ANALYSE THE EFFECT OF CLAD RATIO ON STRESS-STRAIN CURVE OF TITANIUM-CLAD BIMETALLIC STEEL FOR DIFFERENT STRAIN RATES AND TEMPERATURES USING JOHNSON-COOK MODEL

A Thesis Submitted

In partial fulfillment for the award of the degree of

Master of technology

In

Production Engineering

SUBMITTED BY

Harshit Rohatgi
(2K19/PIE/15)

UNDER THE GUIDANCE OF

Dr. N. Yuvaraj
Assistant Professor

DEPARTMENT OF MECHANICAL ENGINEERING
DELHI TECHNOLOGICAL UNIVERSITY
BAWANA ROAD, DELHI-110042
JUNE 2021

CANDIDATE'S DECLARATION

I, HARSHIT ROHATGI, hereby certify that the work which is being presented in this thesis entitled " Analyse the effect of clad ratio on stress-strain curve of Titanium-clad bimetallic steel for different strain rates and different temperatures using Johnson-cook model" being submitted by me is an authentic record of my own work carried out under the supervision of Dr. N. Yuvaraj, Assistant Professor, Department of Mechanical Engineering, Delhi Technological University, Delhi.

The matter presented in this thesis has not been submitted to any other University/Institute for the award of M.Tech Degree.

Place: Delhi HARSHIT ROHATGI

Date: 24/10/2021 (2K19/PIE/15)

CERTIFICATE

I, HARSHIT ROHATGI, hereby certify that the work which is being presented in this thesis entitled "ANALYSE THE EFFECT OF CLAD RATIO ON STRESS-STRAIN CURVE OF TITANIUM-CLAD BIMETALLIC STEEL FOR DIFFERENT STRAIN RATES AND TEMPERATURES USING JOHNSON-COOK MODEL " in the partial fulfillment of the requirement for the award of the degree of Masters of Technology in Production Engineering submitted in the Department of Mechanical Engineering at Delhi College Of Engineering, Delhi University, is an authentic record of my own work carried out during a period from July 2020 to July 2021, under the supervision of Dr. N. YUVARAJ, Assistant Professor, Department of Mechanical Engineering, Delhi College of Engineering, Delhi.

The matter presented in this thesis has not been submitted to any other University/Institute for the award of an M.Tech Degree.

Place: Delhi

Date: 25/10/2021

Dr. N. Yuvaraj
Assistant Professor
Department of Mechanical Engineering
Delhi Technological University

ABSTRACT

Titanium–clad bimetallic steel plate finds its application in the construction of large pressure vessels which are used for storage and processing of petrochemicals. Mechanical properties can be imparted to any material according to its application by a technique known as cladding. To improve material, two main functions are performed by cladding. The first is to improve the material's surface properties like wear resistance in conditions like erosion, abrasion, and Corrosion. The second is to impart bulk-dependent properties like strength, hardness, etc. Titanium-clad bimetallic steel finds its application in various industrial fields like shipbuilding, construction of bridges and buildings, and high-pressure vessels used in the petrochemical industry. Titanium-clad steel enhances the service life of welded pipes as well as reduces the material cost.

The finite element analysis (FEA) technique is an efficacious numerical method for solving several engineering problems. This technique not only provides reliable test results but also reduces the cost of the experiment. The aim of this report is to analyze the effect of clad ratio on stress-strain curves of titanium-clad bimetallic steels for different strain rates and different temperatures using the Johnson-Cook flow stress model. The ratio of the cladding layer thickness (tc) to the total thickness of Titanium-Clad bimetallic steel plate (t) is known as Clad ratio (α). In this report, Titanium Grade 5 is used as a cladding material and AISI 1006 is a parent metal. Furthermore, model constants were estimated from the analyzed result by using material constant for both cladding material and parent material from the research papers. The dimensions of the specimens were taken from GB/T228.1–2010 testing standard. The three-dimensional design of the specimens was created in Solidworks 20 and analyzed in Ansys Explicit Dynamics. A tension test was performed using Ansys for three different temperatures (293K,673K, and 973K) and for three different strain rates (1/sec, 100/sec, and 500/sec). In this report, the reference strain rate was taken as 1/sec and the reference temperature as 293K.

ACKNOWLEDGEMENT

It is a matter of great pleasure for me to present my dissertation report on "ANALYSE THE EFFECT OF CLAD RATIO ON STRESS-STRAIN CURVE OF TITANIUM-CLAD BIMETALLIC STEEL FOR DIFFERENT STRAIN RATES AND TEMPERATURES USING JOHNSON-COOK FLOW STRESS MODEL". First and foremost, I am profoundly grateful to my guide Dr. N. YUVARAJ, Assistant Professor, Mechanical Engineering Department for his expert guidance and continuous encouragement during all stages of the thesis. I feel lucky to get an opportunity to work with him. Not only understanding the subject but also interpreting the results drawn thereon from the graphs was very thought-provoking. I am thankful for the kindness and generosity showed by him towards me, as it helped me morally complete the project before actually starting it.

Finally and most importantly, I would like to thank my family members for their help, encouragement, and prayers through all these months. I dedicate my work to them.

Date: Delhi HARSHIT ROHATGI

Place: 6 October 2021 (2K19/PIE/15)

Table Of Content

CANDIDATE'S DECLARATION…….....i

CERTIFICATE ……...ii

ABSTRACT…….....iii

ACKNOWLEDGEMENT……...iv

LIST OF FIGURES…….....vii

LIST OF TABLES……...xiii

LIST OF GRAPHS…….....xiv

CHAPTER 1……..1

INTRODUCTION…….....1

1.1 Overview…….....1

1.2 Cladding……...1-2

1.3 Titanium…….....2
1.3.1 Grades of Titanium……...…2-3

1.4 Steel……..4
1.4.1 Types and grades of Steel……..4-5

1.5 Methods Used For Cladding Titanium on Mild Steel and Their Application Areas …..5-7

CHAPTER 2……...8
LITERATURE REVIEW……..….8-17

CHAPTER 3……..…18
MATERIAL SELECTION……..…..18

CHAPTER 4……...19
METHODOLOGY ……...….19
4.1 True Stress- True Strain Curve ..……..20
4.2 Tension Test……..22-25

CHAPTER 5……...26
MODELING AND ANALYSIS OF TEST SPECIMENS……26-75
5.1 Modeling ……..26-27
5.2 Analysis……27-75
5.2.1 Johnson-cook model…….....27-28
5.2.2 Procedure and parameters used for analysis…….....28-30
5.2.3 Equivalent (von-mises) stress and equivalent plastic strain along with true stress-true strain curves of specimens using Ansys 19.2…….....31-75

CHAPTER 6…….....77
CALCULATION AND RESULT ……..77-98
Calculation…….....77
6.1 Determination of material constant……...77
6.1.1 Material Constant A, B, and n…….....77
6.1.2 Material Constant C……77
6.1.3 Material Constant, m……..77-78
Result……78
6.2 Material Constants for Clad Ratio-0.17, clad ratio-0.29, and clad ratio-0.5…….78
6.2.1 Material Constants for Clad Ratio-0.17…….....78-79
6.2.2 Material Constant for Clad Ratio-0.29……...80-81
6.2.3 Material Constant for Clad Ratio-0.5…….....81-83
6.3 Effect of Temperature and Strain Rate on the stress-strain curve of TC-bimetallic steel……84-92
6.4 Effect of Clad ratio on Yield stress, Modulus of Elasticity, and Ultimate stress……...93-98
CHAPTER 7……..99
CONCLUSION……99
REFERENCES……100-102

LIST OF FIGURES

Figure 1 Bimetallic steel……1

Figure 2 Titanium-clad steel heater……....2

Figure 3 Roll bonding ……....6

Figure 4 Explosive bonding process……..6

Figure 5 The Explosive roll bonding process……7

Figure 6 Diffusion bonding process……7

Figure 7 General view of Ti-clad steel wide groove joint design……...8

Figure 8 Process Involved……...21

Figure 9 Comparison of true and engineering stress-strain curve……..22

Figure 10 Dimensions of Tensile Test Specimen……26

Figure 11 CAD model of Tensile Specimens (a)Clad Ratio-0, (b) Clad Ratio-1(c)Clad Ratio-0.17,(d) Clad Ratio-0.29, (e) Clad Ratio-0.5…….....27

Figure 12 The meshing of Tensile Specimen of AISI 1006 Steel……27

Figure 13 Boundary condition of tensile specimen…….....28

Figure 14 Applying Velocity in positive X-axis of tensile specimen..…….28

Figure 15 Equivalent(Von-Mises) Stress of Specimen TC-10-0-1..…….31

Figure 16 Equivalent Plastic Strain of Specimen TC-10-0-1……31

Figure 17 Equivalent(Von-Mises) Stress of Specimen TC-10-0-2..…….32

Figure 18 Equivalent Plastic Strain of Specimen TC-10-0-2……32

Figure 19 Equivalent(Von-Mises) Stress of Specimen TC-10-0-3..…….33

Figure 20 Equivalent Plastic Strain of Specimen TC-10-0-3……33

Figure 21 Equivalent(Von-Mises) Stress of Specimen TC-10-0-4……....34

Figure 22 Equivalent Plastic Strain of Specimen TC-10-0-4……34

Figure 23 Equivalent(Von-Mises) Stress of Specimen TC-10-0-5……....35

Figure 24 Equivalent Plastic Strain of Specimen TC-10-0-5……35

Figure 25 Equivalent(Von-Mises) Stress of Specimen TC-10-0-6……36

Figure 26 Equivalent Plastic Strain of Specimen TC-10-0-6……36

Figure 27 Equivalent(Von-Mises) Stress of Specimen TC-10-0-7……37

Figure 28 Equivalent Plastic Strain of Specimen TC-10-0-7……37

Figure 29 Equivalent(Von-Mises) Stress of Specimen TC-10-0-8……38

Figure 30 Equivalent Plastic Strain of Specimen TC-10-0-8……38

Figure 31 Equivalent(Von-Mises) Stress of Specimen TC-10-0-9……39

Figure 32 Equivalent Plastic Strain of Specimen TC-10-0-9……39

Figure 33 Equivalent(Von-Mises) Stress of Specimen TC-10-2-1……40

Figure 34 Equivalent Plastic Strain of Specimen TC-10-2-1……....40

Figure 35 Equivalent(Von-Mises) Stress of Specimen TC-10-2-2……41

Figure 36 Equivalent Plastic Strain of Specimen TC-10-2-2……41

Figure 37 Equivalent(Von-Mises) Stress of Specimen TC-10-2-3……42

Figure 38 Equivalent Plastic Strain of Specimen TC-10-2-3……42

Figure 39 Equivalent(Von-Mises) Stress of Specimen TC-10-2-4……43

Figure 40 Equivalent Plastic Strain of Specimen TC-10-2-4……43

Figure 41 Equivalent(Von-Mises) Stress of Specimen TC-10-2-5……44

Figure 42 Equivalent Plastic Strain of Specimen TC-10-2-5……...44

Figure 43 Equivalent(Von-Mises) Stress of Specimen TC-10-2-6..……45

Figure 44 Equivalent Plastic Strain of Specimen TC-10-2-6……...45

Figure 44 Equivalent(Von-Mises) Stress of Specimen TC-10-2-7..……....46

Figure 45 Equivalent Plastic Strain of Specimen TC-10-2-7……...46

Figure 46 Equivalent(Von-Mises) Stress of Specimen TC-10-2-8..……47

Figure 47 Equivalent Plastic Strain of Specimen TC-10-2-8……...47

Figure 48 Equivalent(Von-Mises) Stress of Specimen TC-10-2-9..……....48

Figure 49 Equivalent Plastic Strain of Specimen TC-10-2-9……...48

Figure 50 Equivalent(Von-Mises) Stress of Specimen TC-5-2-1..……..49

Figure 51 Equivalent Plastic Strain of Specimen TC-5-2-1……49

Figure 52 Equivalent(Von-Mises) Stress of Specimen TC-5-2-2..……..50

Figure 53 Equivalent Plastic Strain of Specimen TC-5-2-2……50

Figure 54 Equivalent(Von-Mises) Stress of Specimen TC-5-2-3..……..51

Figure 55 Equivalent Plastic Strain of Specimen TC-5-2-3……51

Figure 56 Equivalent(Von-Mises) Stress of Specimen TC-5-2-4..……..52

Figure 57 Equivalent Plastic Strain of Specimen TC-5-2-4……52

Figure 58 Equivalent(Von-Mises) Stress of Specimen TC-5-2-5..……..53

Figure 59 Equivalent Plastic Strain of Specimen TC-5-2-5……53

Figure 60 Equivalent(Von-Mises) Stress of Specimen TC-5-2-6..……..54

Figure 61 Equivalent Plastic Strain of Specimen TC-5-2-6……54

Figure 62 Equivalent(Von-Mises) Stress of Specimen TC-5-2-7..……..55

Figure 64 Equivalent(Von-Mises) Stress of Specimen TC-5-2-8..……56
Figure 65 Equivalent Plastic Strain of Specimen TC-5-2-8……56
Figure 67 Equivalent(Von-Mises) Stress of Specimen TC-5-2-9..……57
Figure 68 Equivalent Plastic Strain of Specimen TC-5-2-9……57
Figure 69 Equivalent(Von-Mises) Stress of Specimen TC-2-2-1..……58
Figure 70 Equivalent Plastic Strain of Specimen TC-2-2-1……58
Figure 71 Equivalent(Von-Mises) Stress of Specimen TC-2-2-2..……59
Figure 72 Equivalent Plastic Strain of Specimen TC-2-2-2……59
Figure 73 Equivalent(Von-Mises) Stress of Specimen TC-2-2-3..……60
Figure 74 Equivalent Plastic Strain of Specimen TC-2-2-3……60
Figure 75 Equivalent(Von-Mises) Stress of Specimen TC-2-2-4..……61
Figure 76 Equivalent Plastic Strain of Specimen TC-2-2-4……61
Figure 77 Equivalent(Von-Mises) Stress of Specimen TC-2-2-5..……62
Figure 78 Equivalent Plastic Strain of Specimen TC-2-2-5……62
Figure 79 Equivalent(Von-Mises) Stress of Specimen TC-2-2-6..……63
Figure 80 Equivalent Plastic Strain of Specimen TC-2-2-6……63
Figure 81 Equivalent(Von-Mises) Stress of Specimen TC-2-2-7..……64
Figure 82 Equivalent Plastic Strain of Specimen TC-2-2-7……....64
Figure 83 Equivalent(Von-Mises) Stress of Specimen TC-2-2-8..……65
Figure 84 Equivalent Plastic Strain of Specimen TC-2-2-8……65
Figure 85 Equivalent(Von-Mises) Stress of Specimen TC-2-2-9..……66
Figure 86 Equivalent Plastic Strain of Specimen TC-2-2-9……66

Figure 87 Equivalent(Von-Mises) Stress of Specimen TC-0-2-1……67

Figure 88 Equivalent Plastic Strain of Specimen TC-0-2-1……67

Figure 89 Equivalent(Von-Mises) Stress of Specimen TC-0-2-2……68

Figure 90 Equivalent Plastic Strain of Specimen TC-0-2-2……68

Figure 91 Equivalent(Von-Mises) Stress of Specimen TC-0-2-3……69

Figure 92 Equivalent Plastic Strain of Specimen TC-0-2-3……69

Figure 93 Equivalent(Von-Mises) Stress of Specimen TC-0-2-4……70

Figure 94 Equivalent Plastic Strain of Specimen TC-0-2-4……70

Figure 95 Equivalent(Von-Mises) Stress of Specimen TC-0-2-5……71

Figure 96 Equivalent Plastic Strain of Specimen TC-0-2-5……71

Figure 97 Equivalent(Von-Mises) Stress of Specimen TC-0-2-6……72

Figure 98 Equivalent Plastic Strain of Specimen TC-0-2-6……72

Figure 99 Equivalent(Von-Mises) Stress of Specimen TC-0-2-7……73

Figure 100 Equivalent Plastic Strain of Specimen TC-0-2-7……..73

Figure 101 Equivalent(Von-Mises) Stress of Specimen TC-0-2-8……...74

Figure 102Equivalent Plastic Strain of Specimen TC-0-2-8……..74

Figure 103 Equivalent(Von-Mises) Stress of Specimen TC-0-2-9……...75

Figure 104 Equivalent Plastic Strain of Specimen TC-0-2-9……..75

Figure 105 Plot between $\ln(\sigma - A)$ and $\ln\varepsilon$ for clad ratio-0.17 under reference Conditions..77

Figure 106 Plot between $\sigma/(A+B\varepsilon^{n})$ and $\ln\dot{\varepsilon}^{*}$ for clad ratio-0.17 under the reference conditions……78

Figure 107Plot between ln $(1-\sigma/(A+B\varepsilon^n))$ and lnT* for clad ratio-0.17 under the reference conditions...……..78

Figure 108 Plot between ln$(\sigma - A)$ and lnε for clad ratio-0.29 under reference Conditions…….....79

Figure 109 Plot between $\sigma/(A+B\varepsilon^n)$ and ln$\dot{\varepsilon}$* for clad ratio-0.29 under the reference conditions..……...79

Figure 110 Plot between ln $(1-\sigma/(A+B\varepsilon^n))$ and lnT* for clad ratio-0.29 under the reference conditions.....80

Figure 111Plot between ln$(\sigma - A)$ and lnε for clad ratio-0.5 under reference conditions.....81

Figure 112Plot between ln$(\sigma - A)$ and lnε for clad ratio-0.5 under reference conditions.....81

Figure 113Plot between ln $(1-\sigma/(A+B\varepsilon^n))$ and lnT* for clad ratio-0.29 under the reference conditions…….....82

Figure 114 True Stress-true strain at various temperatures under strain rate of 1/sec……..83

Figure 115 True Stress-true strain at various temperatures under strain rate of 10/sec.……...84

Figure 116 True Stress-true strain at various temperatures under strain rate of 100/sec……..85

Figure 117 True Stress-true strain at various strain rates under the temperature of 293K…...86

Figure 118 True Stress-true strain at various strain rates under the temperature of 673K…..87

Figure 119 True Stress-true strain at various strain rates under the temperature of 973K…...88

Figure 120 Effect of clad ratio on Yield stress (σy).....93

Figure 121 Fitted line plot between Yield stress (σy) and clad ratio……93

Figure 122 Effect of clad ratio on Modulus Of Elasticity(E).....95

Figure 123 Fitted line plot between Modulus of Elasticity and clad ratio……95

Figure 124 Effect of clad ratio on Ultimate Stress (σu).....97

Figure 125 Fitted line plot between Ultimate stress and clad ratio……...97

LIST OF TABLES

Table 1 Classification of carbon steel……..4-5

Table 2 Different grades of Carbon steels……5

Table 3 Literature Review……10-19

Table 4 Elastic properties of AISI 1006 and Titanium Grade 5..…….20

Table 5 Chemical Composition of AISI 1006 Steel….……20

Table 6 Chemical Composition of Titanium Grade 5……..20

Table 7 Dimensions for specimens with different clad ratios at different temperatures and Strain rates……...23-25

Table 8 J-C constants for hot-rolled Titanium Grade 5 Plate ……29

Table 9 J-C constants for hot-rolled AISI 1006 Plate……...…….……29

Table 10 Parameters required for analysis ……...……30

Table 11 Calculated J-C parameters for clad ratio-0.17,0.29 and 0.5…….……...82

Table 12 Analyzed values of Stress-Strain curve correlated parameters……89-91

LIST OF GRAPHS

Graph 1 True Stress-True Strain curve of Specimen TC-10-0-1……31

Graph 2 True Stress-True Strain curve of Specimen TC-10-0-2……....32

Graph 3 True Stress-True Strain curve of Specimen TC-10-0-3……33

Graph 4 True Stress-True Strain curve of Specimen TC-10-0-4……34

Graph 5 True Stress-True Strain curve of Specimen TC-10-0-5……35

Graph 6 True Stress-True Strain curve of Specimen TC-10-0-6……...36

Graph 7 True Stress-True Strain curve of Specimen TC-10-0-7……...37

Graph 8True Stress-True Strain curve of Specimen TC-10-0-8..……...38

Graph 9 True Stress-True Strain curve of Specimen TC-10-0-9.....……...39

Graph 10 True Stress-True Strain curve of Specimen TC-10-2-1..……....40

Graph 11 True Stress-True Strain curve of Specimen TC-10-2-2.……41

Graph 12 True Stress-True Strain curve of Specimen TC-10-2-3.……42

Graph 13 True Stress-True Strain curve of Specimen TC-10-2-4.……43

Graph 14 True Stress-True Strain curve of Specimen TC-10-2-5……..44

Graph 15 True Stress-True Strain curve of Specimen TC-10-2-6……..45

Graph 16 True Stress-True Strain curve of Specimen TC-10-2-7..……46

Graph 17 True Stress-True Strain curve of Specimen TC-10-2-8..……47

Graph 18True Stress-True Strain curve of Specimen TC-10-2-9...……48

Graph 19 True Stress-True Strain curve of Specimen TC-5-2-1……...49

Graph 20 True Stress-True Strain curve of Specimen TC-5-2-2...……50

Graph 21 True Stress-True Strain curve of Specimen TC-5-2-3...……51

Graph 22 True Stress-True Strain curve of Specimen TC-5-2-4...……52

Graph 23 True Stress-True Strain curve of Specimen TC-5-2-5……...……53

Graph 24 True Stress-True Strain curve of Specimen TC-5-2-6……...…54

Graph 25 True Stress-True Strain curve of Specimen TC-5-2-7……...55

Graph 26 True Stress-True Strain curve of Specimen TC-5-2-8…….……..56

Graph 27 True Stress-True Strain curve of Specimen TC-5-2-9…….……..57

Graph 28 True Stress-True Strain curve of Specimen TC-2-2-1…….……..58

Graph 29 True Stress-True Strain curve of Specimen TC-2-2-2……..59

Graph 30 True Stress-True Strain curve of Specimen TC-2-2-3…….……..60

Graph 31 True Stress-True Strain curve of Specimen TC-2-2-4…….……..61

Graph 32 True Stress-True Strain curve of Specimen TC-2-2-5…….……..62

Graph 33 True Stress-True Strain curve of Specimen TC-2-2-6…….……..63

Graph 34 True Stress-True Strain curve of Specimen TC-2-2-7…….……..64

Graph 35 True Stress-True Strain curve of Specimen TC-2-2-8…….……..65

Graph 36 True Stress-True Strain curve of Specimen TC-2-2-9…….……..66

Graph 37 True Stress-True Strain curve of Specimen TC-0-2-1…….……..67

Graph 38 True Stress-True Strain curve of Specimen TC-0-2-2…….……..68

Graph 39 True Stress-True Strain curve of Specimen TC-0-2-3…….……..69

Graph 40 True Stress-True Strain curve of Specimen TC-0-2-4…….……..70

Graph 41 True Stress-True Strain curve of Specimen TC-0-2-5…….……..71

Graph 42 True Stress-True Strain curve of Specimen TC-0-2-6…….……..72

Graph 43 True Stress-True Strain curve of Specimen TC-0-2-7…….……..73

Graph 44 True Stress-True Strain curve of Specimen TC-0-2-8…….……..74

Graph 45 True Stress-True Strain curve of Specimen TC-0-2-9…….……..75

CHAPTER -1

INTRODUCTION

1.1 Overview

Titanium-steel composite has found usage due to its ability to withstand high pressure, good corrosion resistance, and low price. In the production of titanium vessels, titanium-steel composite becomes the important structural material, in which base material load-carrying steel is guarded against the liquid environment which is corrosive in nature by a clad of titanium alloy. In these years, sustainable development is a hot topic to be focused on, i.e., to make metallic materials more efficient which are derived from the limited resources to the maximum level at a minimum cost.

In marine environments, titanium-clad steels find their application in large pressure vessels due to their excellent corrosion resistance property. Cladding is a technique to protect low-grade materials so that their service life cycle will become better or to substitute costly base materials. It was profound that the product's performance has been improved with cladding.

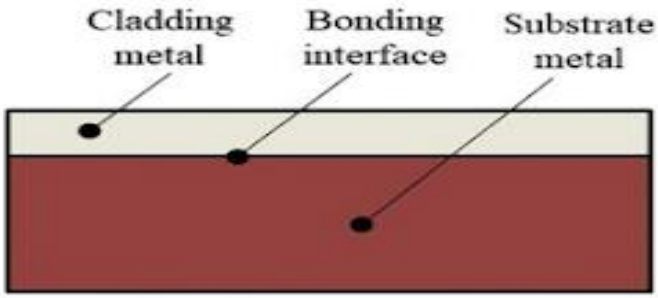

Fig.1. Bimetallic steel

1.2 Cladding

Cladding is a technique that is widely employed to modify surfaces. It is a process in which a metallic layer of material is mechanically or metallurgically bonded to a corrosion-prone material to enhance its corrosion resistance and/or impart high strength to increase its service life. The coating is used to refine product performance in the modern manufacturing industry. A combination of properties of alloys or two or more metals is offered by the cladding technique. Cladding also provides some distinct advantages such as resistance to corrosion or erosion, improved hardness, favorable microstructure, and strong bonding.

Cladding on low carbon steel (mild steel) through welding, an important role played by the heat input to achieve a high hardness of the surface. The hardness of the surface can be enhanced through the cladding and this method is known as hard facing. Hard facing is an extensively used method to treat surfaces that are subjected to corrosion or oxidation, severe wear, erosion, and cavitations from high-velocity fluid flow.

Fig.2. Titanium-clad steel heater

1.3 Titanium

Titanium and its alloys find the use of their properties like excellent fatigue resistance, wide temperature range stability, low value of thermal conductivity and thermal expansion coefficient, excellent corrosion resistance for some industrial chemicals which create problems, sterling resistance to erosion and cavitations caused by flow high-velocity fluid, etc for a variety of applications such as chemical equipment, jet engines, aerospace equipment, electroplating equipment, etc. In industrial application corrosion resistance of titanium is the most important property while in an aerospace application mechanical properties of titanium are the primary consideration. A strong adherent oxide film (TiO_2) is formed when a fresh surface of titanium is exposed to moisture and air. This film is chemically stable and protective due to which titanium has high corrosion resistance. This film is not detected by naked eyes because it is transparent in nature.

1.3.1 Grades of Titanium

There are 4 varieties of titanium alloys and 6 grades of pure titanium(grades 1,2,3,4,7 and 11). Titanium alloys have traces of vanadium, aluminum, niobium, molybdenum, tantalum, manganese, zirconium, chromium, iron, cobalt, copper, and nickel.
Titanium alloy four grades or varieties are Ti 6Al 4V, Ti 3AL 2.5, Ti 6AL 4V ELI, Ti 5Al 2.5Sn.

1. **Titanium alloy Grade 5 (Ti 6Al 4V)**
   Most commonly used titanium alloy. Therefore it is commonly referred to as a titanium alloy workhorse. This grade has high corrosion resistance and good formability.
   Hence it is commonly used to make:
   1. Engine components
   2. Aerospace fasteners
   3. Aircraft turbines
   4. High-performance automatic parts
   5. Aircraft structural components
   6. Sports equipment
   7. Marine applications

2. **Titanium alloy Grade 12 (Ti 3AL 2.5)**
   This alloy has the best weldability. It also has high strength at high temperatures. It is unique because it shows the characteristics of stainless steel and is heavier than other titanium alloys. It shows high corrosion resistance and is used in many applications and industries as follows:
   1. Hydrometallurgical applications
   2. Shell & tube heat exchangers
   3. Marine applications
   4. Chemical manufacturing at elevated temperature.

3. **Titanium alloy Grade 23 (Ti 6AL 4V ELI)**
   Commonly known as surgical titanium as it found a major application in surgery.
   This alloy can be easily molded and cut into small strands, wires, & coils. It has high corrosion resistance & the same strength as Ti 6AL 4V. It is lightweight and highly resistant to damage as compared to other titanium alloys. It has exceptional biocompatibility which makes it easier to implant in & attach to the bone without having side effects.
   Some common surgical applications of Ti 6AL 4V ELI are :
   1. Orthopedic cables
   2. Orthopedic pins and screws
   3. Surgical staples
   4. Springs
   5. In joint replacements
   6. Bone fixation devices
   7. Cryogenic vessels
   8. Orthodontic applications

4. **Titanium alloy Grade 6 (Ti 5AL 2.5Sn)**
   It is a non-heat treatable alloy that possesses high-temperature stability, good weldability, good corrosion resistance, & high strength. It has high creep resistance and found its application in aircraft and airframes.

1.4 Carbon Steel

It is an iron-carbon alloy having 2.1 wt.% of carbon. For alloying carbon steels, there is no specified minimum limit of alloying elements. The maximum amount of silicon, manganese, and copper should be less than 0.6 wt.%, 1.65 wt.%, and 0.6 wt.% respectively.

1.4.1 Carbon steel types and their properties:-

Table.1. Classification of carbon steel

Type	Carbon content (wt.%)	Properties	Microstructure	Applications	Images
Low Carbon Steel	Less than 0.25	High ductility, low hardness, high toughness, weldability, & machinability.	Ferrite and pearlite	Automobile body components, pipes, food cans, construction and bridge components, structural shapes (channel, angle iron, and I-beams)	
Medium Carbon Steel	0.25 to 0.6	Resistance to wear, medium strength, toughness, ductility, and low hardenability.	Martensite	Train wheels, railway tracks, crankshafts, machinery parts, and gears.	
High Carbon Steel	0.6 to 1.25	Low ductility, high strength, and hardness.	Pearlite	Springs, cutting tools, high-strength wire, and dies.	

Ultra-high carbon steel	1.25 to 2	Extreme strength, sharpness, and resilience	Ferrite	Knives, axles, and punches.	

Table.2. Different grades of carbon steels

Type	ASTM name	Carbon content (wt.%)	Applications
Low	1010	0.1	Nails, automobile panels, wire
Low	1020	0.2	Structural steel, pipes, sheet steel
Low	A36	0.29	Structural
Low	A516 Grade70	0.31	Low-temperature pressure vessels
Medium	1030	0.27-0.34	Gears,axles, machinery parts, bolts
Medium	1040	0.37-0.44	Couplings, crankshaft
High	1080	0.75-0.88	Music wire
High	1095	0.90-1.04	Cutting tools, springs

1.4.2 AISI 1006 -

AISI 1006 plates of steel have extremely low carbon content and other alloying materials that's why they are called dead mild steel.

Properties-

1. Low hardness and plasticity
2. Excellent weldability and formability

Applications-

1. Panels for automobiles or appliances
2. Shipbuilding Plate
3. Boiler Plate

4. Flange Plate used in fuel and water pipelines.

1.5 Methods Used For Cladding Titanium on Mild Steel and Their Application Areas

1. Roll bonding process- A manufacturing process in which sufficient pressure is applied by a pair of flat rollers when two metal layers pass through it which causes plastic deformation at the interface of substrate and cladding material. Wide titanium-clad plates and sheets are manufactured by this process with high manufacturing efficiencies, low energy consumption, and low pollution [22]. The cost of this process is less than the conventional explosive bonding process. The improved microstructure of clad plates and voids at the interface is also eliminated by this process.

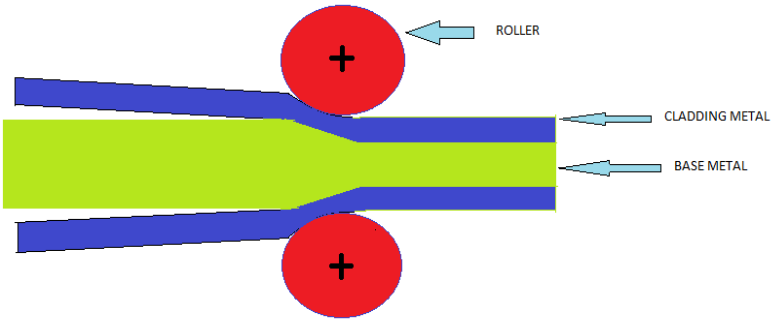

Fig.3. Roll bonding

2. Explosive bonding process- A solid-state welding process in which welding clad of heterogeneous metal is achieved by energy released by explosive material detonation. This is mostly used to combine steel- titanium because the layer of intermetallic phases formed at the joint surface and its thickness is lower than in other methods [22]. The use of this process is limited due to low yield rate, high costs, variable strength at bonding surfaces, environmental and noise pollution.

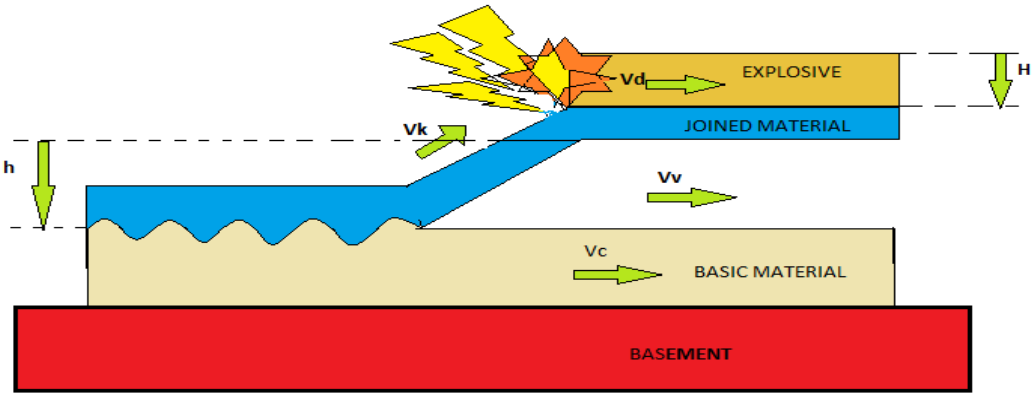

Fig.4. Explosive bonding process

3. Explosive roll bonding process- It combines the advantages of both roll bonding and explosive bonding processes [27]. In this process, explosive bonding is used as a primary process to manufacture thick clad plates, and hot or cold rolling is used as a secondary process to obtain the finished product. This process is used to manufacture a wide variety of products.

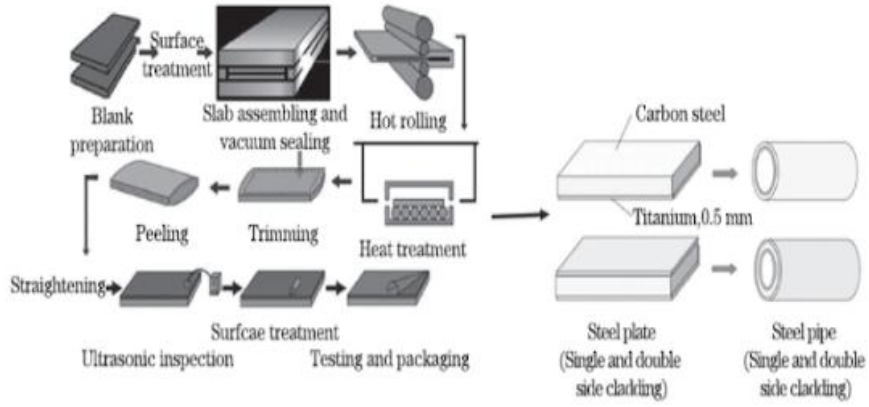

Fig.5. The explosive roll bonding process

4. Diffusion bonding process- It is also a solid-state joining process in which metal plates are compressed under high pressure and temperature below their melting point resulting in an undetectable original bond line. Bond is formed between the base material and cladding material by atomic diffusion across the interface. This process does not require filler material but it is time-consuming and is limited to manufactured small-size products [22]. Therefore this process is not applicable to producing titanium clad steel plates at an industrial scale.

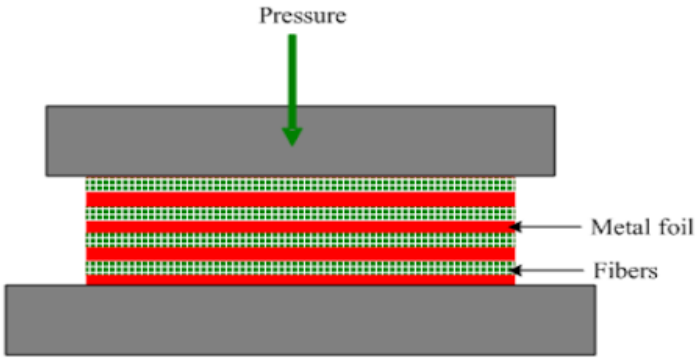

Fig.6. Diffusion bonding process

5. Cladding of Titanium-Steel by Welding-

Welding is considered the effective and most popular process to clad titanium on mild steel. Various welding processes are solid-state welding like explosive welding, diffusion welding, etc., friction welding, brazing, arc welding process like CSC-GMAW, GTAW, etc., different high energy intensity welding like Plasma Arc Welding (PAW), laser beam welding (LBW), etc [2].

The cladding of titanium on mild steel by explosive welding has some disadvantages as it requires a special space to carry out the joining process and welding parameters should be the

correct choice [26,28]. Tungsten inert gas welding can also be used to clad titanium on mild steel but it results in cracks at joints caused by the formation of intermetallic phases due to incomplete solubility of iron in titanium. One of the main disadvantages of TIG welding is that it uses very costly sheets of vanadium.

Friction stir welding finds its less usage in the fabrication of titanium clad steel plate due to its high labor requirement, use of interlayer like vanadium which increases the cost of joint preparation because of its high price and also makes the joint process time-consuming [24]. Gas metal arc welding is a reliable, cost-effective, all-position capability, clean, popular, and semi-automatic technique to produce titanium-clad steel plates.

The CSC-GMAW is the advanced version of short circuit GMAW in which a reciprocating wire feed is used to develop consistent drop transfer at low currents.CSC-GMAW process results in less heat input and dilution as compared to other arc welding processes[25].

Fig.7. General view of Ti-clad steel wide groove joint design

CHAPTER -2

LITERATURE REVIEW

Mechanical properties can be imparted to any material according to its application by a technique known as cladding. Titanium is used as a marine metal due to its high corrosion resistance but it is costly so to make use of titanium's high corrosion resistance and less cost and good mechanical properties of steel, cladding of titanium is done on mild steel which is very much suitable for severely corrosive environments. Titanium-clad steel plate finds its application in various industrial fields like shipbuilding, construction of bridges and buildings, and high-pressure vessels used in the petrochemical industry. Titanium-clad steel enhances the service life of welded pipes as well as reduces the material cost. This paper contains various methods, used for cladding titanium on mild steel.

The bonding strength and formability of clad material depend on the properties and thickness of the intermetallic compounds that are formed in each interface's diffusion layer [32]. It was observed that Knoop hardness of mild steel decreases with the increase in temperature during post-heat treatment while the hardness of titanium get decreased up to 600°C [34] and remains unchanged in-between temperature 600°C to 800°C and then transformation of Ti into brittle BCC β-Ti takes place which results in an increase of hardness of Ti rapidly beyond 800°C when titanium is clad on mild steel by roll bonding. Formation of micro-cracks could easily take place in the intermetallic compound due to deformation from applied stress which will act as a stress concentration factor and it can cause a fracture at Ti clad material's bonding interface [33]. It was observed that the hardness of the titanium side is greater than the mild steel side.

Roll bonding of titanium mild steel joints using Nb as an interlayer has a higher shear strength than joints without any interlayer while using Mo as an interlayer will result in lower shear strength of joints as compared to without interlayer [35]. At the different preheat temperatures shear strength increases with the increase in starting rolling temperature then it gets stable up to some temperature then rapidly decreases as a further increase in starting rolling temperature [11].In explosively welded steel-titanium-clad components 80% initiation of fatigue cracks starts at the steel side while at the interface of Ti and steel, 20% initiation of fatigue cracks, and no crack initiation at the titanium side when it is subjected to push-pull loading [14]. The titanium-clad mild steel plate's shear strength depends on the amount of the titanium carbide film on the interface of iron and Titanium. It was observed that the hardness of both materials titanium and steel is higher than before cladding [9].

The increase in hardness of titanium is more than mild steel was also observed after rolling of titanium-clad steels. In explosively welded steel/titanium components, there can be crack growth at the points of weaker bond formation. cracks formed in titanium due to which is able to protect the steel from corrosion [12]. It was recognized that micro-cracks also occur at the interfaces of the Titanium mild steel joints [13].

It was espied that at the interface of titanium and interlayer and around the Ti first layer have the highest hardness when the titanium is clad on mild steel using different types of interlayer through controlled short circuit gas metal arc welding process. Fabrication of Ti-clad steel welded joints by using Ni, NiCu, and NiCr as interlayer, it was found that 607, 554, and 568 $HV_{0.5}$ were the hardness value for Ni-Ti, NiCr-Ti, and NiCu-Ti respectively[16].
The maximum hardness noticed at the Fe-V interface in the Ti-V and V-Ti systems were 409 and 307 $HV_{0.5}$ respectively. Some micro-cracks were also observed at the Fe-V interface that may influence the hardness value. Ti-clad steel Welded joints made by CSCGMAW show less hardness as compared to welded joints made through a combination of GTAW-P and CSC GMAW processes.
Titanium bimetallic steel plate when subjected to tension test fine dimples was observed on their fractured surface which gives an indication of ductile fracture of Titanium bimetallic steel plate. As the value of clad ratio decreases, the elastic modulus of the Titanium bimetallic steel plate increases because titanium has higher yield stress as compared to mild steel. It was also observed that as the clad ratio increases, 0.2 % proof stress of titanium clad steel plate increases. Hardness at the interface of the Ti cladding layer & the mild steel are observed lower than the individual hardness because of the formation of compounds like FeTi and TiC at the interface during the hot rolling process [2]. The maximum shear strength at the bonding temperature of 835 °C approximately 150 MPa was observed between steel and titanium when cladding of titanium on mild steel was carried by an explosive welding process [36-37]. For joining the interface of clad plates effectively, fracture of the matrix can be considered an important factor. The maximum value of shear strength of approximately 225 MPa was observed between Ti and steel for diffusion bonding of titanium on mild steel [30-31]. It was examined when cladding of titanium on mild steel using Ni interlayer only 224 Mpa shear strength in the matrix because Nickel interlayer unable to constrain the diffusion of Fe and Ti at 1000°C and brittle compounds like TiFe and TiC at the interface was formed[29].

Table.3. Literature Review

SI No.	**Author**	**Process**	**Material and filler metal**	**Results**
1.	**Xinpei Liu et.al. (2019)**	Hot rolling	Clad metal -TA2 Titanium and Base metal -Q235 steel	1. Stress-Strain curves of Titanium clad bimetallic steel plates with different clad ratios( ) were obtained. 2. Notice that as the clad ratio increases the strength increases.

2.	**Dariusz Rozumek et.al. (2012)**	Explosive welding	Clad metal - Titanium Grade1 Base metal - S355J2 N	1. Examine that composite's hardness at all its sections is more than the hardness of the parent material before cladding. And at the interface line, the highest hardness for steel is observed. 2. Two different cases of crack growth were observed, in one case the crack grows along the interface line, in the other case the crack crosses the interface line.
3.	**T.N. Prasanthi et.al. (2015**)	Explosive welding	Clad metal - Titanium Grade 2 Base metal -Mild steel	1. For load ratio 1.07, a wavy interface having a sinusoidal-like pattern was observed in an explosive Ti-clad mild steel plate. 2. At the isolated regions in the wave vortices of the clad interface, a brittle intermetallic phase Fe2Ti was obtained. 3. Fine grains and dendritic structures were formed at high energetic conditions during cladding.
4.	**Qiaoling Chu et.al. (2017)**	Explosive welding	Clad metal- Titanium Grade1 Base metal -Q345 steel	1. It is found that at the interface deformation-recovery-recrystallization takes place due to a rapid increase in temperature and followed by a fast cooling rate. 2. FeTi intermetallics of nano-size are observed at the titanium and iron interface. 3. In the melted zone high hardness was observed and the localized strain can be accommodated by recrystallized structure.

5.	**Xiongwei Tong et.al. (2020)**	Explosive welding	Clad metal- CP Titanium Base metal-Q235 steel Filler wire - Cu-Nb	1. It was observed that there were cracks in welded joints which were filled by Cu30Nb and Cu5Nb wires. 2. Sensitive regions of cracking are rich in Fe-Ti, Cu-Ti, and Fe-Nb intermetallics. The average strength of 334 Mpa had been observed in welded joints.
6.	**Jianxiong Li et.al. (2020)**	Vaporizing foil actuator welding	Clad metal -Ti-1.2ASN Base metal-436 stainless steel Interlayer material-Pure niobium	1. Ti/Nb/SS welds absorbed more energies than Ti/SS welds at temp 300-700◦C due to the Nb interlayer prohibits interdiffusion between Titanium and Stainless steel. 2. At the fracture surfaces various intermetallics such as FeTi, Cr2Ti, Fe2Ti and their mixtures for Titanium stainless steel welds, and Fe7Nb6, □-Ti, and Fe2Nb phases for Ti/Nb/SS welds after thermal exposure at high temperature.
7.	**Sweta Saroj et.al. (2020)**	Tungsten inert gas welding	Clad metal-Inconel 825 Base metal -AISI 304 steel	1. As the increase in processing current the clad layer height, width, dilution ratio, dilution depth/area, maximum pool depth/area, and clad angle increased. 2. There is a minor improvement in hardness value(300–350 HV) for produced Inconel 825 clad as compared to the AISI 304 steel substrate (260–270 HV).

8.	**Qiaoling Chu et.al. (2019)**	Explosive welding	Clad metal-Titanium Grade1 Base metal -Low carbon steel (S235)	1. It was observed that typical wave structure with mixing zone at the explosive interface and Fe-Ti intermetallics dominated at mixing zone. 2. Intermetallic compounds like Fe2Ti (14.2 GPa) and FeTi(20.6GPa) showed more hardness than Fe base metal which have only a 2.2 GPa hardness value. The ultimate strength (432MPa) of Titanium steel bimetallic joints is observed.
9.	**Mohsen Saboktakin et.al. (2011)**	Hot roll bonding	Clad metal-Titanium Grade1 Base metal-Plain carbon steel Interlayer material-CP copper foil	1. It was observed that the interdiffusion between titanium and steel can be prevented by using copper interlayer during roll bonding at high temperatures. 2. The reaction layers of TiCu4, Ti3Cu4, Ti2Cu3, Ti2Cu, and TiCu along with their mixtures formed at the CuTi interface. 3. Average peeling strength decreases because of the formation of intermetallic compounds in the titanium-copper mixed layer.

10.	**Y Mahmood et.al. (2020)**	Explosive welding	Clad metal- Titanium Grade 5 Base metal- SS304 Interlayer material- Al-Cu composite plate	1. It was observed that the interlayer reduces the formation of intermetallics by controlling the energy loss. Better quality welded joints majorly depend on threshold values of plastic deformation and impact pressure and these parameters can be controlled by the interlayer. 2. Numerical simulation results showed that maximum deformation appears at the flyer-interlayer interface as compared to the interlayer-base interface. 3. Simulation results indicated that the probability of brittle intermetallics formation was increased due to the formation of continuous packets of melted regions by the Al interlayer. 4. Welded composite plate joint strength could decrease as Cu yield strength was very much lower than parent materials.
11.	**D.S. Bae et.al. (2011)**	Cold rolling	Clad metal- Titanium Grade1 Base metal - Mild steel(SPCC) grade	1. The Knoop hardness of titanium decreased in the 500~600 ◦C range & show a uniform value up to 800◦C and then increased up to 900◦C while mild steel Knoop hardness gets decreased with post-heat treatment temperature. 2. The diffusion layer showed a high Knoop hardness value as compared to Ti and mild steel matrices at 600◦C. 3. At the interface of Ti/Mild steel, bonding force gets decreased up to 800◦C and then increased to some extent due to post-heat treatment temperature.

12.	**Xi-yang Chai et.al. (2017)**	Hot roll bonding	Clad metal-Titanium Grade 2 Base metal-Q390 steel Interlayer material-Mo or Nb	1. With no interlayer, a shear strength value of 225 Mpa was observed in clad plates. 2. Shear strength of the joint increases by 65 MPa when the Nb interlayer was inserted.While bonding strength decreases by 20 MPa when the Mo interlayer is inserted. 3. At the interface of the clad plates, various intermetallic phases were formed like TiC, □-Ti, and Fe2Ti when no interlayer is used. While at Ti/Mo and Ti/Nb interface no intermetallic reaction takes place, but at the interface, Mo/steel, and Nb/ steel some micro-voids were found.
13.	**Jiang Haitao et.al. (2014)**	Explosive roll bonding	Clad metal-Titanium Grade 2 Base metal-Q235B steel	1) During heat treatment of titanium-stell explosive-rolled clad plate, at the interface a diffusion-reaction layer was formed due to which bonding strength was decreased at 850 °C and above. 2. At 850 °C, near the titanium side of the interface, TiC was formed due to diffusion-reaction. formation of TiC. FeTi, Fe2Ti, and few TiC formed near the steel side of the interface during diffusion-reaction at 950°C. 3. During heat treatment, there was a decline in bonding strength due to the discontinuous formation of bulk-shaped intermetallics.

14.	**Aleksander Karolczuk et.al. (2012)**	Explosive welding	Clad metal- Titanium Grade 1 Base metal-S355J2 N	1. It was observed that fatigue crack initiation starts at 20% in interface and 80% in steel but in titanium, there is no crack initiation. Specimens with wavy interface show lower fatigue life than flat interface specimens under the same force amplitude. 2. At the interface thin layer of melted metal is observed and some microcracks at the border. Amorphous solid material with a titanium percentage of 69 was formed with 80% of cracks in the steel.
15.	**Yakup Kaya et.al. (2019)**	Explosive welding	Clad metal- Titanium Grade 2 Base metal- Ship steel Grade A	1. At the explosive ratio of 2, a smooth bimetallic composite surface with no diffusion is formed as per EDS and SEM analysis. 2. It was also observed that as the value of explosion ratio increases, hardness value increased at both sides of the bimetallic composite bonding interface, while there is no change in hardness value at the thickness center of bimetallic composite steels. 3. The tensile-shear tests showed that an increase in explosion ratio tensile-shear strength of bimetallic composite specimens increases.

16.	**Fumio Kurosawa et.al. (1988)**	Hot roll bonding	Clad metal- CP Titanium Base metal-Plain carbon steel	1. It was observed that at the interface of iron-titanium various intermetallic compounds like FeTi, Fe2Ti, TiH2 (titanium hydride), and □ -Ti containing Fe were found. 2. Shear strength of titanium-iron interface depends on the amount of Titanium carbide film but it has lease influence on the shear strength of intermetallic compounds like FeTi, Fe2Ti and □-Ti.
17.	**Boxin Li et.al. (2018)**	Diffusion bonding	Clad metal-CP Titanium Base metal-Plain carbon steel	1. During the diffusion bonding process carbon atoms from steel parts diffuse to the Titanium part. Diffusion of carbon atoms in α-Ti is more favorable in vertical to the c axis as compared to along the c axis. 2. At a diffusion temperature of 750 or 800°C, for the diffusion of Fe atoms TiC layer acts as a barrier. At 850°C, diffusion of iron atoms through the TiC layer takes place which leads to the formation of intermetallic compounds like Fe2Ti and FeTi at the TiC/Ti interface. And at the higher diffusion temperatures, this TiC layer barrier effect reduces.

18.	**Lu Liangyu et.al. (2020)**	Explosive welding	Clad metal-Titanium Grade 1 Base metal-304 SS	1. A periodic wavelike bond is exhibited by the bonding interface of Ti-SS. Melting zones are formed at the interface. It was observed from the line scan that the amount of diffusion in the melting zone is very much severe as compared to at the ordinary interface, which results in the improvement of the cladding plate's interfacial bonding strength. 2. At the interface the Vickers hardness value reaches a max of 413.10, and as the value of the distance from the interface increases it decreases gradually. After explosion welding, it was that the tensile strength of SS is 865 Mpa. The data of the shear test showed that the cladding plate had a 325 Mpa as longitudinal shear strength and 309 Mpa as the transverse shear strength.

19.	**Zongan LUO et.al. (2013)**	Vacuum hot roll bonding	Clad metal- Pure titanium Base metal-304 SS Interlayer material- Niobium	1. Excellent properties were exhibited by Titanium-Stainless Steel clad plate using Nb as an interlayer. At the interface, no cracks and discontinuities were observed and the value of shear strength is more than the minimum standard. 2. It was investigated that there is the absence of intermetallic compounds at the Titanium-Niobium interface at all roll bonding temperatures while for Niobium- Stainless Steel no reaction products were formed up to 900◦C roll bonding temperatures. 3. It was observed that at 900◦C roll bonding temperature value of shear strength at the interface was approximately 396 MPa and through the Titanium-Niobium interface ductile fracture occurred.
20.	**C. Sudha et.al. (2015)**	Friction welding	Clad metal- Titanium Grade 2 Base metal- Mild steel	1. It was investigated by TEM, that at the interface fine FeTi intermetallic phase is ingrained in the ferrite matrix. 2. It was observed that during the friction welding process, plastic strain is experienced by the mild steel which causes recrystallization and grain growth in the interface of the mild steel.

21.	**Mohsen Saboktakin et.al. (2011)**	Hot roll bonding	Clad metal-CP Titanium Base metal-Plain carbon steel Interlayer material - Copper	1. It was observed that element diffusion between Ti and carbon steel can be blocked by the copper interlayer. 2. It was investigated that no diffusion layer or no reaction takes place at the interface of Fe-Cu while at the interface of copper and titanium different intermetallic compounds formed like Ti2Cu3, TiCu4, TiCu, Ti3Cu4, and Ti2Cu along with their mixtures. 3. Average peel strength decreases because of the formation of the intermetallic compounds at the Titanium-copper interface.

CHAPTER -3

MATERIAL SELECTION

Titanium clad bimetallic steel in the present analysis work is made of two different metals: for clad metal Titanium Grade 5 is used and for base metal AISI 1006.

Table.4. Elastic properties of AISI 1006 Steel and Titanium Grade 5

Materials	**Elastic Modulus(E) (GPa)**	**Poisson's Ratio (μ)**	**Mass Density Kg/m^3**	**Yield Strength (□y) (MPa)**
AISI 1006	210	0.27	7872	285
Titanium Grade 5	110	0.31	4429	862

Table.5. Chemical Composition of AISI 1006 Steel

C(%)	**Fe(%)**	**Mn(%)**	**P (%)**	**S(%)**
0.08	99.43-99.75	0.25-0.4	0.04	0.05

Table.6. Chemical Composition of Titanium Grade 5

Ti(%)	**Al(%)**	**V(%)**	**Fe(%)**	**O(%)**	**C(%)**	**N(%)**	**H(%)**
87.6-91	5.5-6.75	3.5-4.5	0.40	0.20	0.08	0.05	0.015

CHAPTER -4

METHODOLOGY

To illustrate the effect of clad ratio on the stress-strain curve of TC bimetallic steels, a 3D finite element model was developed to simulate the uniaxial tensile coupon test by using the module called explicit dynamic in software ansys19.2.By assembling two layers of components, tensile coupon specimens were formed.

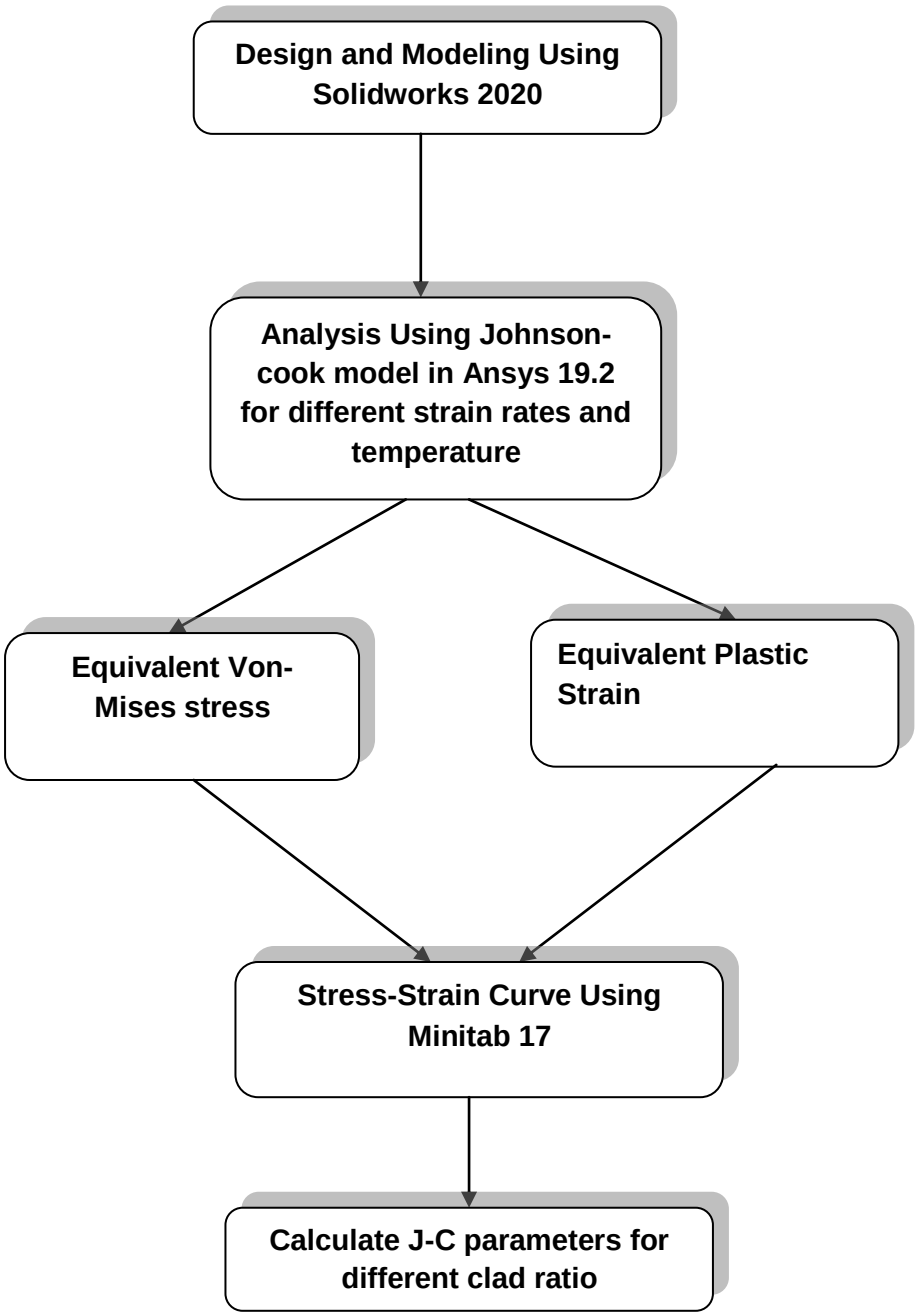

Fig.8. Process Involved

4.1 True Stress- True Strain Curve

The true stress-strain curve gives a characteristic of true indication of deformation of a metal which does not give by the engineering stress-strain curve because it is entirely based on the original dimensions of the specimen, and during the test, these dimensions change continuously. The true stress-strain curve counts the factor of continuously changing dimensions of the specimen. The true stress-strain curve is also known as the flow curve as it represents the plastic flow characteristic of the material.

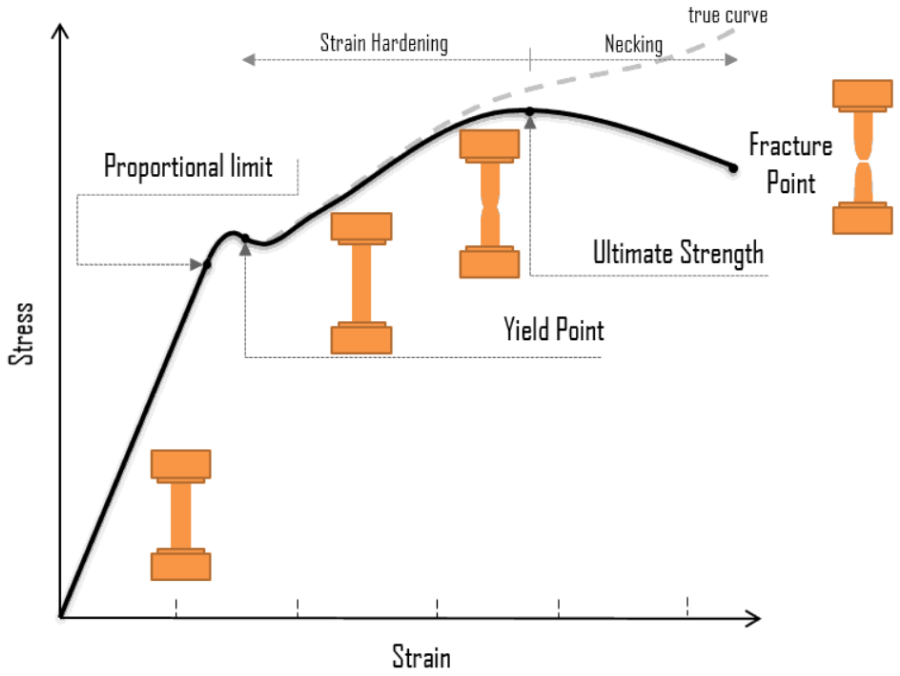

Fig.9. Comparison of true and engineering stress-strain curve

4.2 Tension Test

The tension test is performed by using Ansys 19.2 by giving values to certain parameters. Here the clad ratio is a varying parameter while other parameters like displacement, strain rate, and time are kept constant. The ratio of the cladding layer thickness (tc) to the total thickness of Titanium-Clad bimetallic steel plate (t) is known as Clad ratio (α). A total of 45 tension coupon specimens having different nominal clad ratios α = 0.00, 0.17, 0.29, 0.50, and 1.00 were designed for the tension test using Solidwork 2020. The test specimens' nomenclature is based on the nominal thickness of substrate metal (tb), the nominal thickness of titanium cladding layer (tc), & a specimen's serial number. For example, TC-5–2-1 represents a Titanium-Clad bimetallic steel tension specimen with a 5 mm-thick substrate metal of AISI 1006 steel & cladding layer of Titanium Grade 5 of thickness 2mm, and the end numerate denotes the first specimen in a group of nine specimens with identical geometric dimensions and material composition but different strain rates and temperatures.

Table.7. Dimensions for specimens with different clad ratios at different temperatures and strain rates.

SPECIMENS	CLAD RATIO(α)	TEMPERATURE (K)	STRAIN RATE (/Sec)	Base metal (AISI 1006 Steel) Thickness(mm)	Clad metal (Titanium grade5) Thickness(mm)
TC-10-0-1	0	293	1	10	0
TC-10-0-2	0	673	1	10	0
TC-10-0-3	0	973	1	10	0
TC-10-0-4	0	293	100	10	0
TC-10-0-5	0	673	100	10	0
TC-10-0-6	0	973	100	10	0
TC-10-0-7	0	293	500	10	0
TC-10-0-8	0	673	500	10	0
TC-10-0-9	0	973	500	10	0
TC-10-2-1	0.17	293	1	10	2
TC-10-2-2	0.17	673	1	10	2
TC-10-2-3	0.17	973	1	10	2
TC-10-2-4	0.17	293	100	10	2

TC-10-2-5	0.17	673	100	10	2
TC-10-2-6	0.17	973	100	10	2
TC-10-2-7	0.17	293	500	10	2
TC-10-2-8	0.17	673	500	10	2
TC-10-2-9	0.17	973	500	10	2
TC-5-2-1	0.29	293	1	5	2
TC-5-2-2	0.29	673	1	5	2
TC-5-2-3	0.29	973	1	5	2
TC-5-2-4	0.29	293	100	5	2
TC-5-2-5	0.29	673	100	5	2
TC-5-2-6	0.29	973	100	5	2
TC-5-2-7	0.29	293	500	5	2
TC-5-2-8	0.29	673	500	5	2
TC-5-2-9	0.29	973	500	5	2
TC-2-2-1	0.50	293	1	2	2
TC-2-2-2	0.50	673	1	2	2
TC-2-2-3	0.50	973	1	2	2
TC-2-2-4	0.50	293	100	2	2
TC-2-2-5	0.50	673	100	2	2
TC-2-2-6	0.50	973	100	2	2
TC-2-2-7	0.50	293	500	2	2
TC-2-2-8	0.50	673	500	2	2

TC-2-2-9	0.50	973	500	2	2
TC-0-2-1	1.00	293	1	0	2
TC-0-2-2	1.00	673	1	0	2
TC-0-2-3	1.00	973	1	0	2
TC-0-2-4	1.00	293	100	0	2
TC-0-2-5	1.00	673	100	0	2
TC-0-2-6	1.00	973	100	0	2
TC-0-2-7	1.00	293	500	0	2
TC-0-2-8	1.00	673	500	0	2
TC-0-2-9	1.00	973	500	0	2

CHAPTER -5

MODELLING AND ANALYSIS

5.1 Modeling

To design a tensile test specimen of TC bimetallic steel GB/T228.1–2010 testing standard was used as a reference document to set down the dimensions of the specimen. The CAD geometry for the specimen was developed using Solidworks 2020. The dimensions shown in fig.9 are in mm. The different thickness of the AISI 1006 and Titanium Grade 5 part of the specimen was taken as given in table.8.

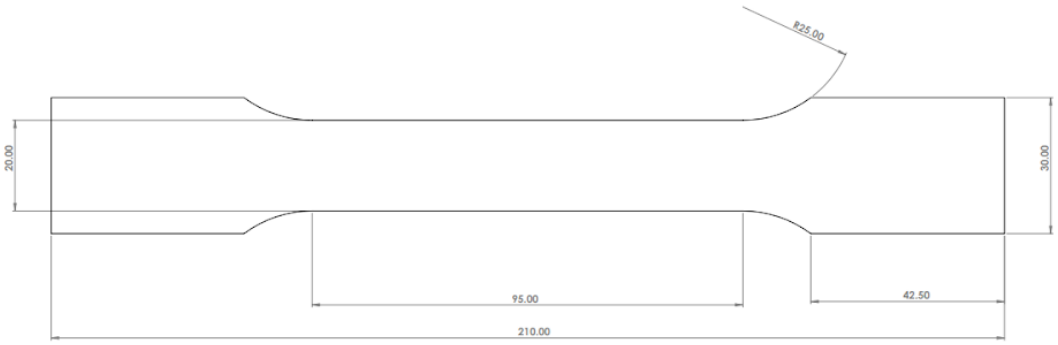

Fig.10. Dimensions of Tensile Test Specimen

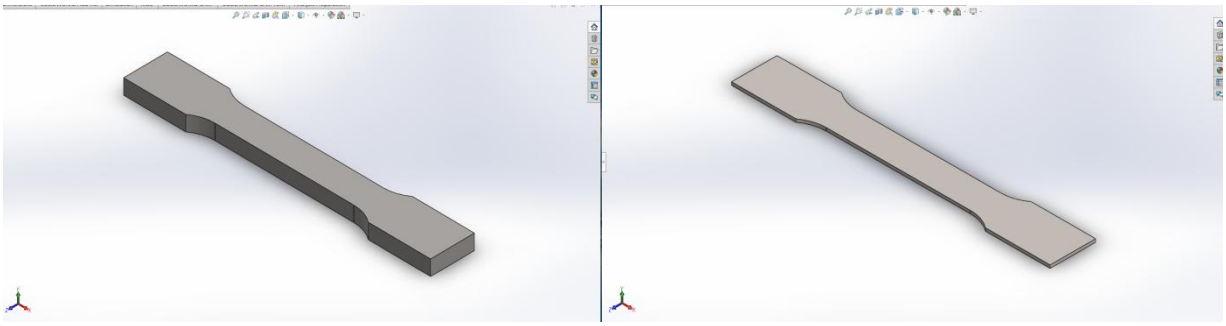

(a) (b)

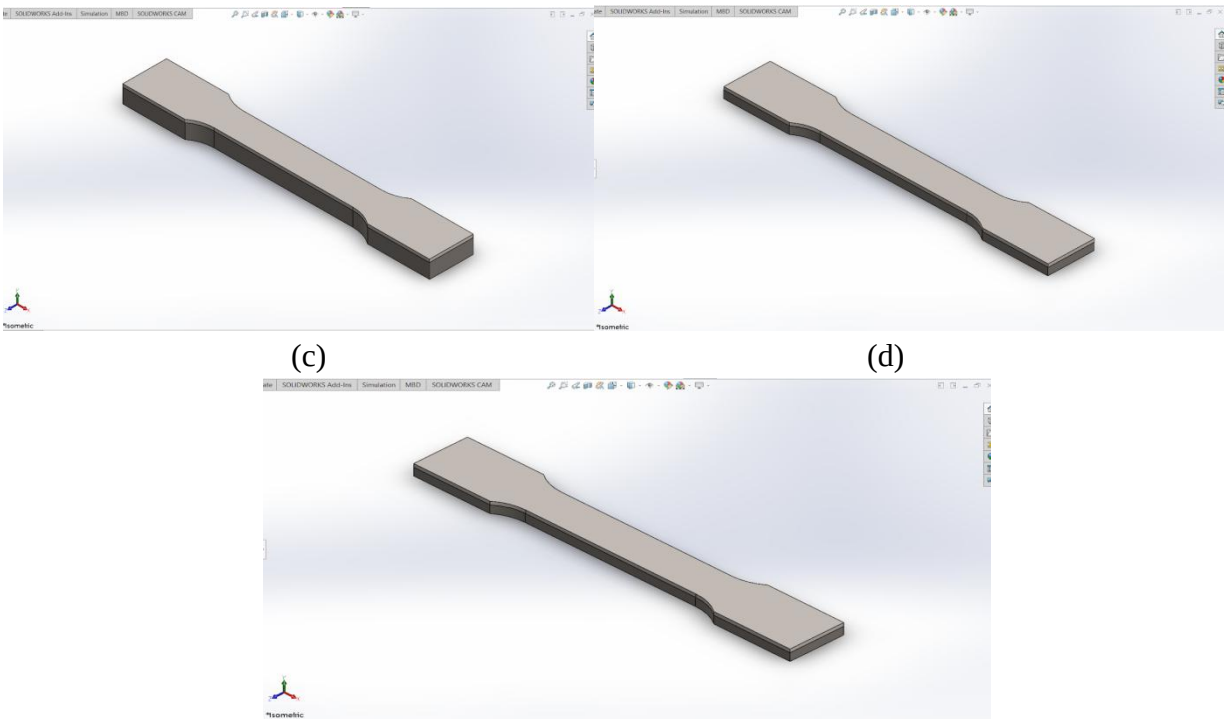

(c) (d)

(e)

Fig.11. CAD model of Tensile Specimens (a)Clad Ratio-0, (b) Clad Ratio-1,(c)Clad Ratio-0.17,(d) Clad Ratio-0.29, (e) Clad Ratio-0.5

5.2 Analysis

5.2.1 Johnson-Cook Model -

The Johnson-Cook model is used to define the metallic material relationship between stress and strain under the conditions of high strain rate, high temperature, and large deformation.
The flow stress model is expressed as :

$$\sigma = (A + B\varepsilon^{n})(1 + C \ln\acute{\varepsilon}^{*})(1 - T^{*}) \text{.....(1)}$$

where **σ** - Equivalent Stress,
ε - Equivalent Plastic Strain.
A- Yield Stress of material under reference conditions
B- Strain Hardening Constant
n- Strain Hardening Coefficient
C- Strengthening Coefficient Of Strain Rate
m-Thermal Softening Coefficient
έ*- Dimensionless strain rate
T*- homologous temperature
In this flow stress model,

ε̇*= ε̇/ ε̇ref

T* = (T − Tref)/ (Tm − Tref) ,

where

Tm - Melting temperature of the material

T- Deformation temperature

ε̇ref and **Tref** are the reference strain rate and the reference deformation temperature, respectively.

In this report, the reference strain rate, ε̇ref, and the reference temperature, Tref, were taken as 1 s−1and 293 K, respectively.

To calculate the material constant for different clad ratios, take the material constant for titanium grade 5 and AISI 1006 as a reference.

Table.8 J-C constants for hot-rolled Titanium Grade 5 Plate[38]

A (MPa)	B(MPa)	n	C	M
874	583	0.316	0.003	0.95

Table.9. J-C constants for hot-rolled AISI 1006 Steel [39]

A (MPa)	B(MPa)	n	C	M
350	275	0.36	0.022	1

5.2.2 Procedure and parameters used for analysis-

For an illustration of the effect of clad ratio on the stress-strain curves yield stress, ultimate stress, and modulus of elasticity is analyzed for different clad ratios using Ansys 19.2 software by giving values shown in the table for parameters like strain rate, displacement, and time. The effects of geometric imperfection & residual stresses were not considered. Plastic formulation with von Mises' yield function, associated isotropic hardening, and plastic flow is commonly used for simulating the static material behavior of metal in 3D Finite element models & is employed in Ansys 19 was applied to analyze both AISI 1006 steel & Titanium Grade 5 materials. The Three Dimensional Model of the specimens are imported in ANSYS 19.2 and discretized into a finite number of elements. This process is commonly known as meshing. The purpose of meshing is to reduce the effort and the amount of time to get accurate results. A fine meshing of the specimen was chosen using 6845 elements and 8988 nodes.

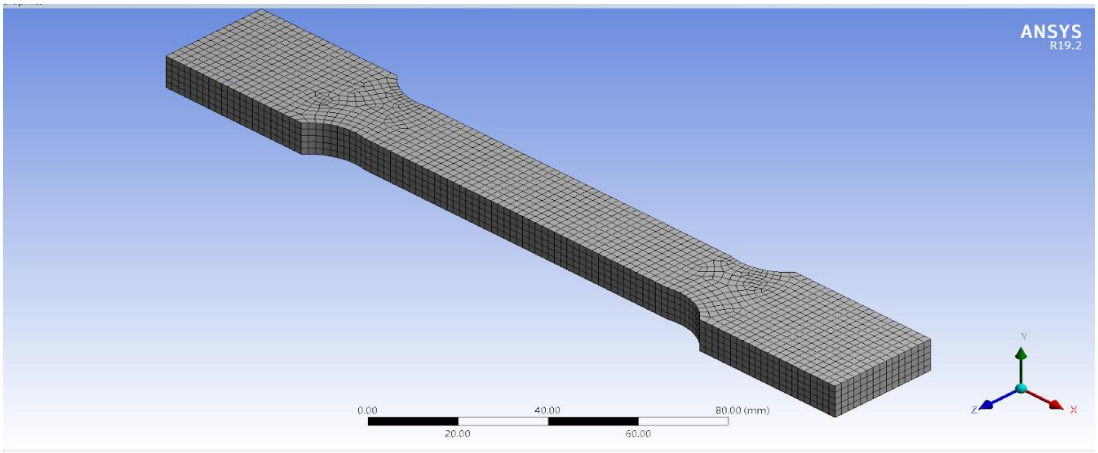

Fig.12. The meshing of Tensile Specimen of AISI 1006 Steel

After mesh, the required constraints are fixed on the specimens in the term of boundary conditions. For a component in ANSYS, there are 6 Degrees of Freedom. In this tensile test, the fixed support is used to restrict the movement of one end of the specimen as shown in Fig. 4 (a). Besides, an axial velocity in the positive X-axis is applied to the other end of the specimen as per Fig. 4 (b).

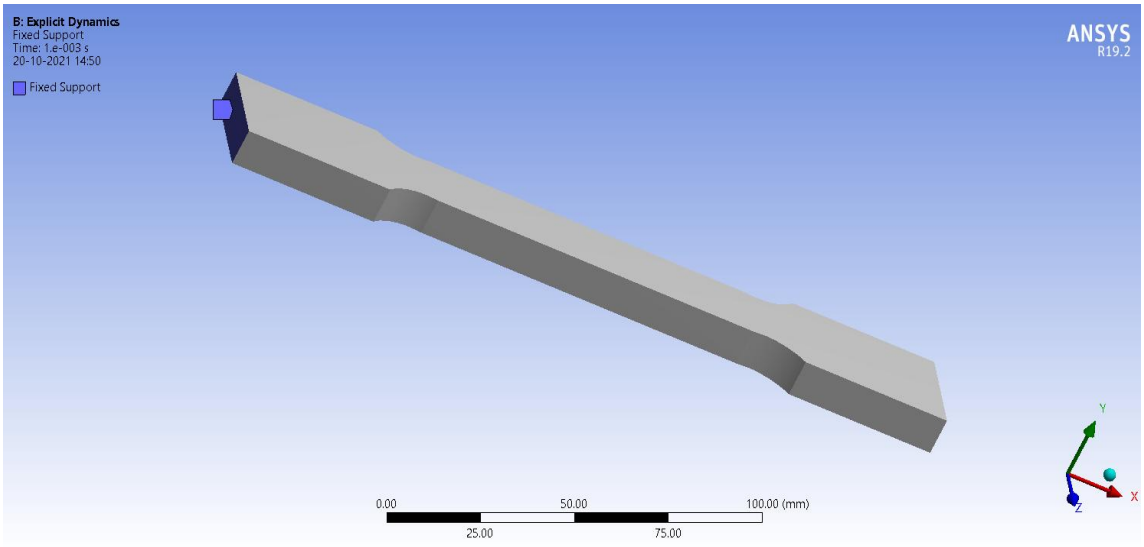

Fig.13. Boundary condition of tensile specimen

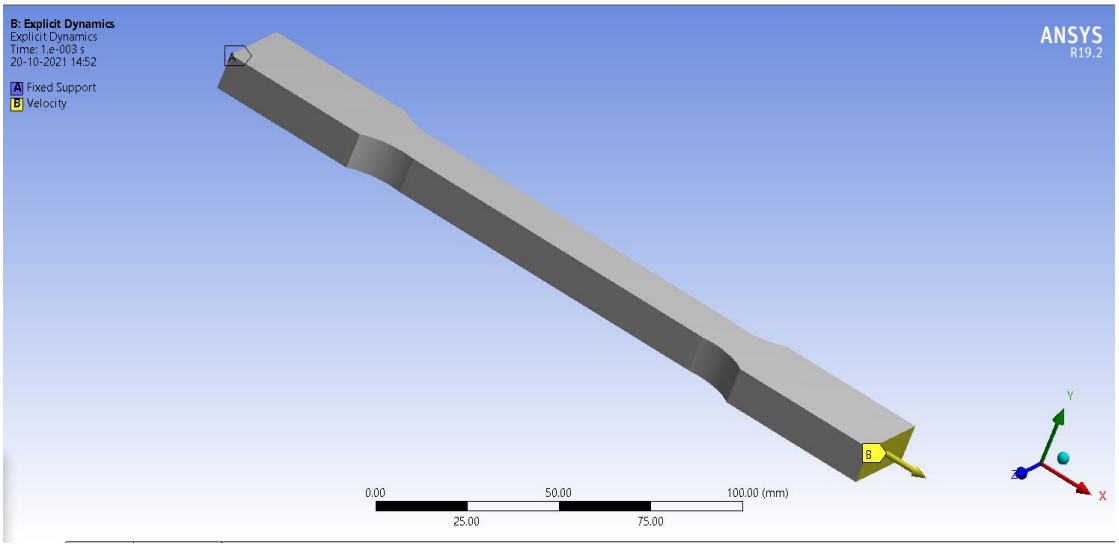

Fig.14. Applying Velocity in positive X-axis of tensile specimen

Table.10. Parameters required for analysis

Parameters	**Value**
Strain rate	1/sec, 10/sec and 100/sec
Temperature	293K, 673K and 973K
Velocity	For different Strain rates ● 1/sec- 95mm/sec ● 10/sec-950mm/sec ● 100/sec-9500mm/sec
Reference strain rate	1/sec
Reference Temperature	293K

5.2.3 Equivalent (von mises) stress and equivalent plastic strain along with true stress-true strain curves of specimens using Ansys 19.2.

Specimen-TC-10-0-1

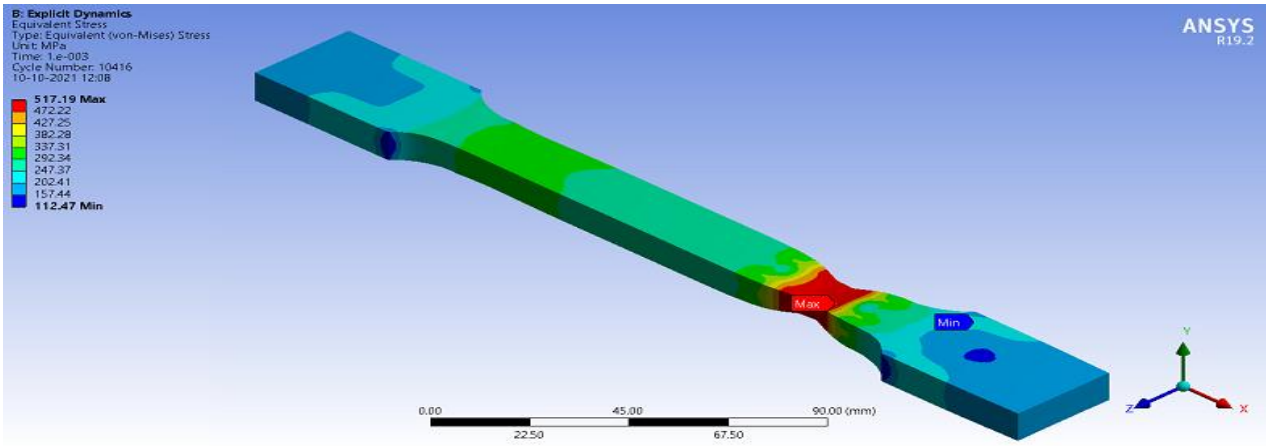

Fig.15. Equivalent(Von-Mises) Stress of Specimen TC-10-0-1

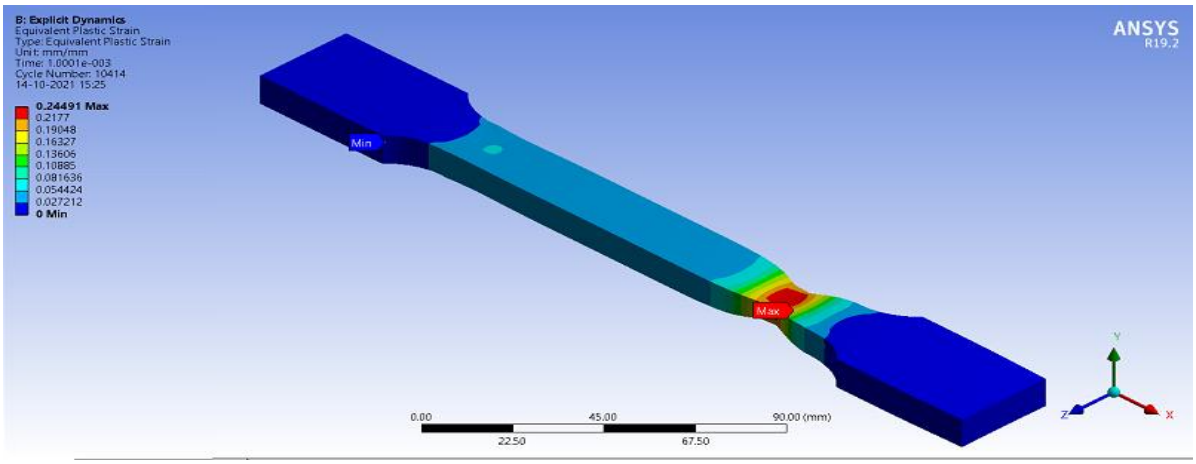

Fig.16. Equivalent Plastic Strain of Specimen TC-10-0-1

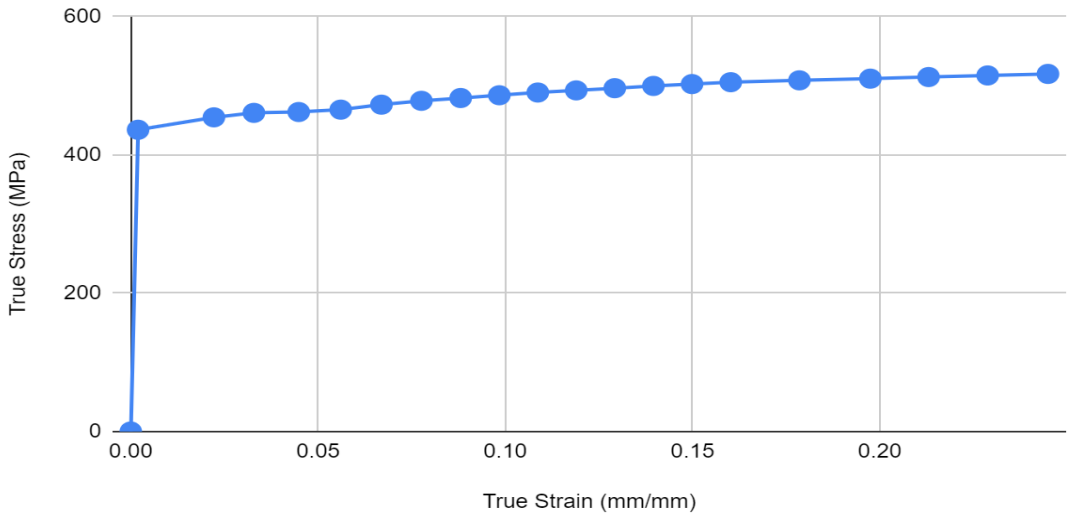

Graph.1. True Stress-True Strain curve of Specimen TC-10-0-1

Specimen -TC-10-0-2

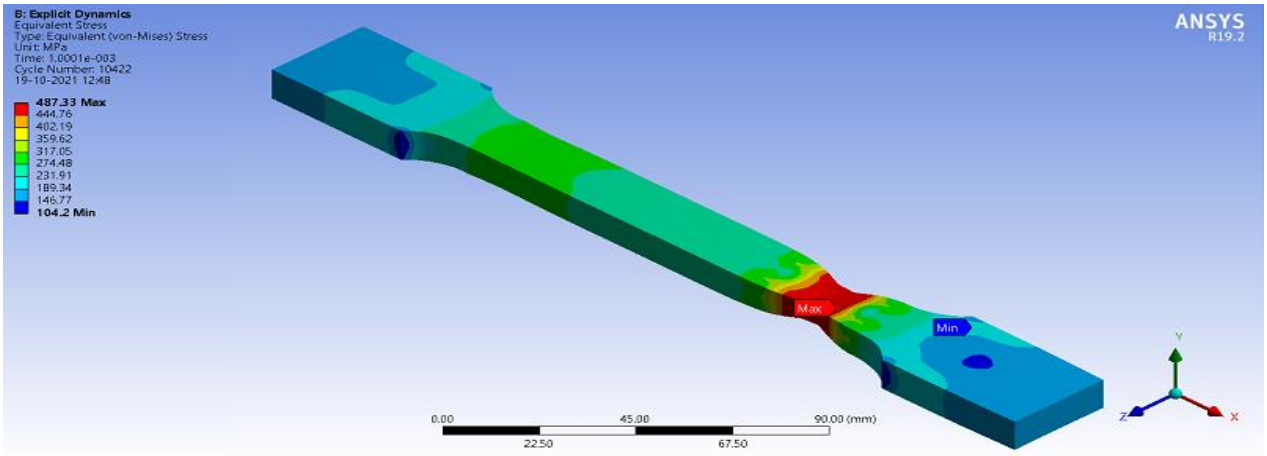

Fig.17. Equivalent(Von-Mises) Stress of Specimen TC-10-0-2

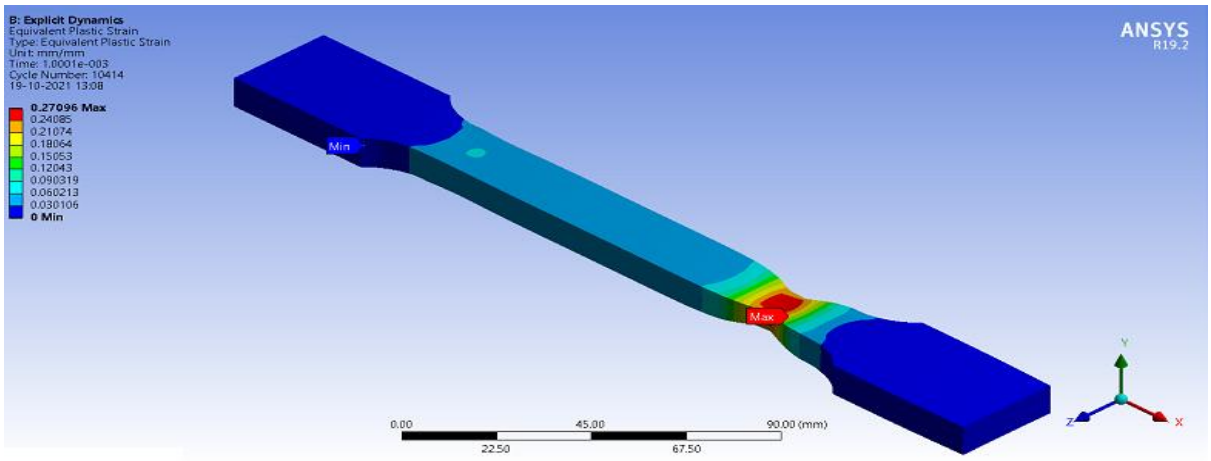

Fig.18. Equivalent Plastic Strain of Specimen TC-10-0-2

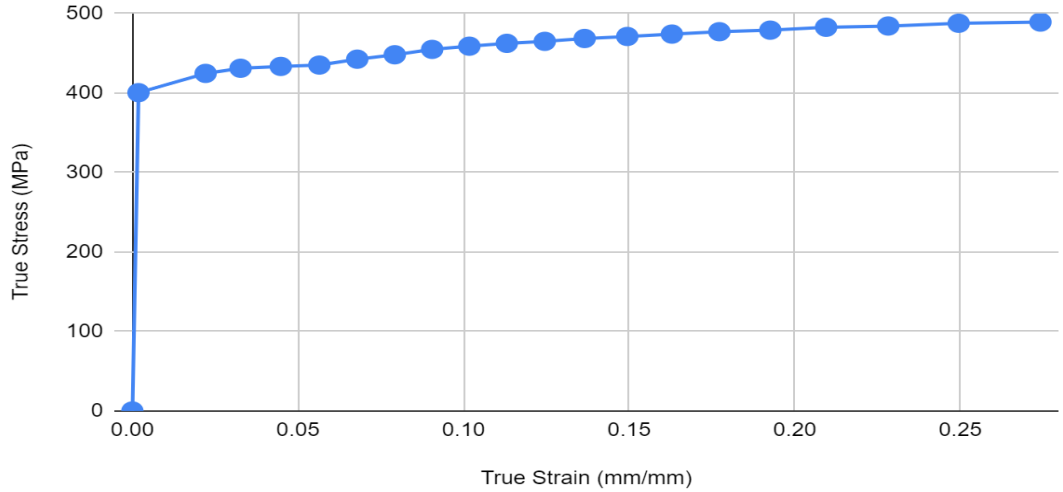

Graph.2. True Stress-True Strain curve of Specimen TC-10-0-2

Specimen-TC-10-0-3

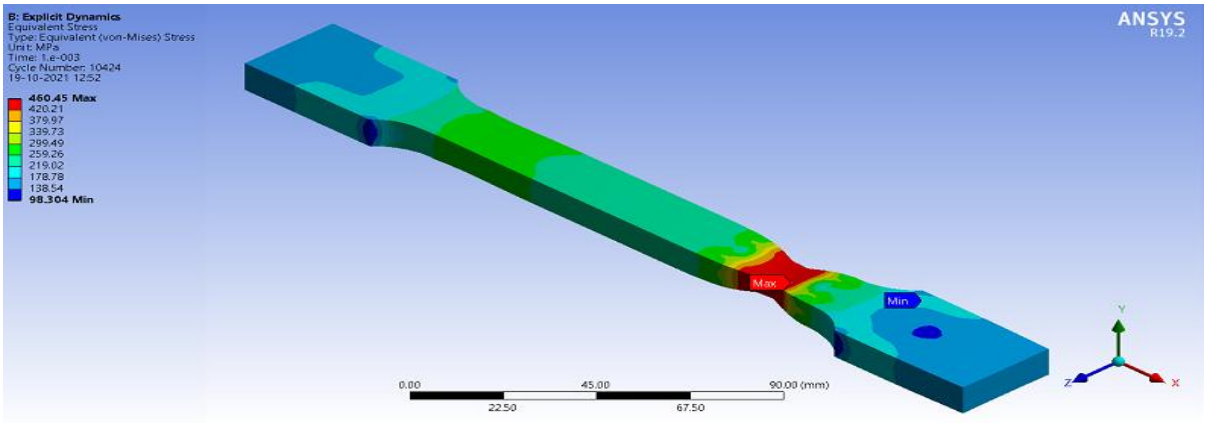

Fig.19. Equivalent(Von-Mises) Stress of Specimen TC-10-0-3

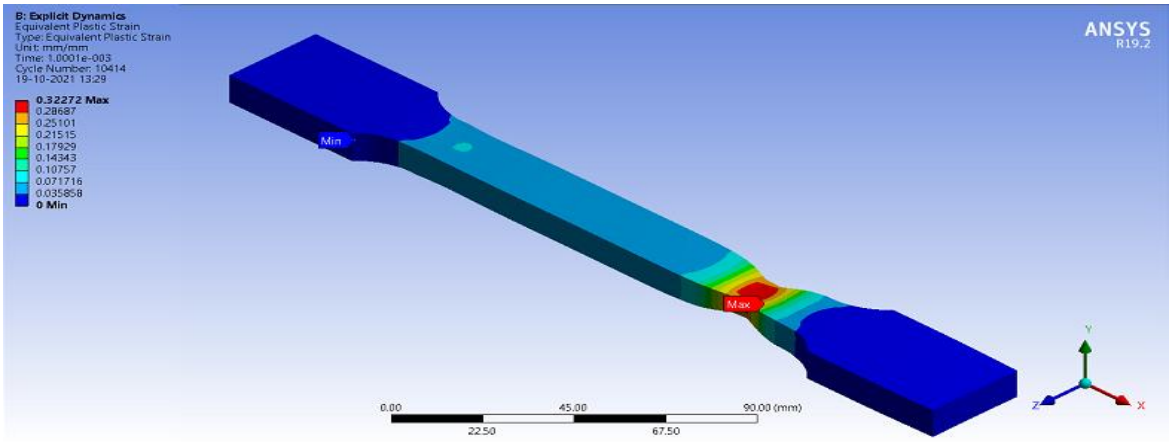

Fig.20. Equivalent Plastic Strain of Specimen TC-10-0-3

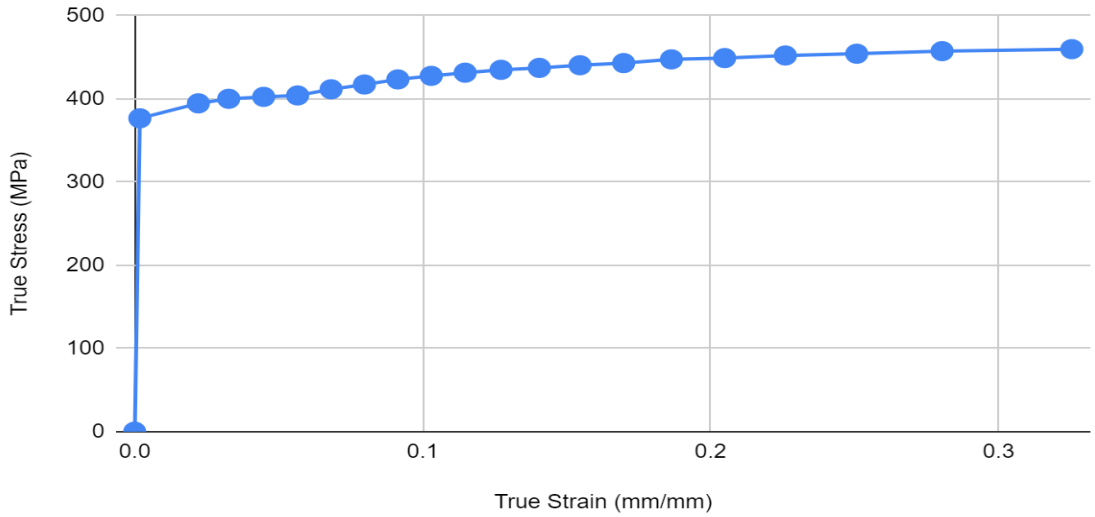

Graph.3. True Stress-True Strain curve of Specimen TC-10-0-3

Specimen -TC-10-0-4

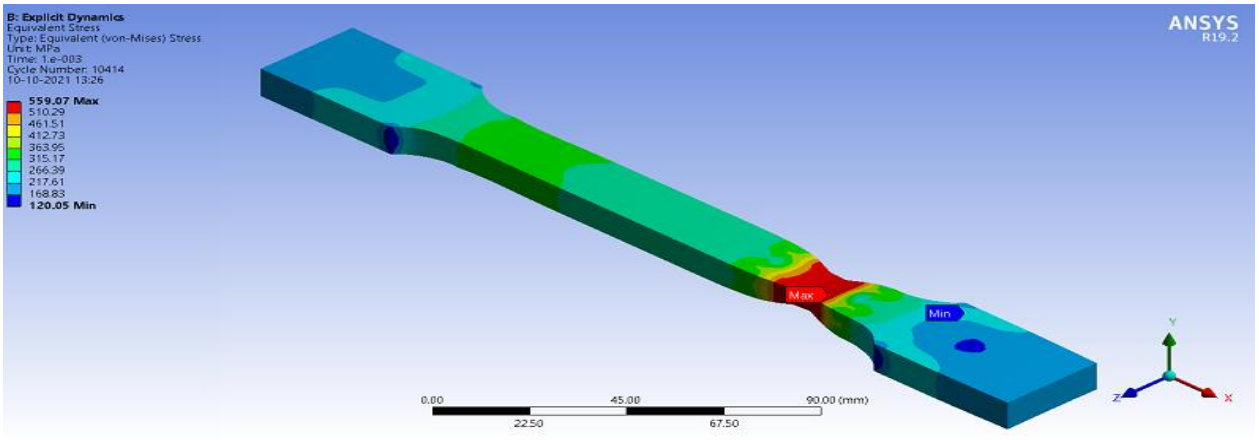

Fig.21. Equivalent(Von-Mises) Stress of Specimen TC-10-0-4

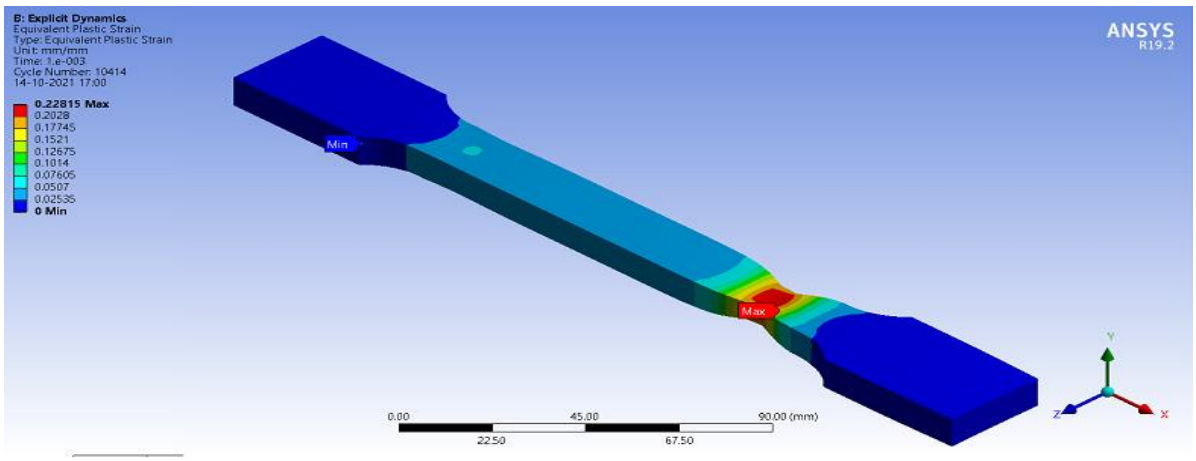

Fig.22. Equivalent Plastic Strain of Specimen TC-10-0-4

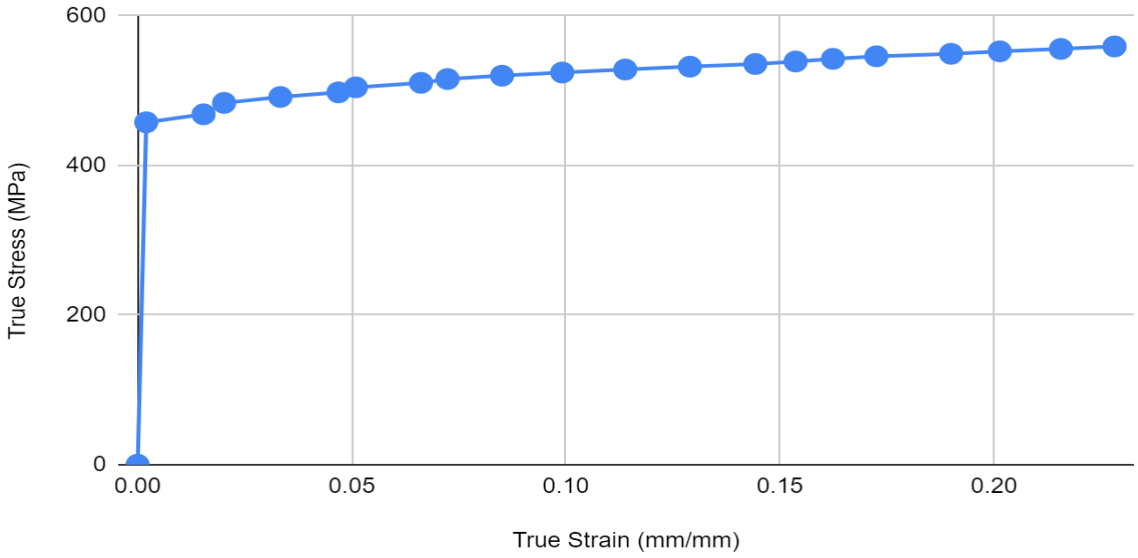

Graph.4. True Stress-True Strain curve of Specimen TC-10-0-4

Specimen -TC-10-0-5

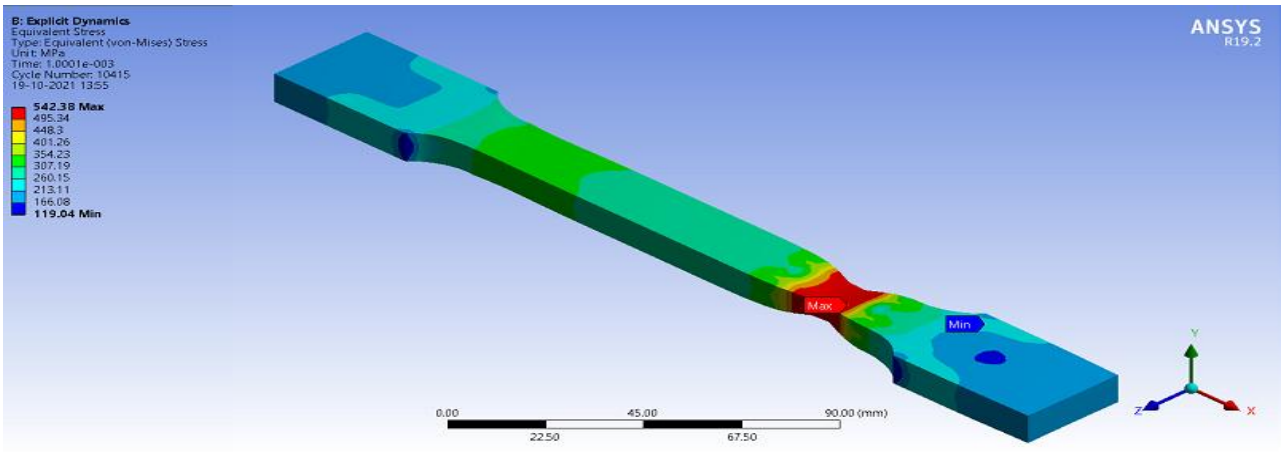

Fig.23. Equivalent(Von-Mises) Stress of Specimen TC-10-0-5

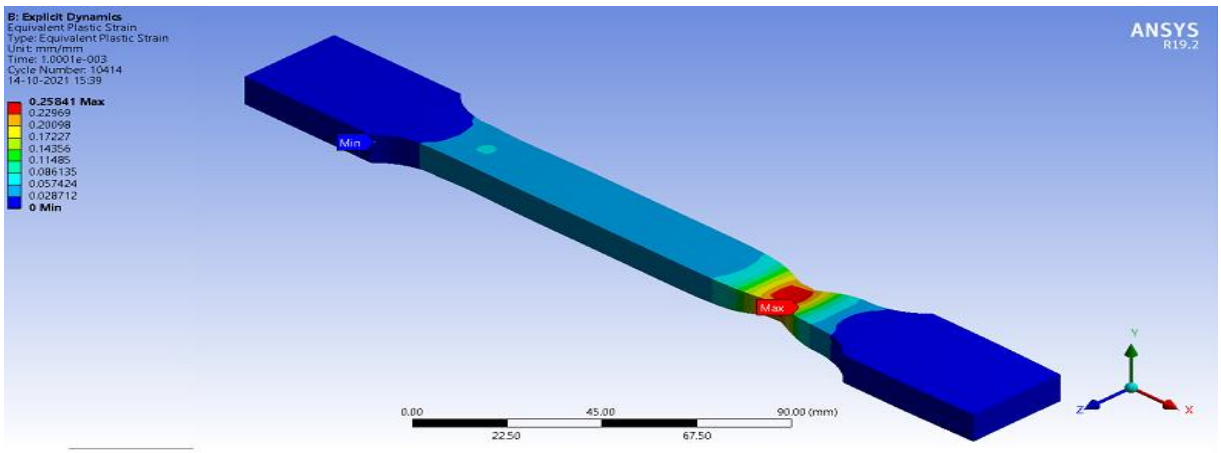

Fig.24. Equivalent Plastic Strain of Specimen TC-10-0-5

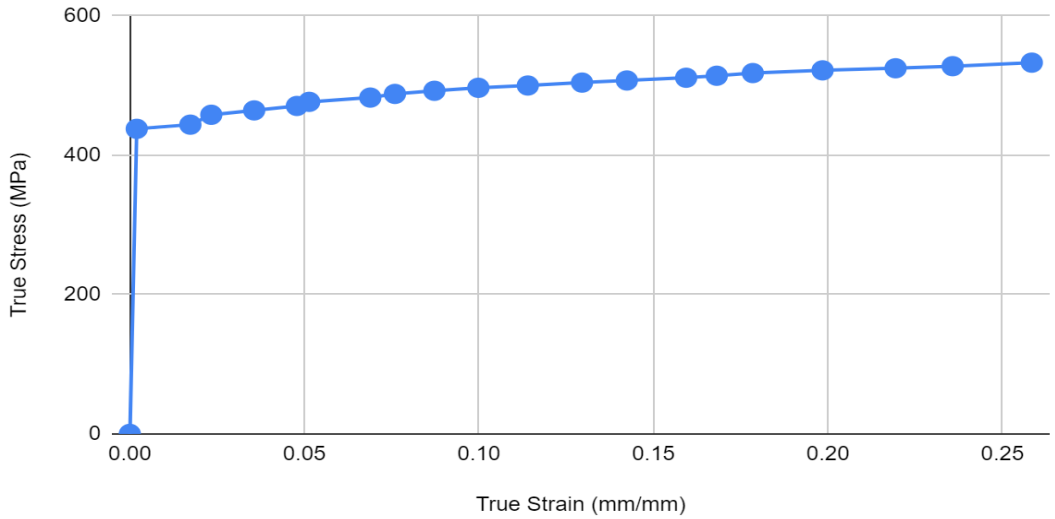

Graph.5. True Stress-True Strain curve of Specimen TC-10-0-5

Specimen -TC-10-0-6

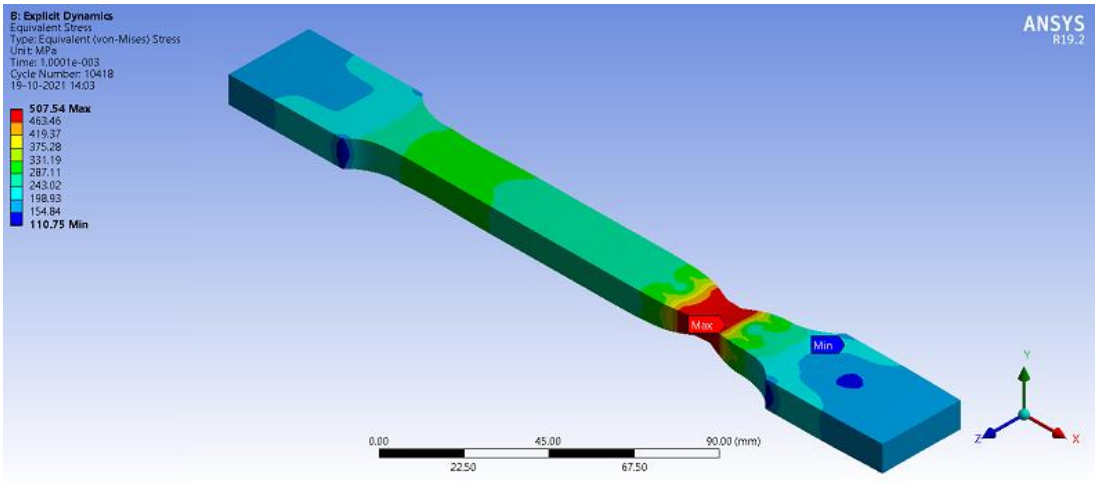

Fig.25. Equivalent(Von-Mises) Stress of Specimen TC-10-0-6

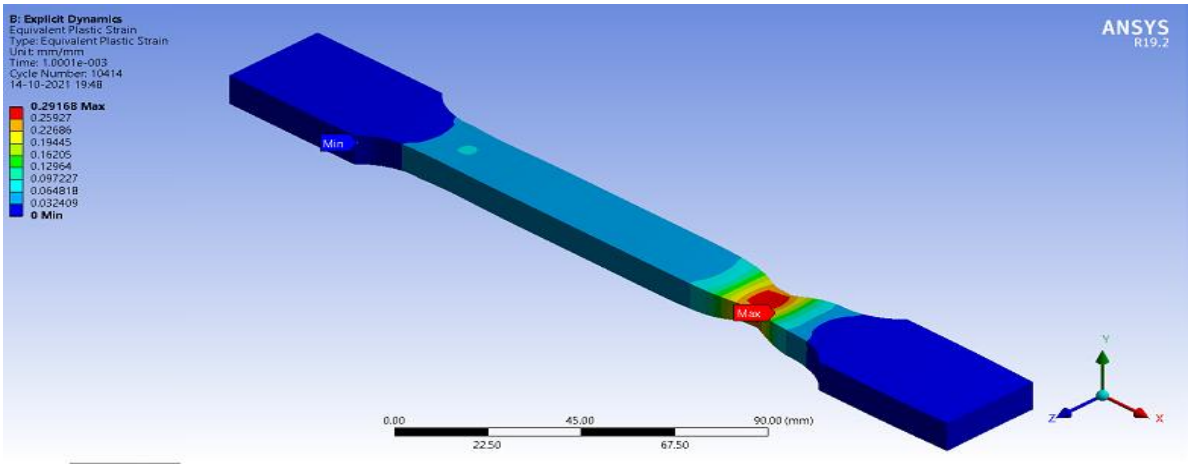

Fig.26. Equivalent Plastic Strain of Specimen TC-10-0-6

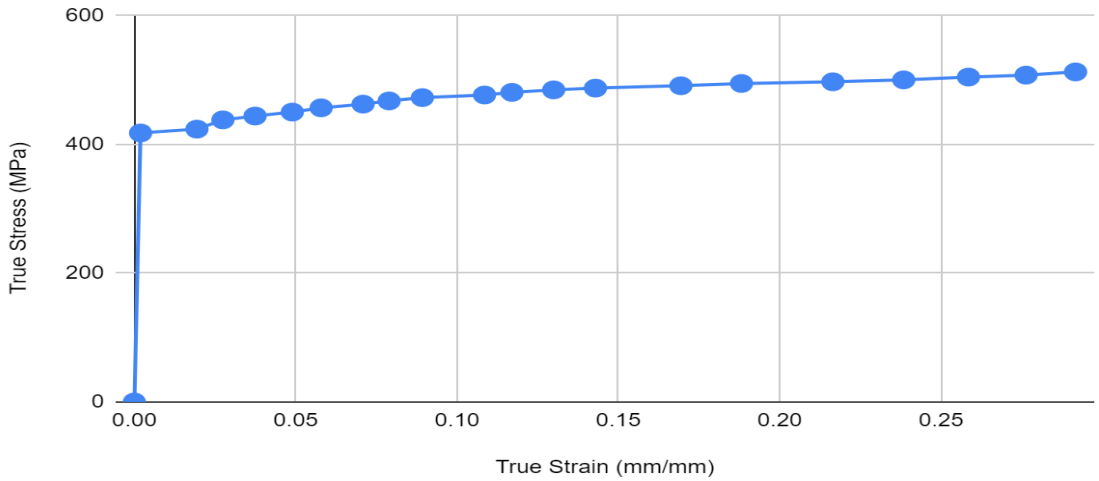

Graph.6. True Stress-True Strain curve of Specimen TC-10-0-6

Specimen -TC-10-0-7

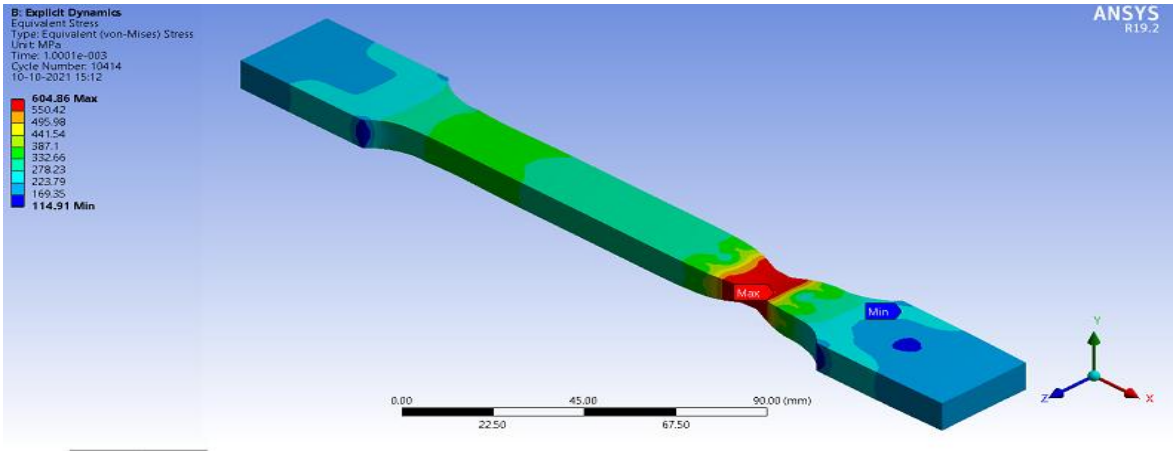

Fig.27. Equivalent(Von-Mises) Stress of Specimen TC-10-0-7

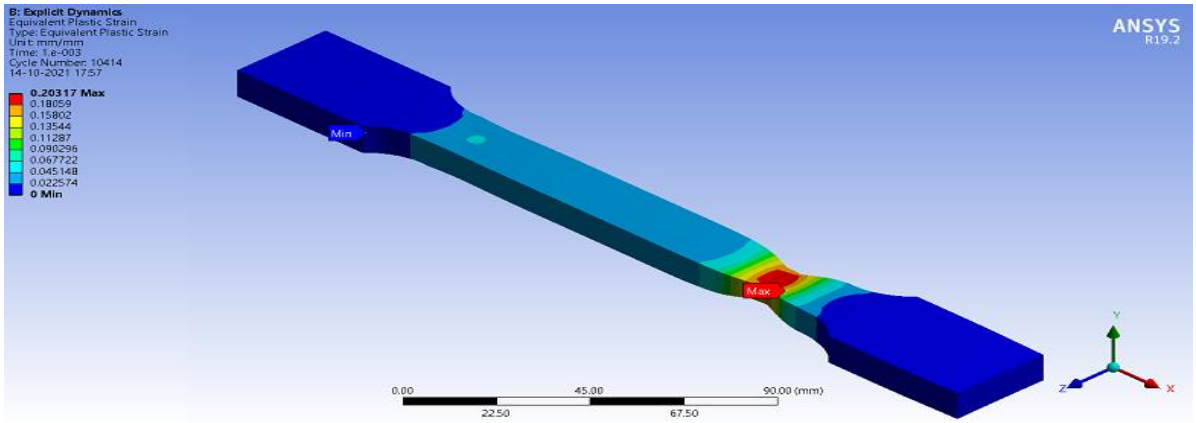

Fig.28. Equivalent Plastic Strain of Specimen TC-10-0-7

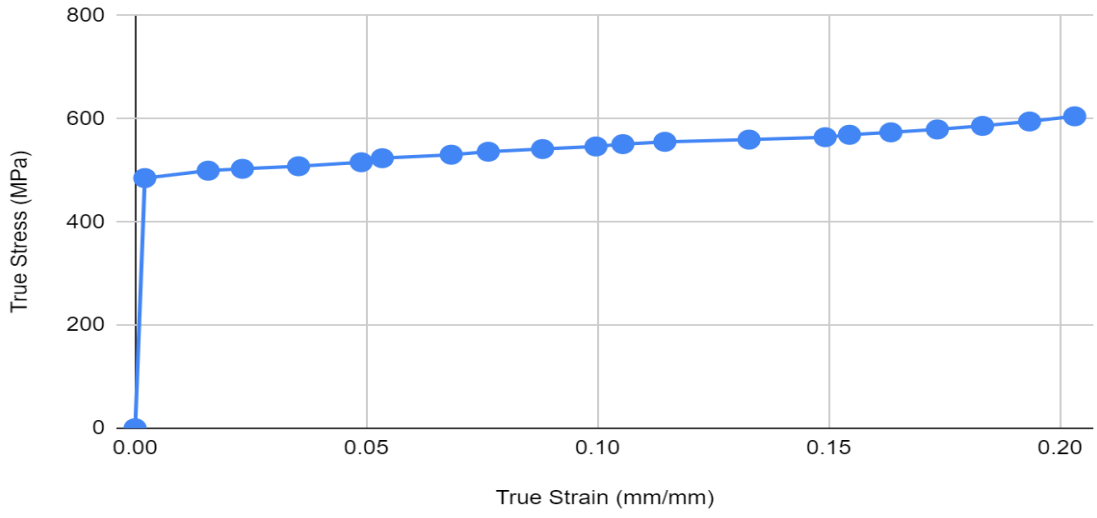

Graph.8. True Stress-True Strain curve of SpecimenTC-10-0-7

Specimen TC-10-0-8

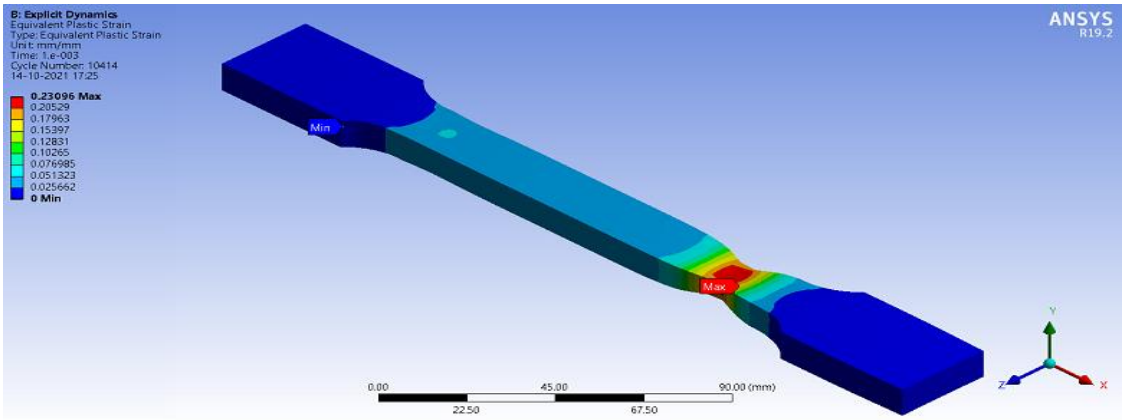

Fig.29. Equivalent(Von-Mises) Stress of Specimen TC-10-0-8

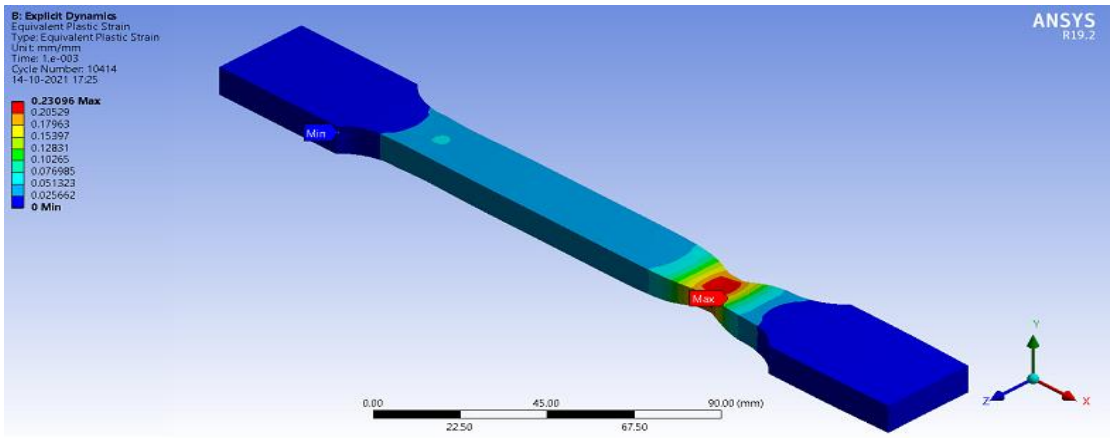

Fig.30. Equivalent Plastic Strain of Specimen TC-10-0-8

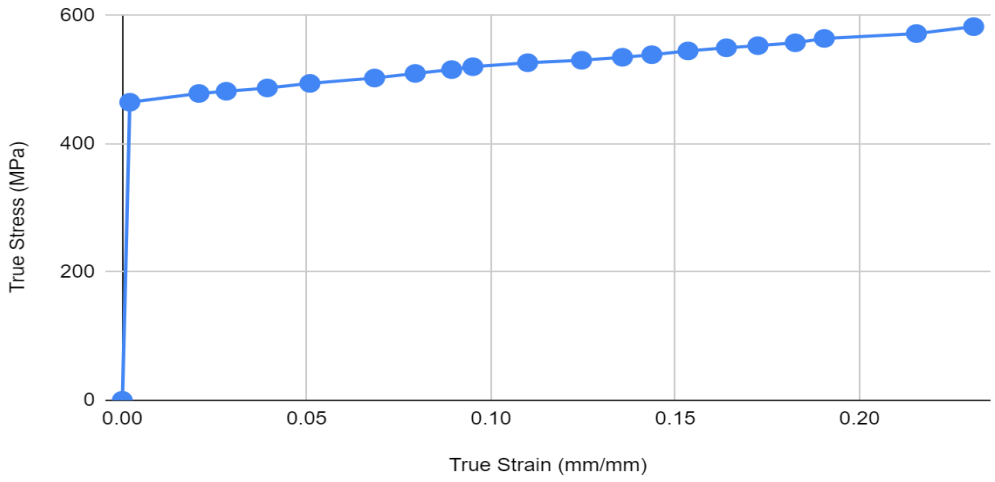

Graph.8. True Stress-True Strain curve of Specimen TC-10-0-8

Specimen TC-10-0-9

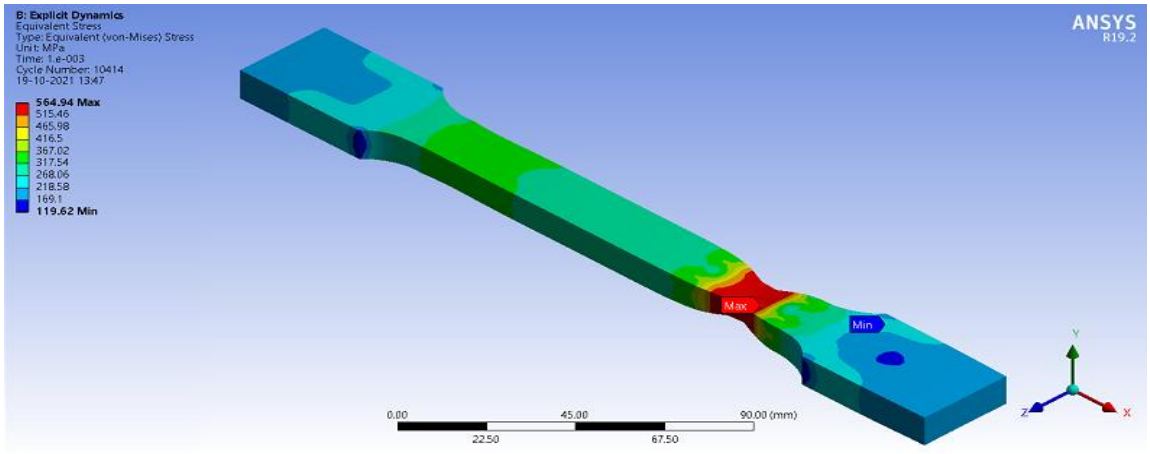

Fig.31. Equivalent(Von-Mises) Stress of specimen TC-10-0-9

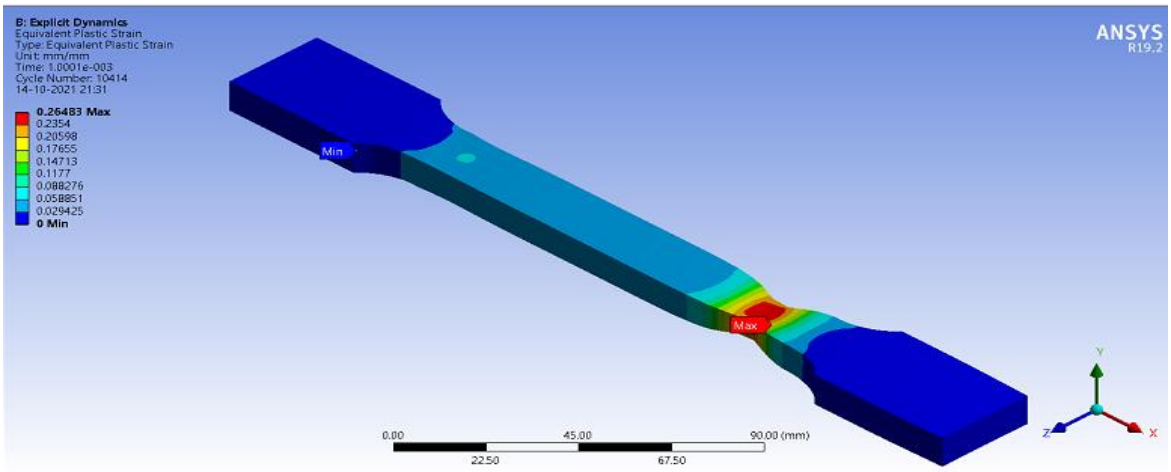

Fig.32. Equivalent Plastic Strain of Specimen TC-10-0-9

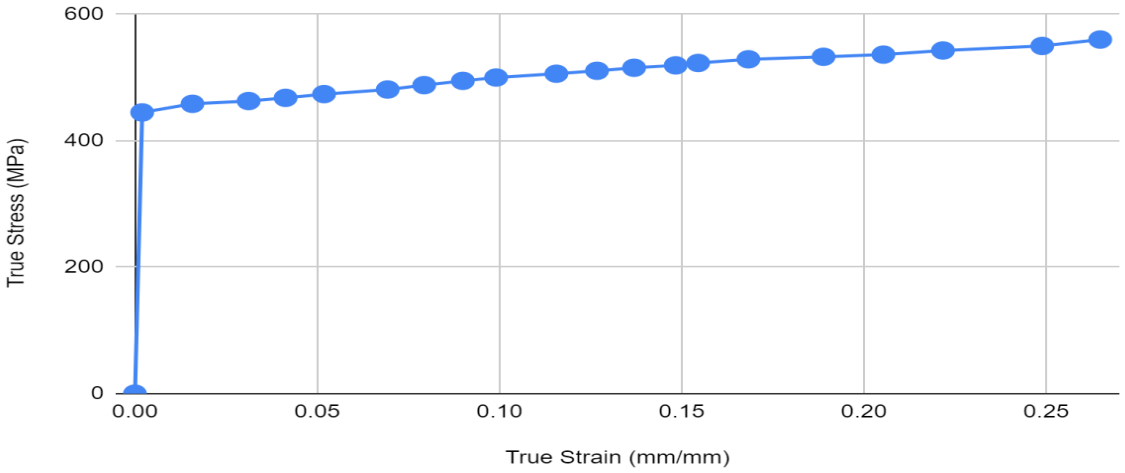

Graph.9. True Stress-True Strain curve of Specimen TC-10-0-9

Specimen TC-10-2-1

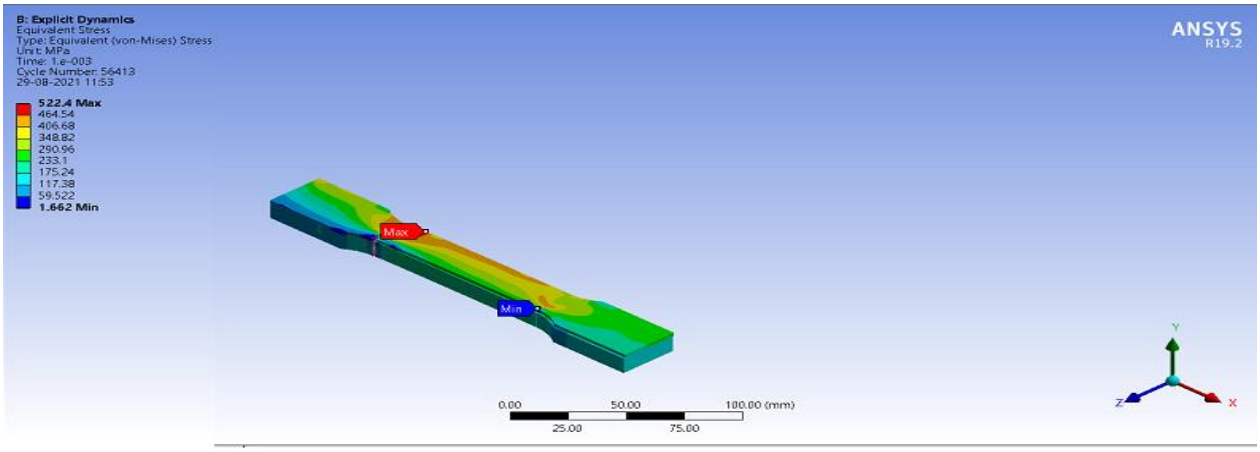

Fig.33. Equivalent(Von-Mises) Stress of Specimen TC-10-2-1

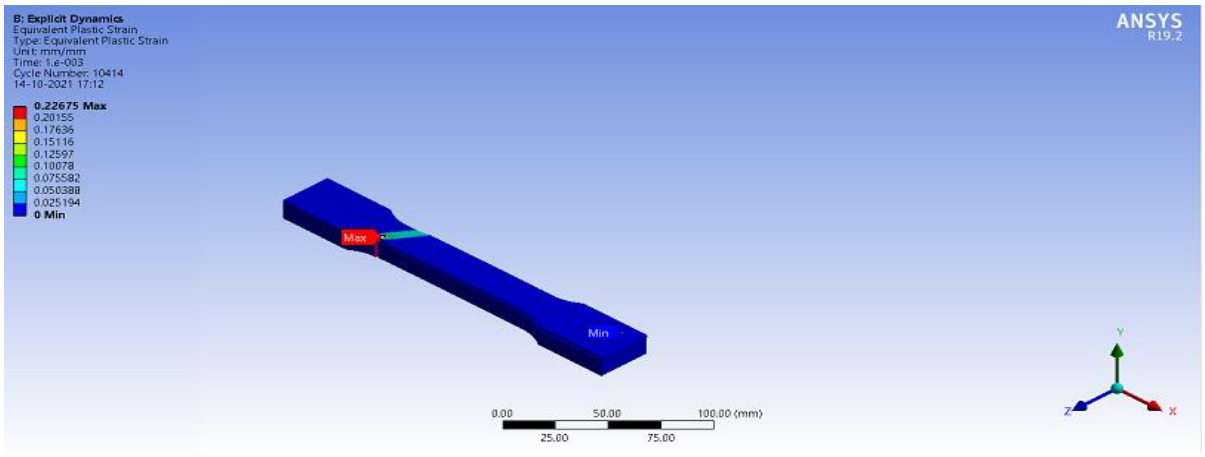

Fig.34. Equivalent Plastic Strain of Specimen TC-10-2-1

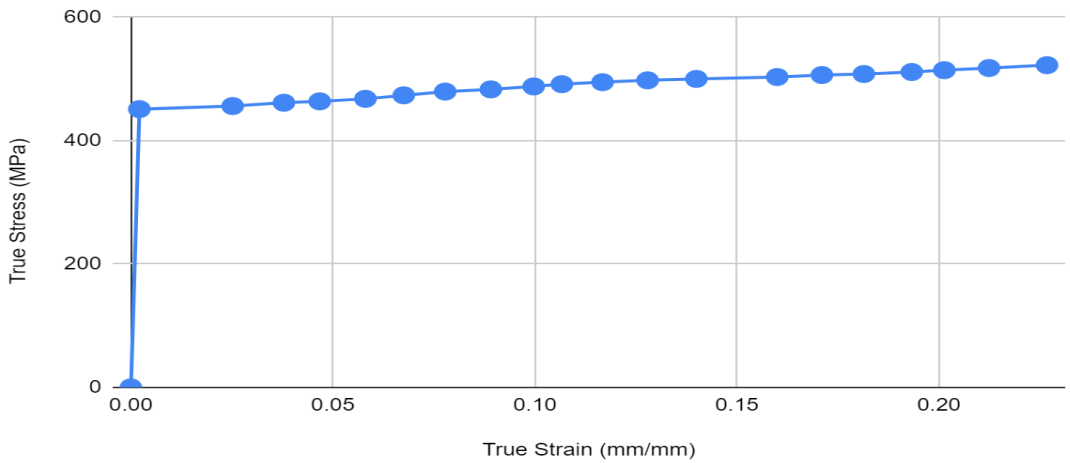

Graph.10. True Stress-True Strain curve of Specimen TC-10-2-1

Specimen TC-10-2-2

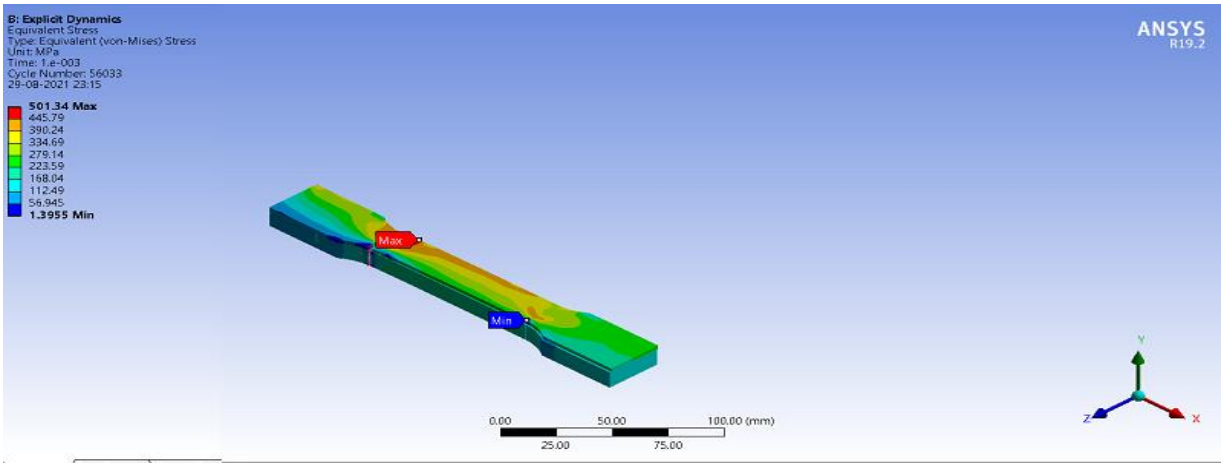

Fig.35. Equivalent(Von-Mises) Stress of Specimen TC-10-2-2

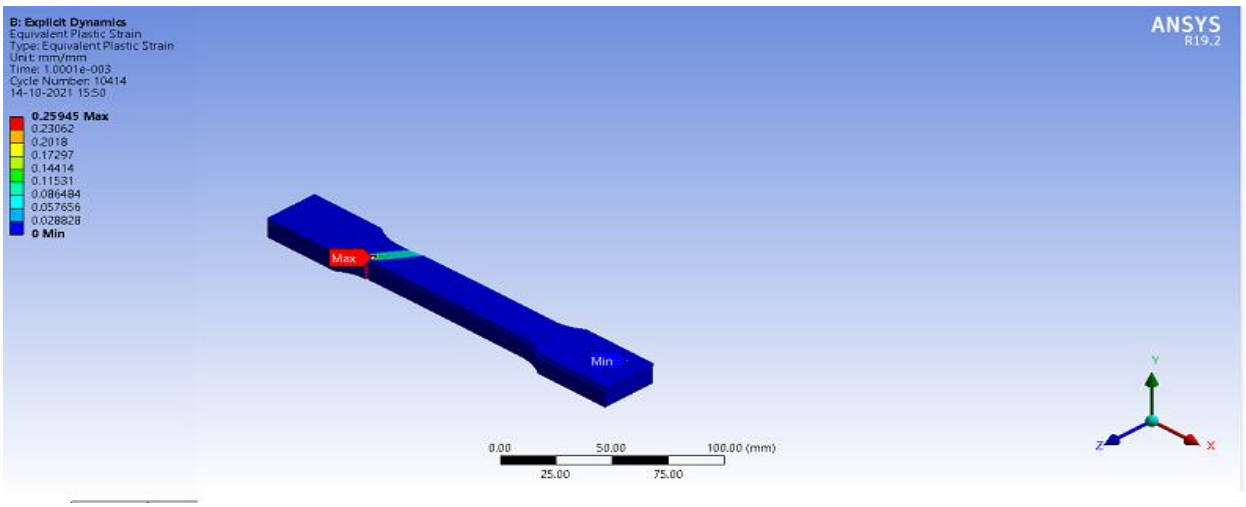

Fig.36. Equivalent Plastic Strain of Specimen TC-10-2-2

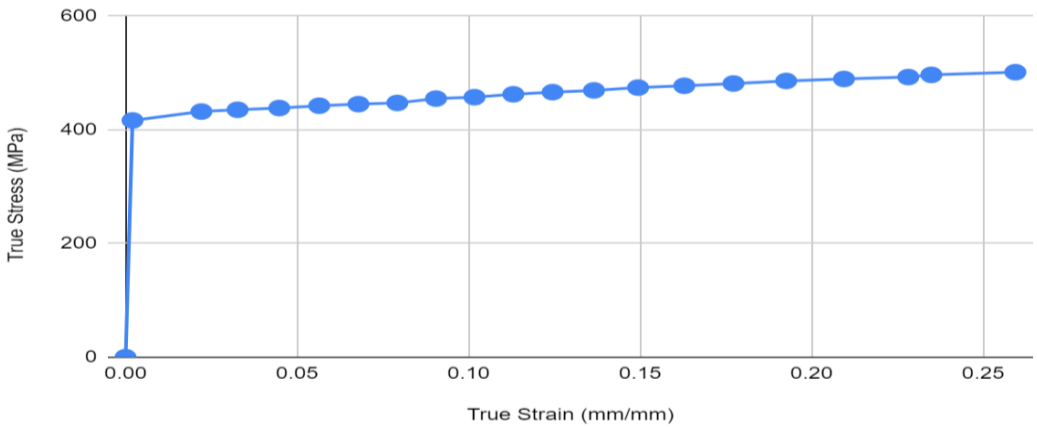

Graph.11. True Stress-True Strain curve of Specimen TC-10-2-2

Specimen TC-10-2-3

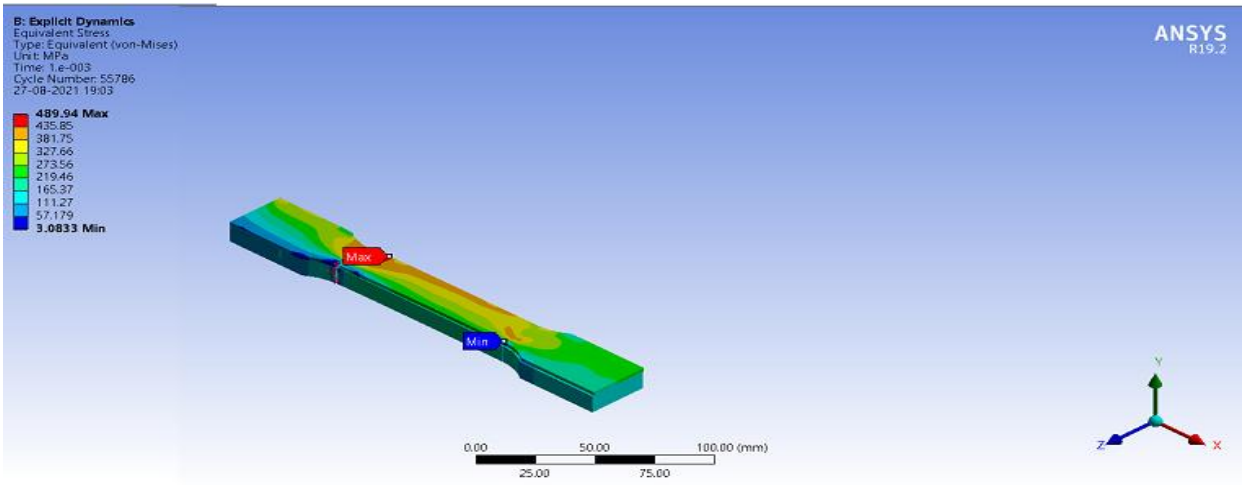

Fig.37. Equivalent(Von-Mises) Stress of Specimen TC-10-2-3

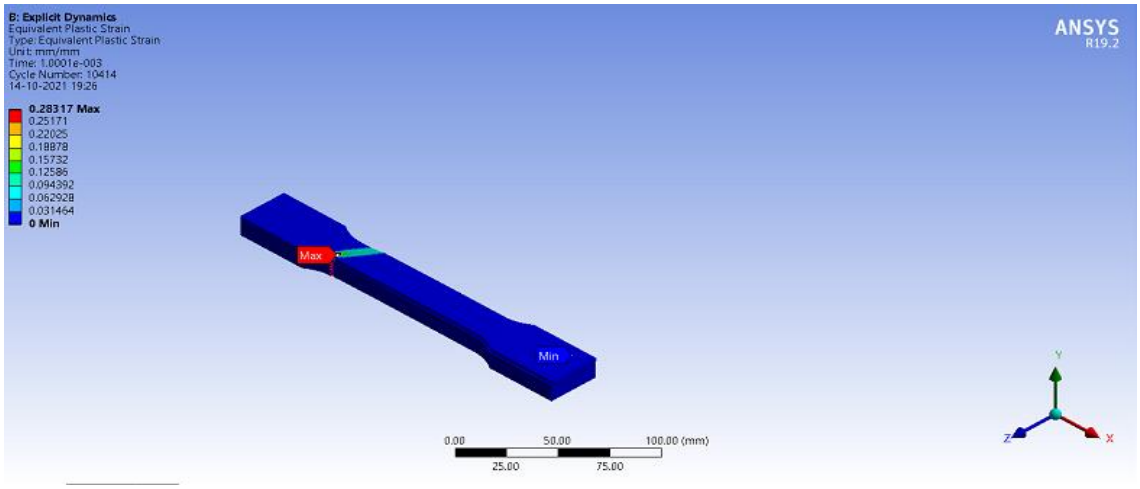

Fig.38. Equivalent Plastic Strain of Specimen TC-10-2-3

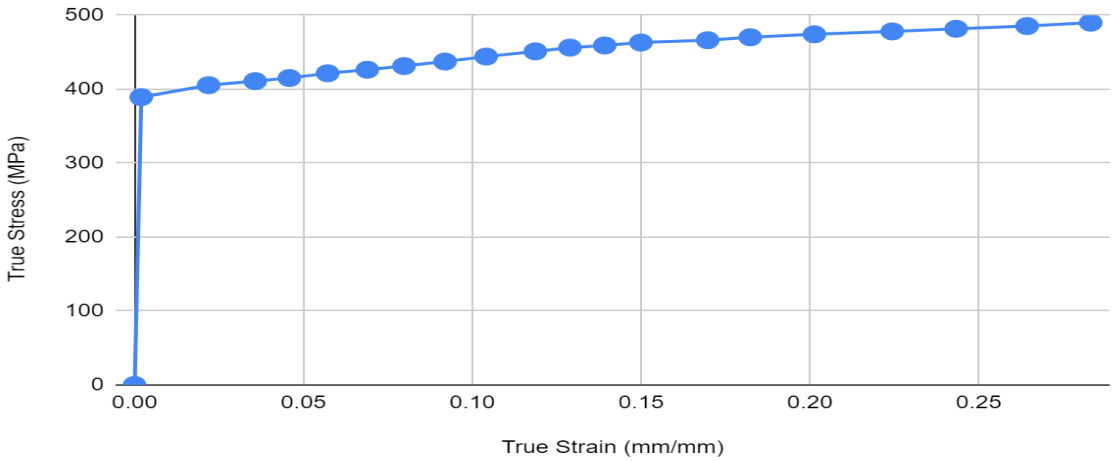

Graph.12. True Stress-True Strain curve of Specimen TC-10-2-3

Specimen TC-10-2-4

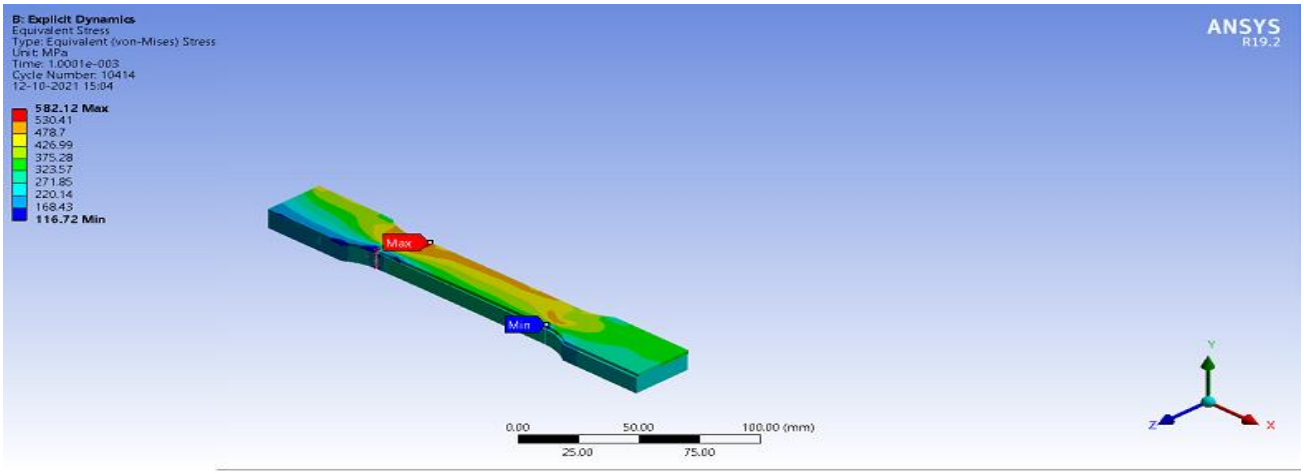

Fig.39. Equivalent(Von-Mises) Stress of Specimen TC-10-2-4

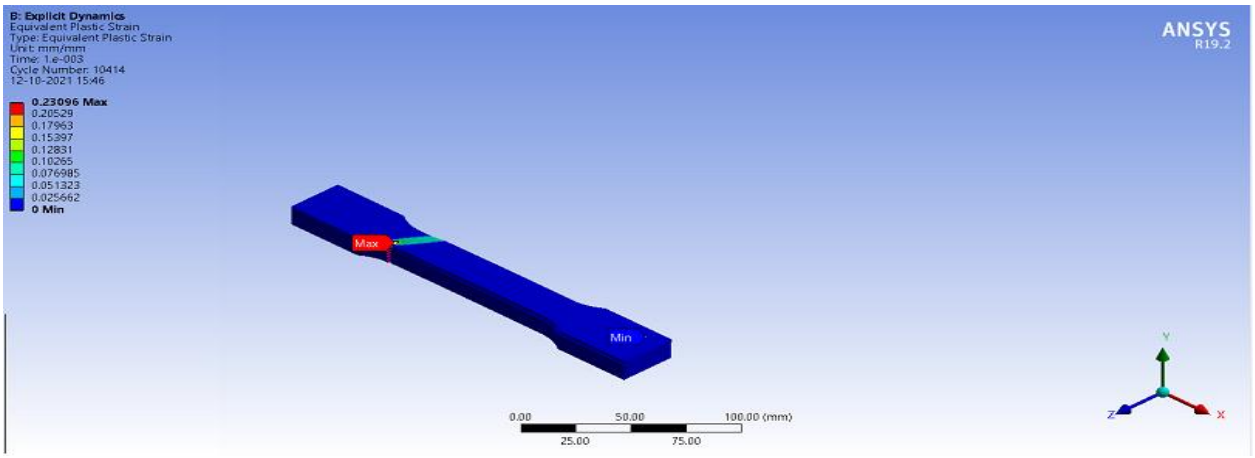

Fig.40. Equivalent Plastic Strain of Specimen TC-10-2-4

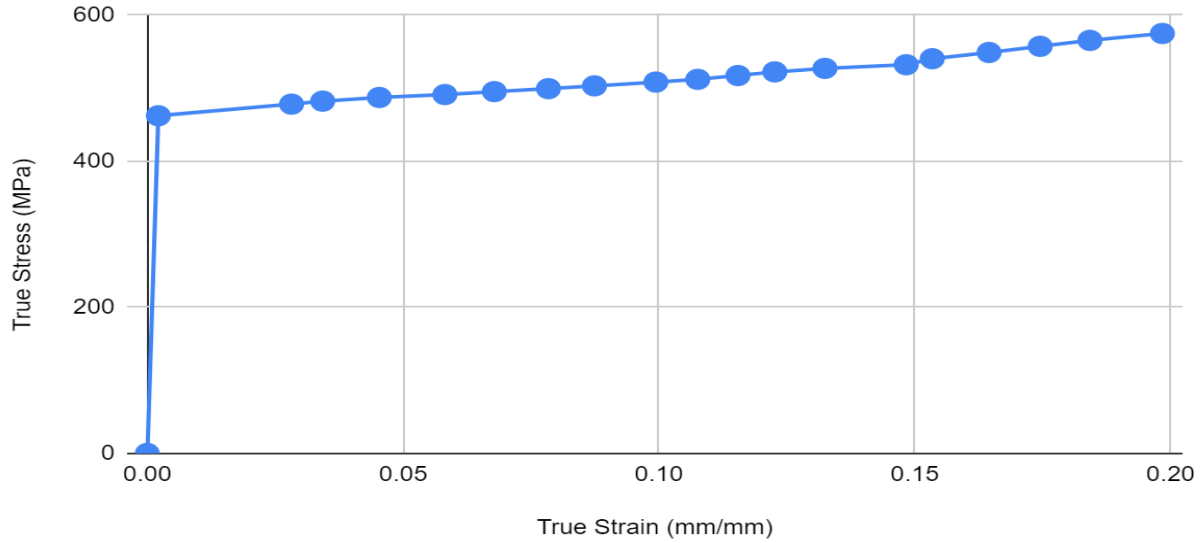

Graph.13. True Stress-True Strain curve of Specimen TC-10-2-4

Specimen TC-10-2-5

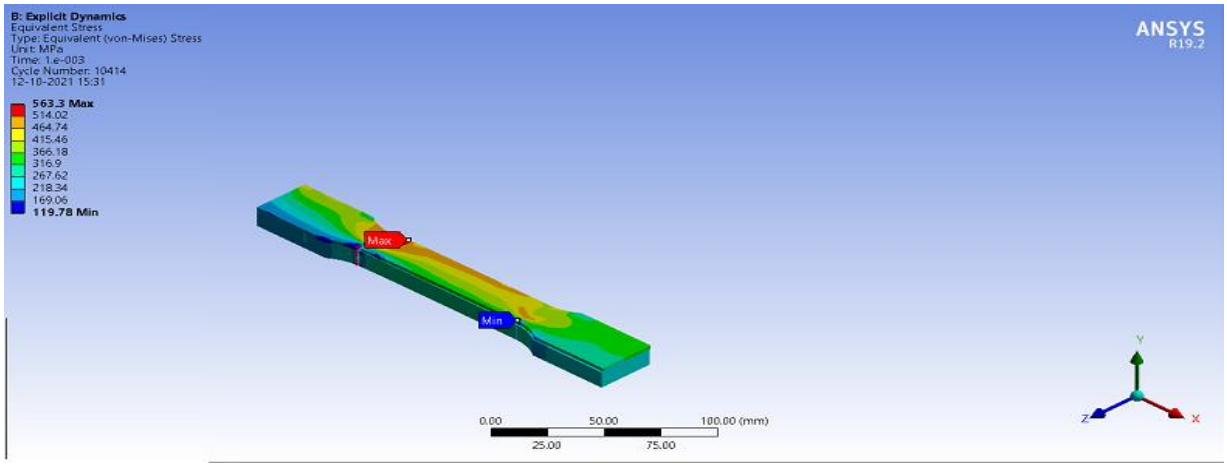

Fig.41. Equivalent(Von-Mises) Stress of Specimen TC-10-2-5

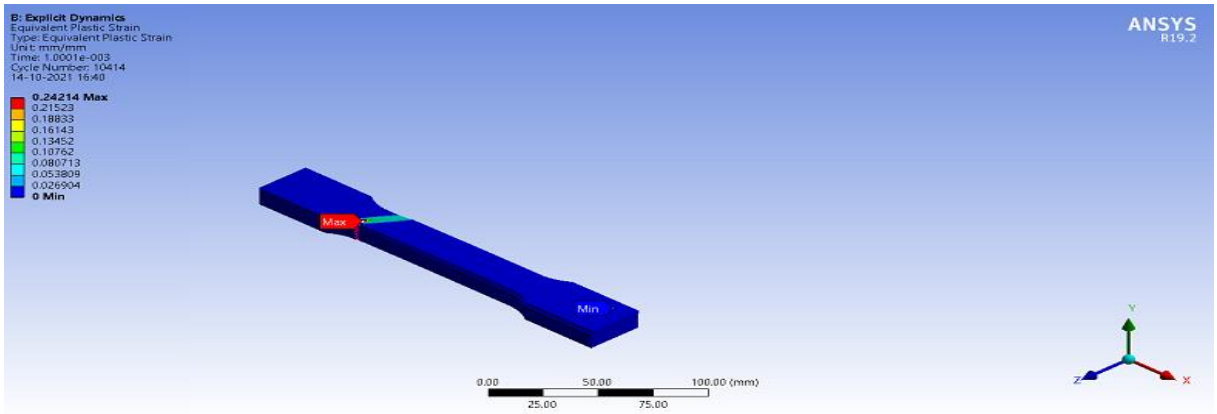

Fig.42. Equivalent Plastic Strain of Specimen TC-10-2-5

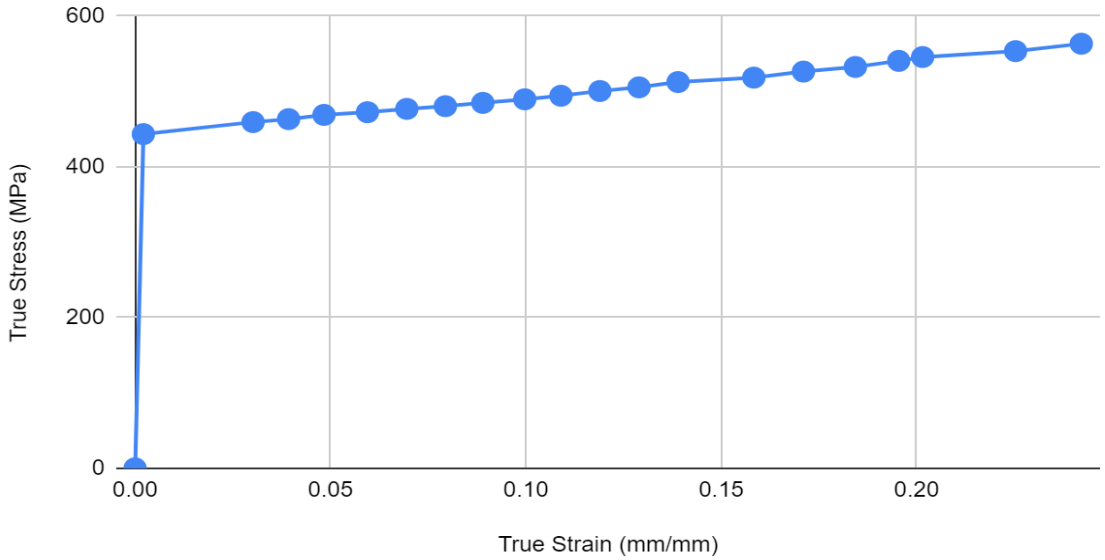

Graph.14. True Stress-True Strain curve of Specimen TC-10-2-5

Specimen TC-10-2-6

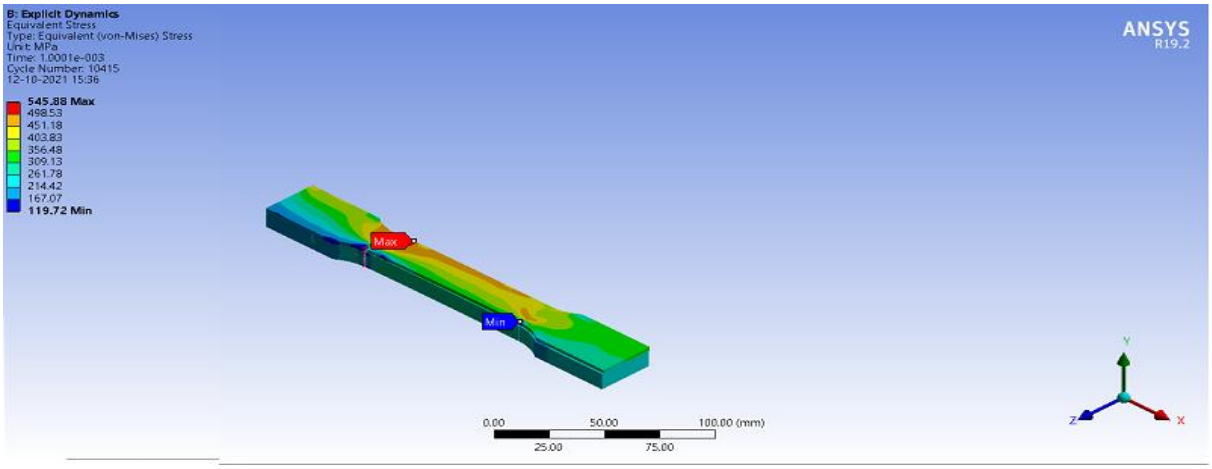

Fig.43. Equivalent(Von-Mises) Stress of Specimen TC-10-2-6

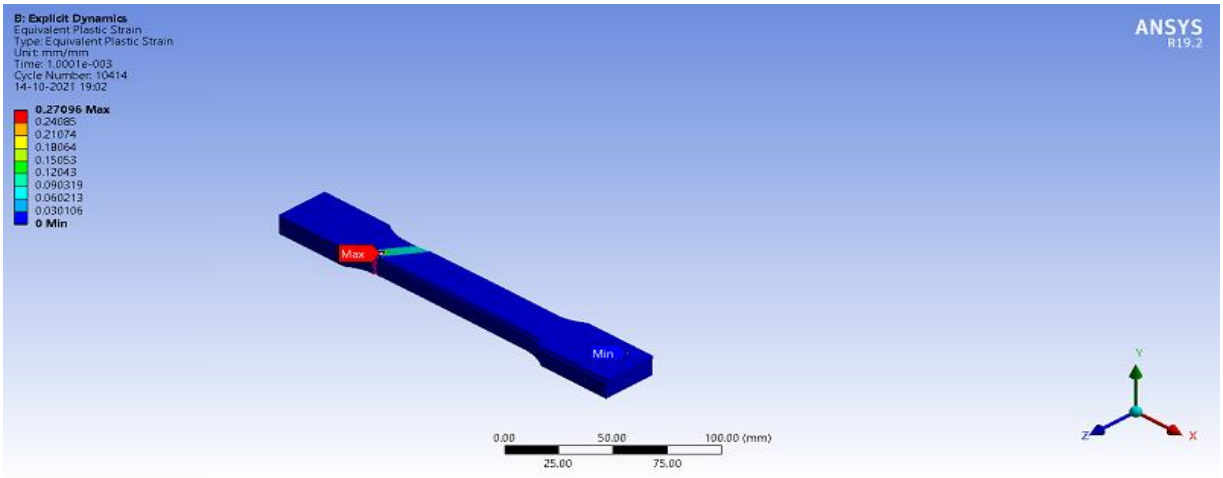

Fig.44. Equivalent Plastic Strain of Specimen TC-10-2-6

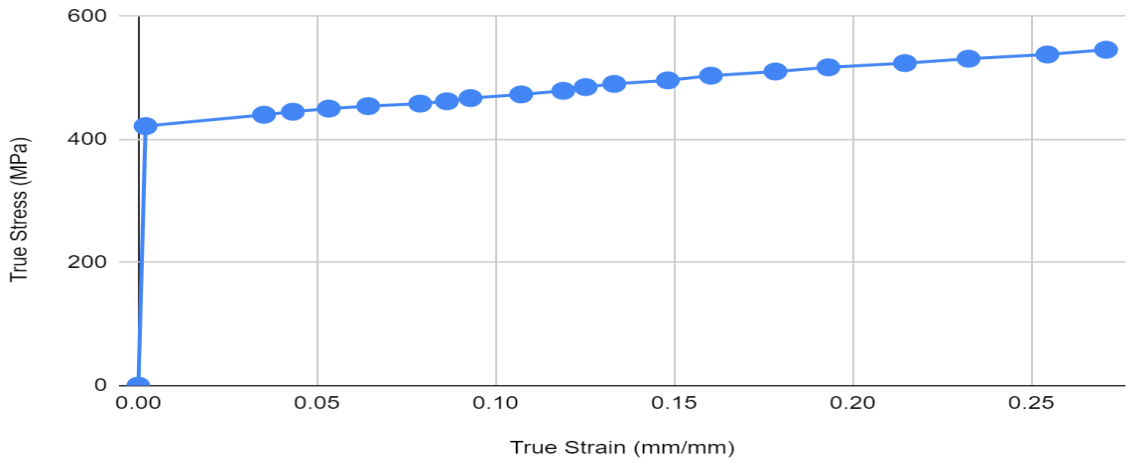

Graph.15. True Stress-True Strain curve of Specimen TC-10-2-6

Specimen TC-10-2-7

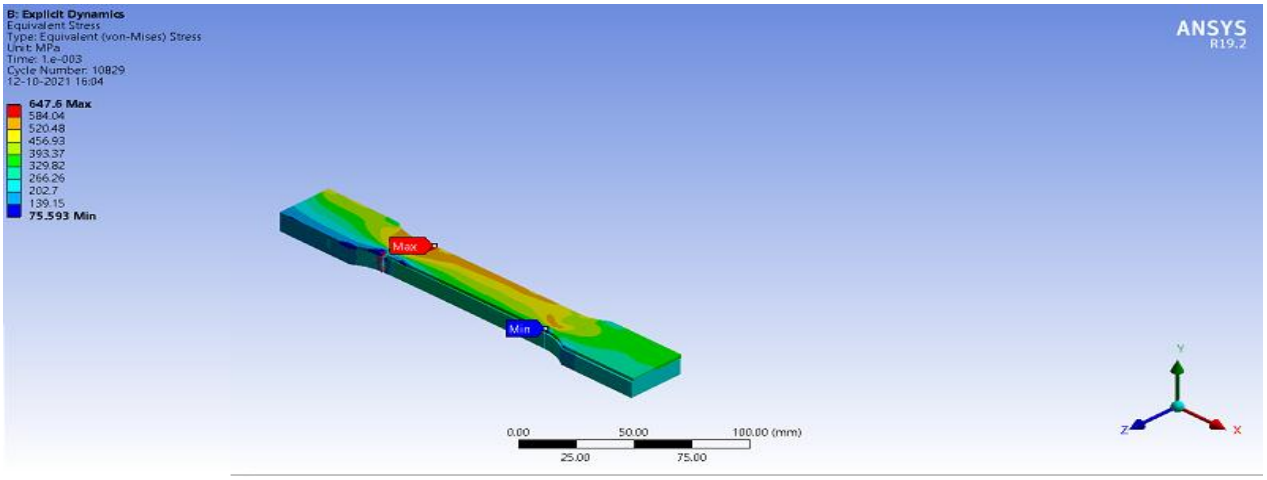

Fig.45. Equivalent(Von-Mises) Stress of Specimen TC-10-2-7

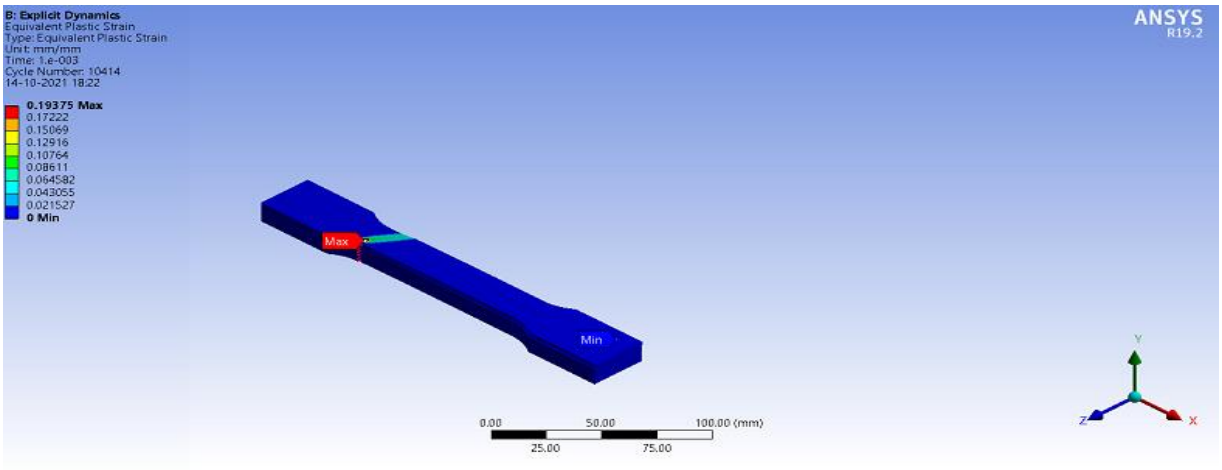

Fig.46. Equivalent Plastic Strain of Specimen TC-10-2-7

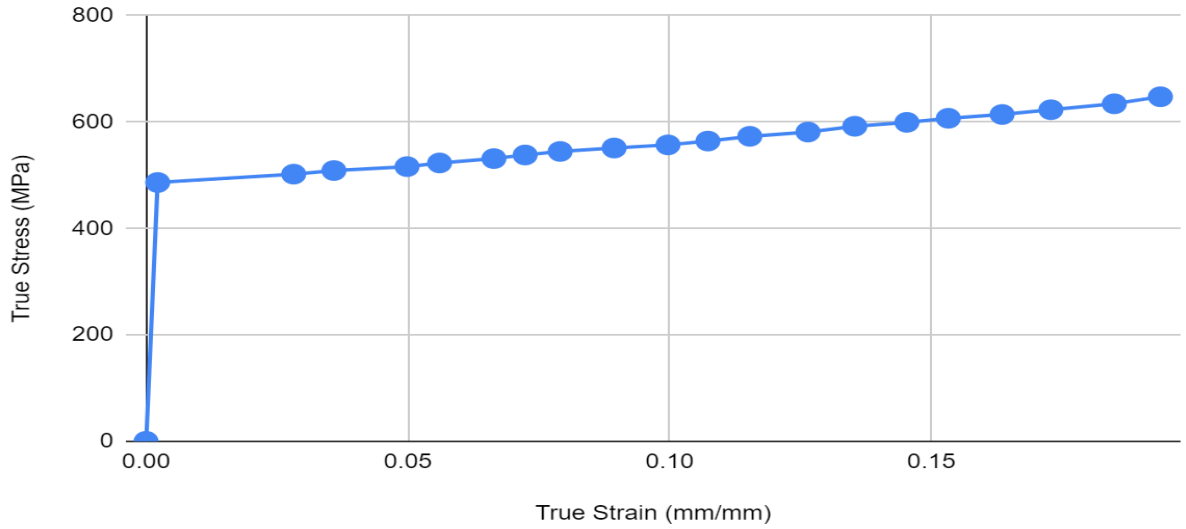

Graph.16. True Stress-True Strain curve of Specimen TC-10-2-7

Specimen TC-10-2-8

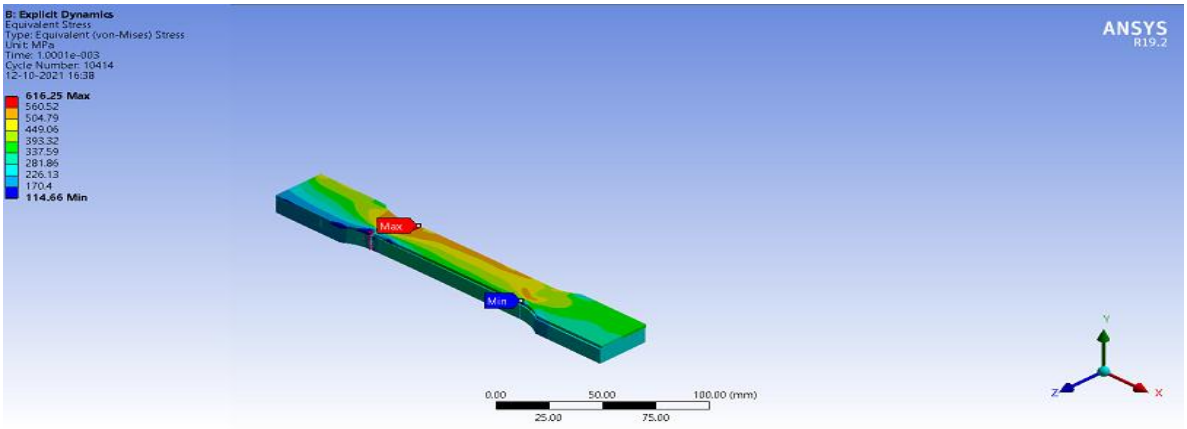

Fig.47. Equivalent(Von-Mises) Stress of Specimen TC-10-2-8

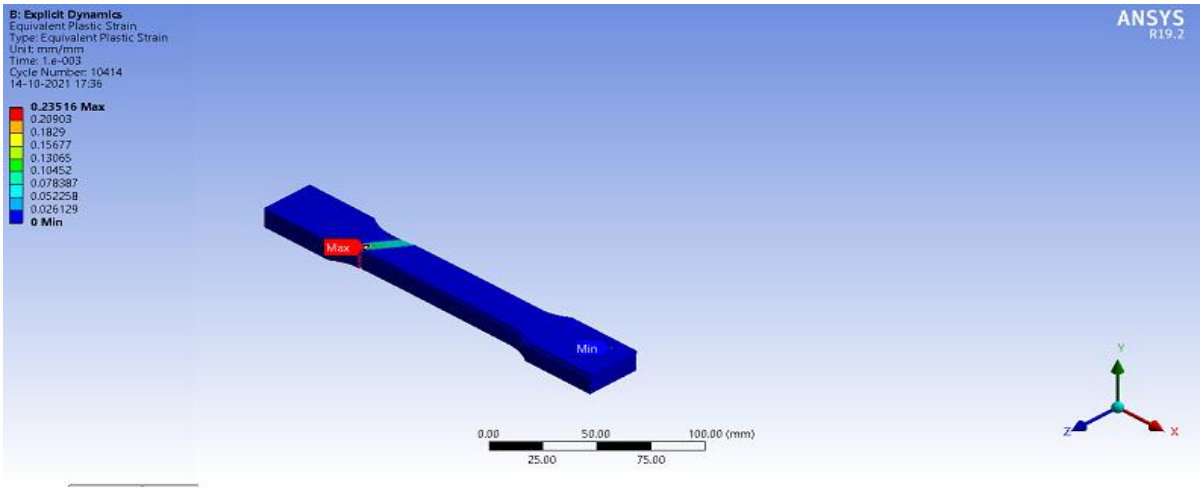

Fig.48. Equivalent Plastic Strain of Specimen TC-10-2-8

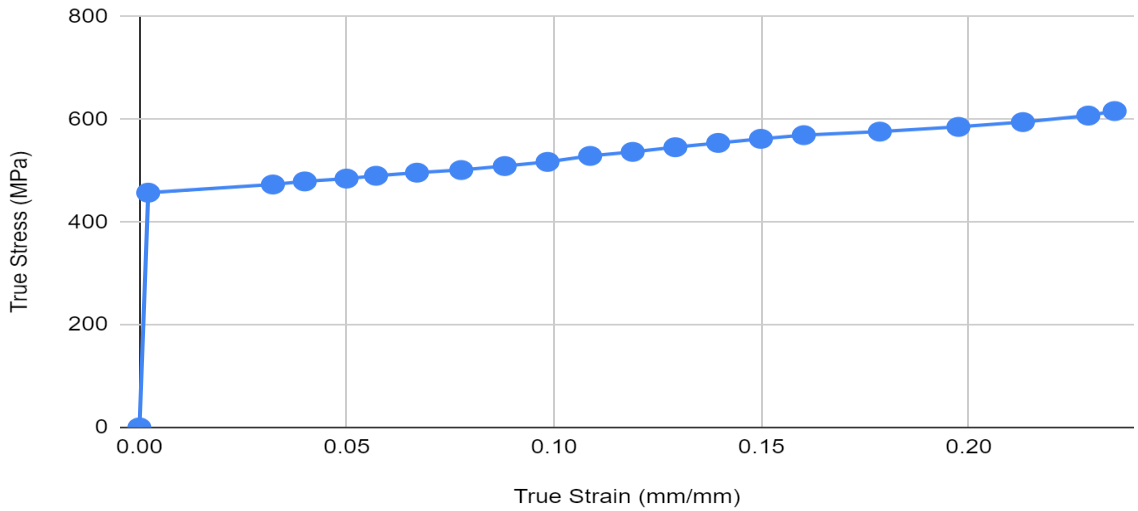

Graph.17. True Stress-True Strain curve of Specimen TC-10-2-8

Specimen TC-10-2-9

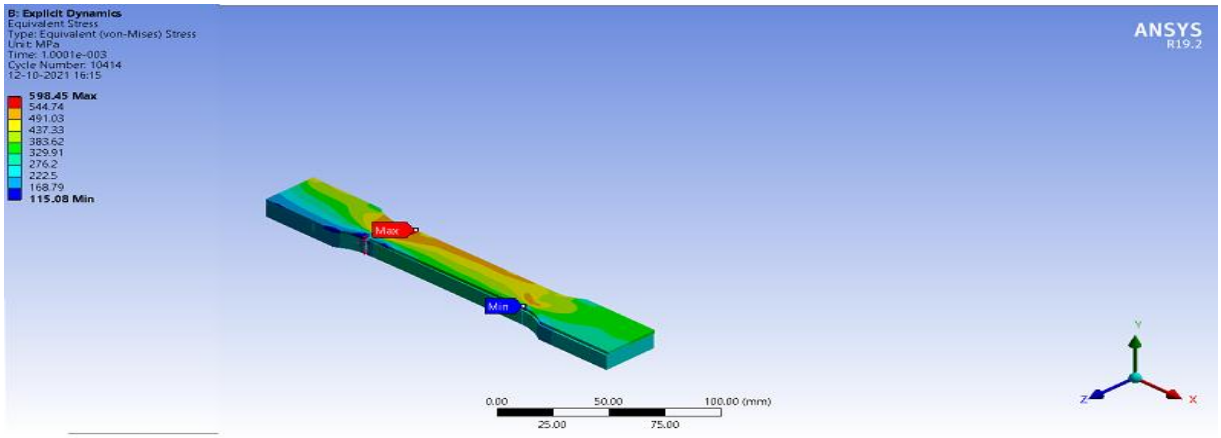

Fig.49. Equivalent(Von-Mises) Stress of Specimen TC-10-2-9

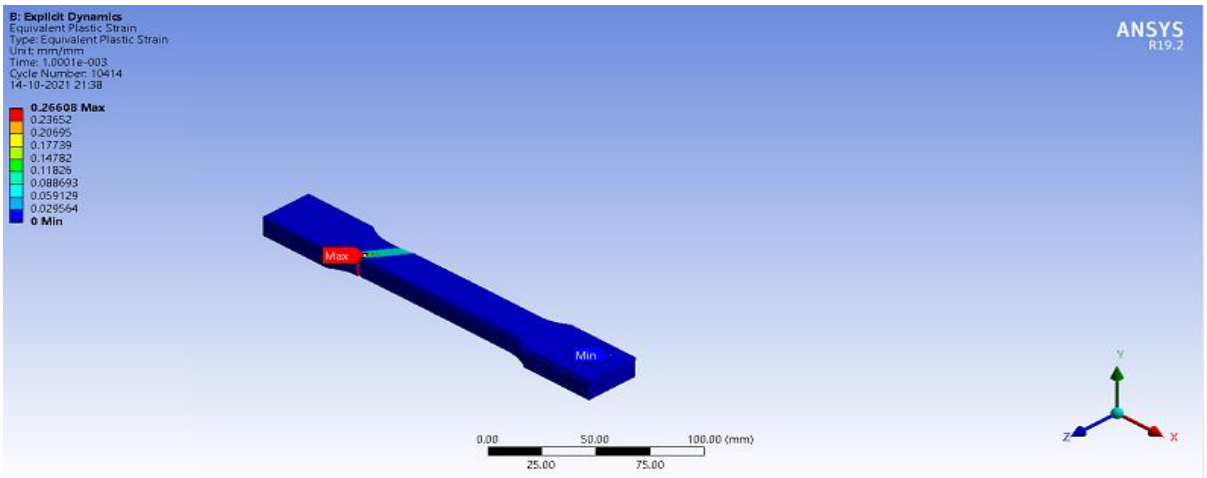

Fig.50. Equivalent Plastic Strain of Specimen TC-10-2-9

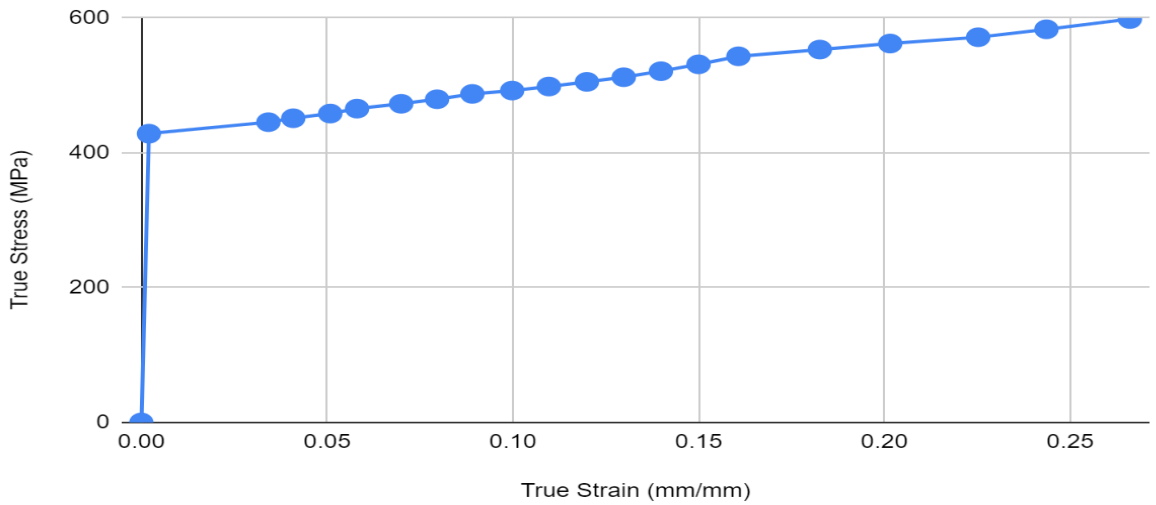

Graph.18. True Stress-True Strain curve of Specimen TC-10-2-9

Specimen TC-5-2-1

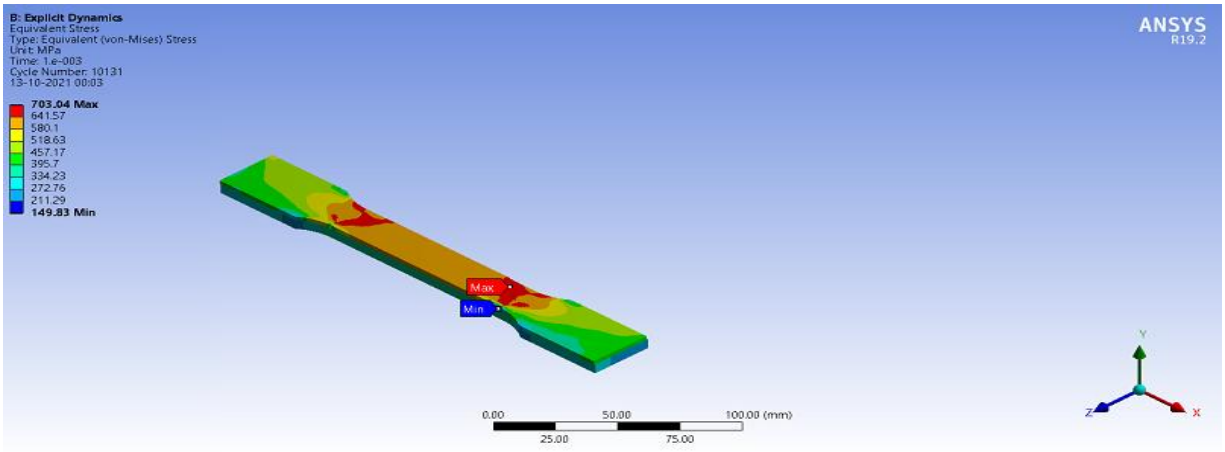

Fig.51. Equivalent(Von-Mises) Stress of Specimen TC-5-2-1

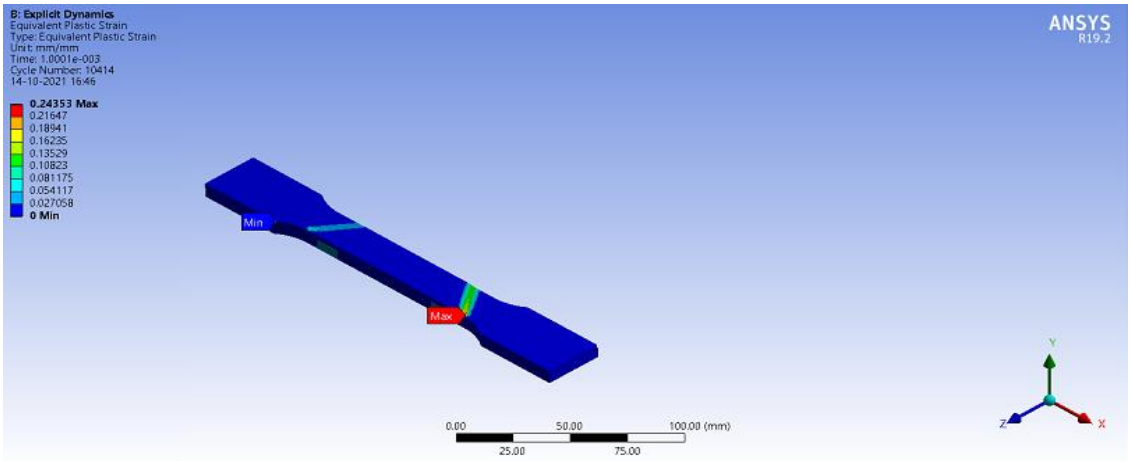

Fig.52. Equivalent Plastic Strain of Specimen TC-5-2-1

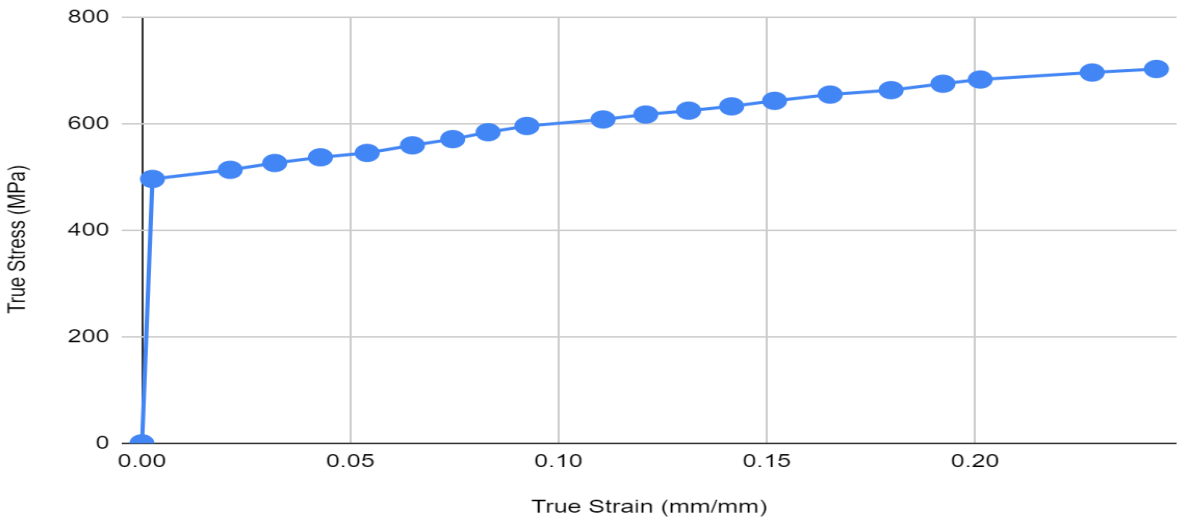

Graph.19. True Stress-True Strain curve of Specimen TC-5-2-1

Specimen TC-5-2-2

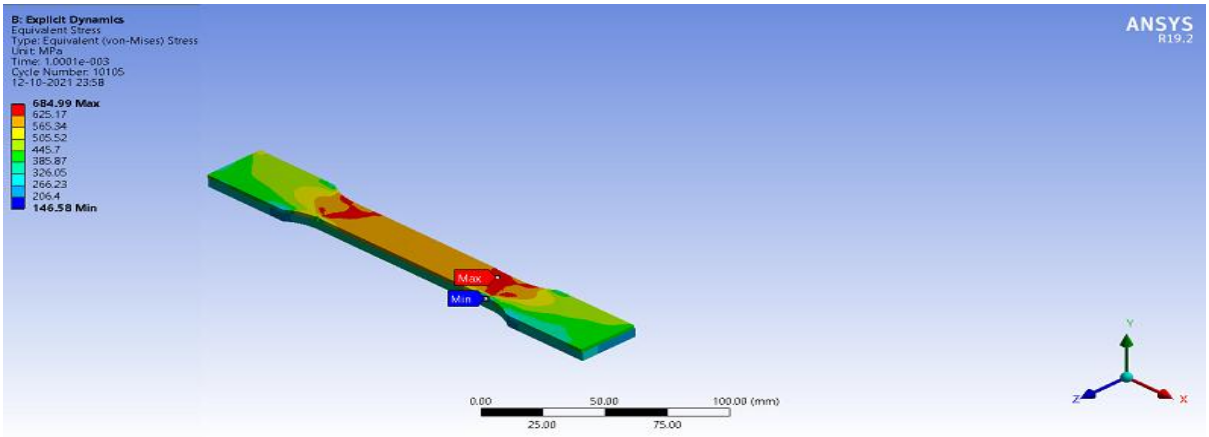

Fig.53. Equivalent(Von-Mises) Stress of Specimen TC-5-2-2

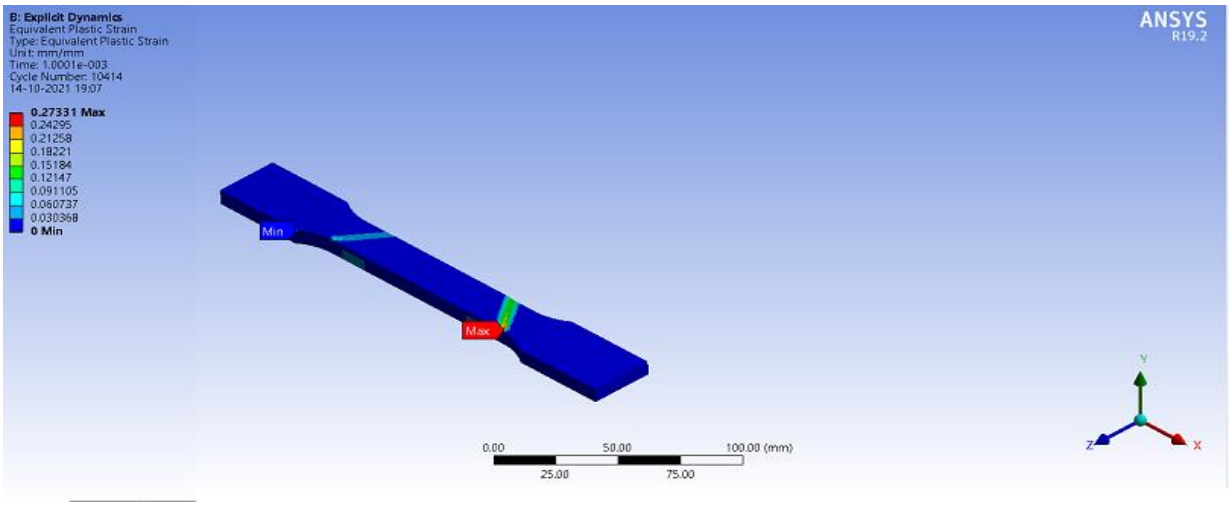

Fig.54. Equivalent Plastic Strain of Specimen TC-5-2-2

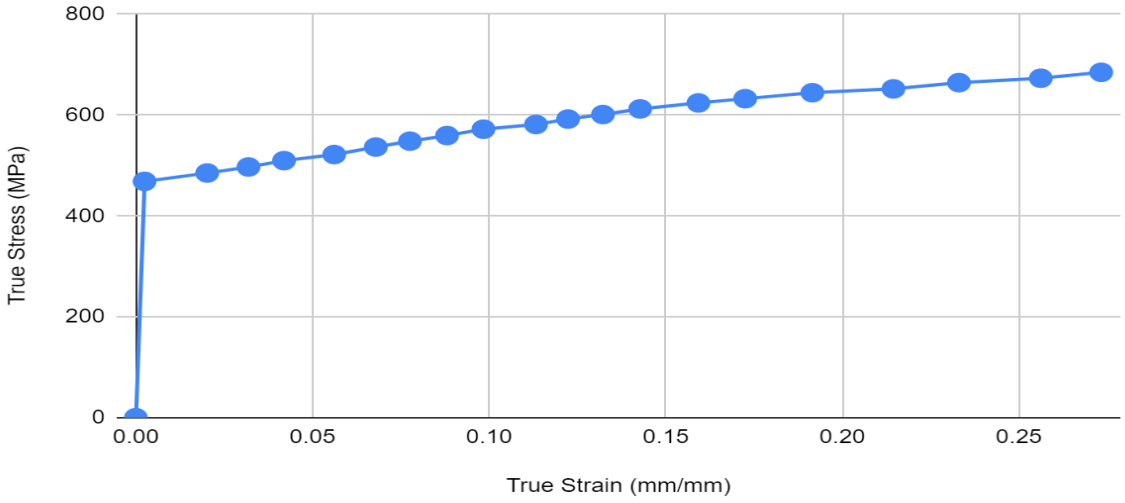

Graph.20. True Stress-True Strain curve of Specimen TC-5-2-2

Specimen TC-5-2-3

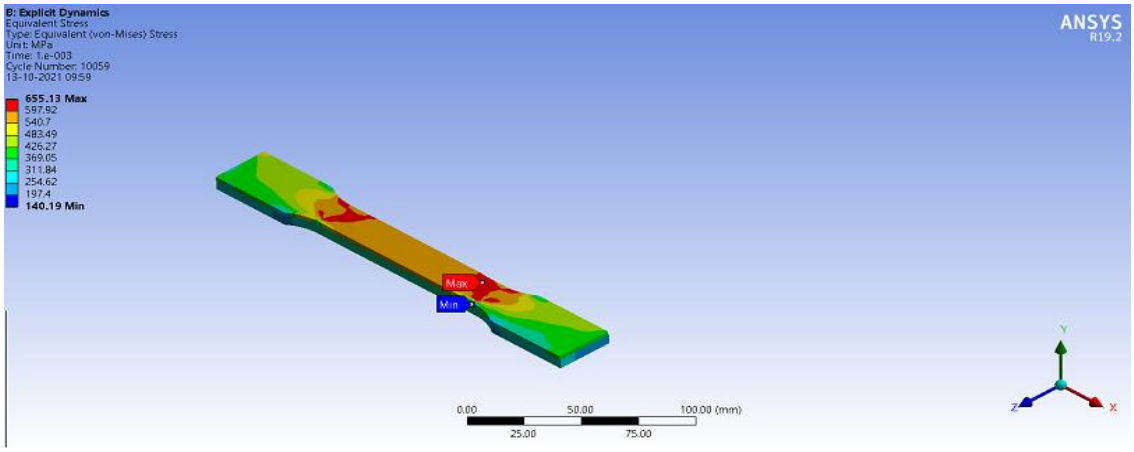

Fig.55. Equivalent(Von-Mises) Stress of Specimen TC-5-2-3

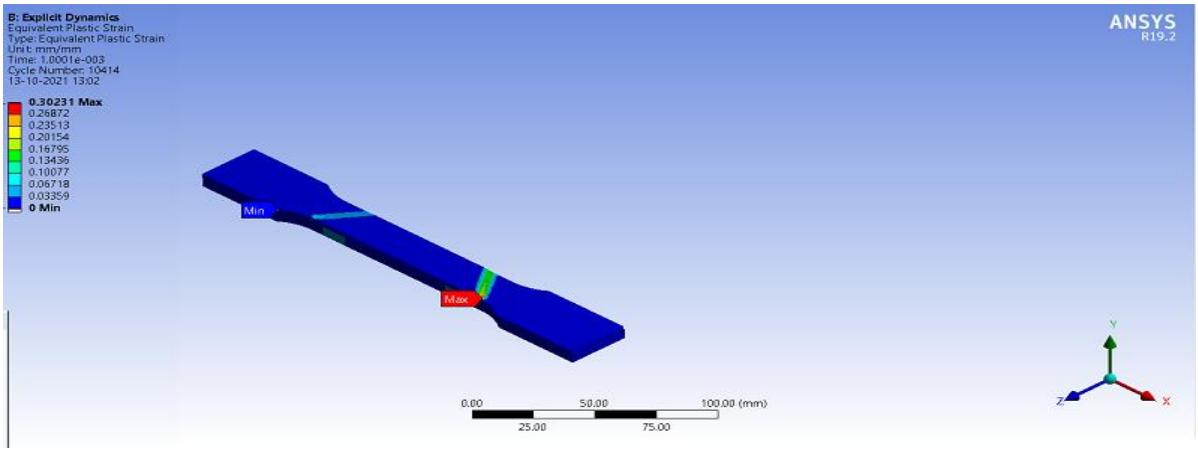

Fig.56. Equivalent Plastic Strain of Specimen TC-5-2-3

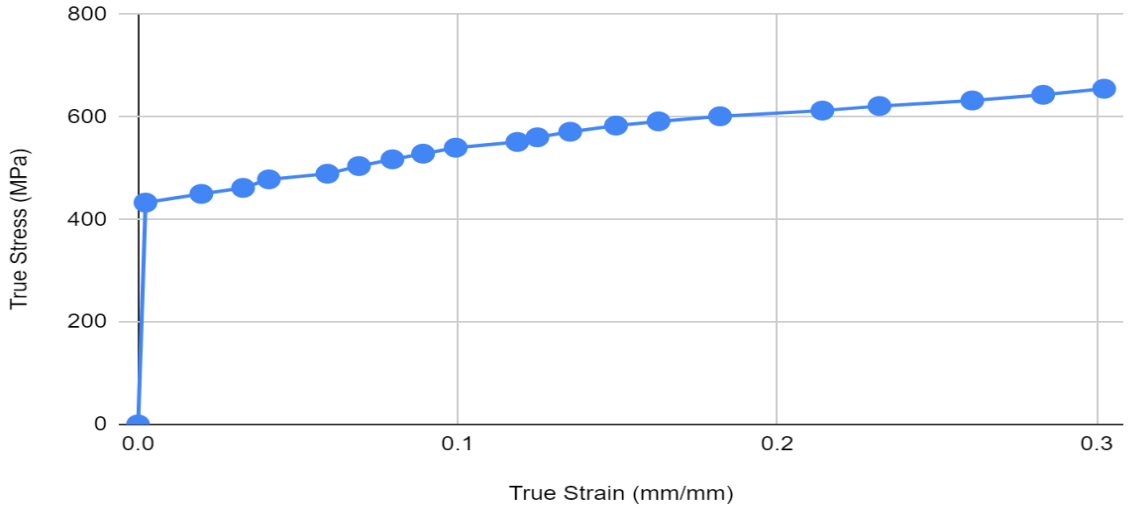

Graph.21. True Stress-True Strain curve of Specimen TC-5-2-3

Specimen TC-5-2-4

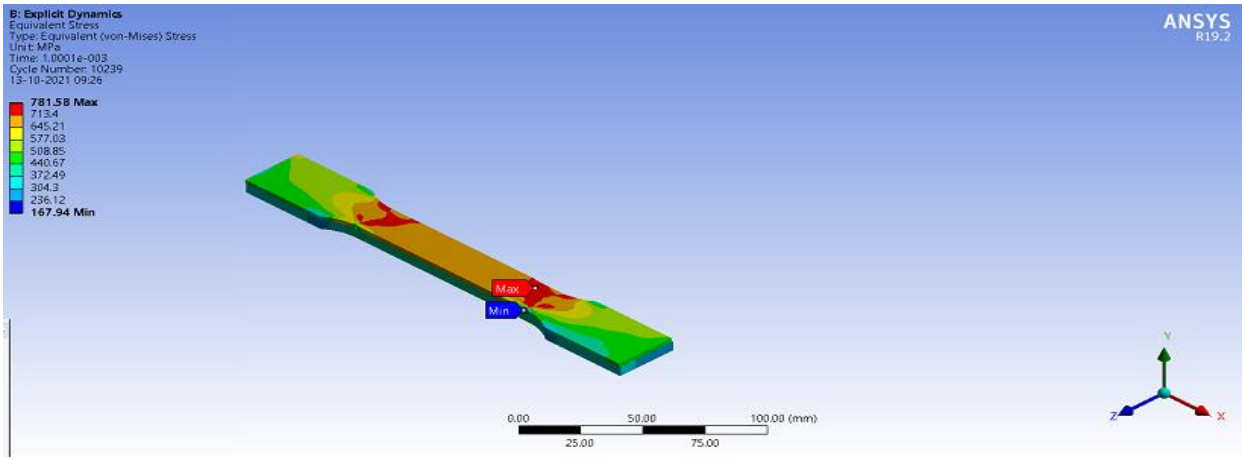

Fig.57. Equivalent(Von-Mises) Stress of Specimen TC-5-2-4

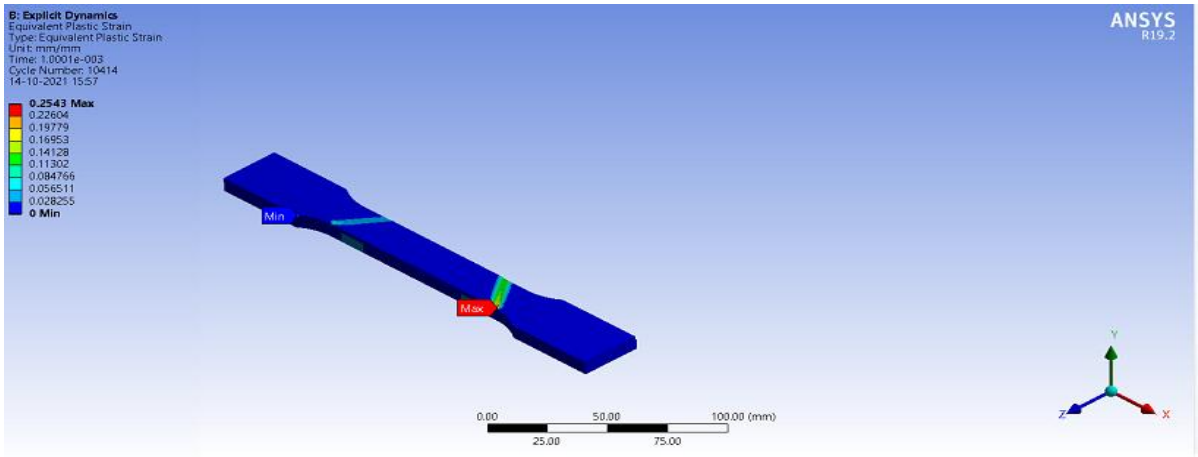

Fig.58. Equivalent Plastic Strain of Specimen TC-5-2-4

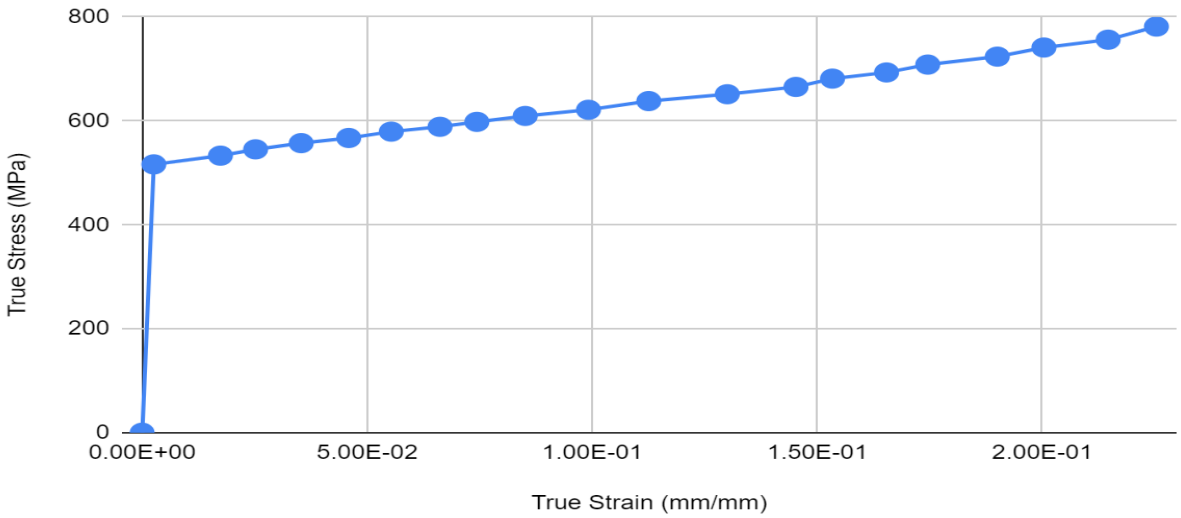

Graph.22. True Stress-True Strain curve of Specimen TC-5-2-4

Specimen TC-5-2-5

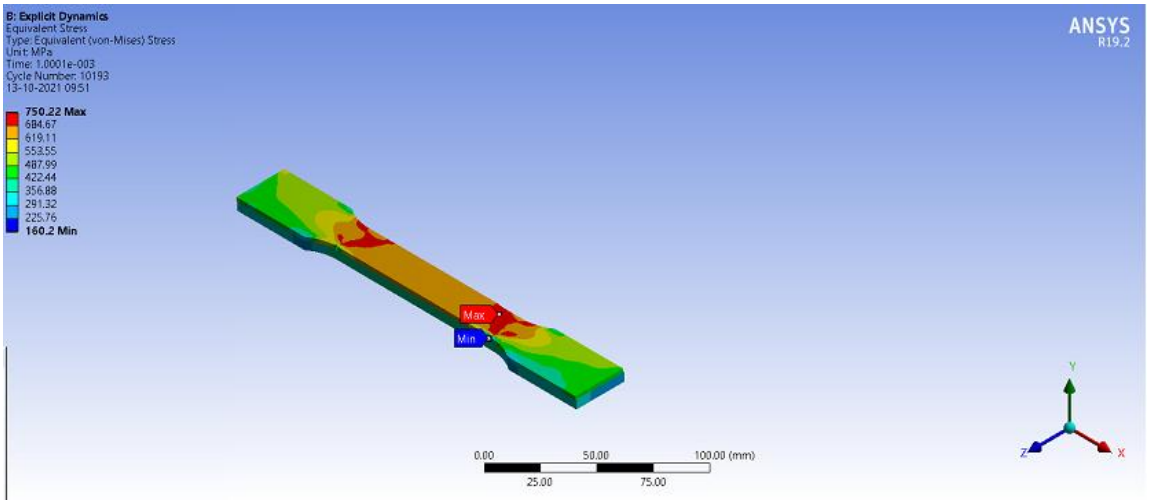

Fig.59. Equivalent(Von-Mises) Stress of Specimen TC-5-2-5

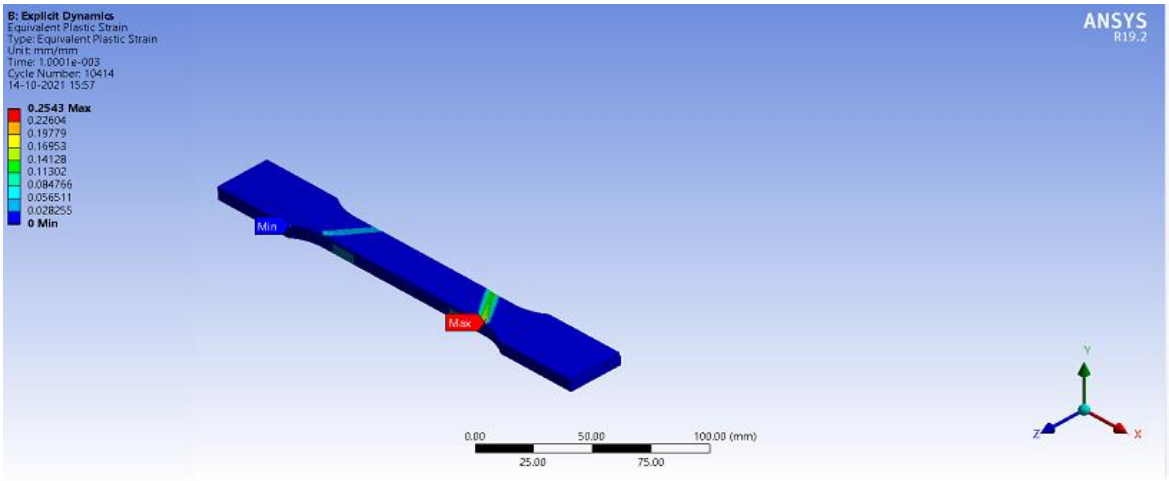

Fig.60. Equivalent Plastic Strain of Specimen TC-5-2-5

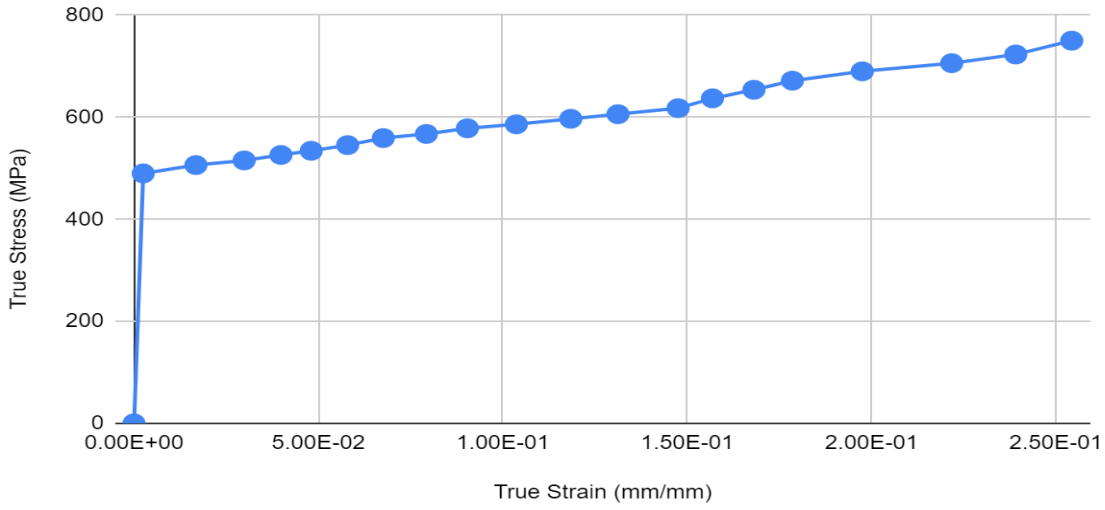

Graph.23. True Stress-True Strain curve of Specimen TC-5-2-5

Specimen TC-5-2-6

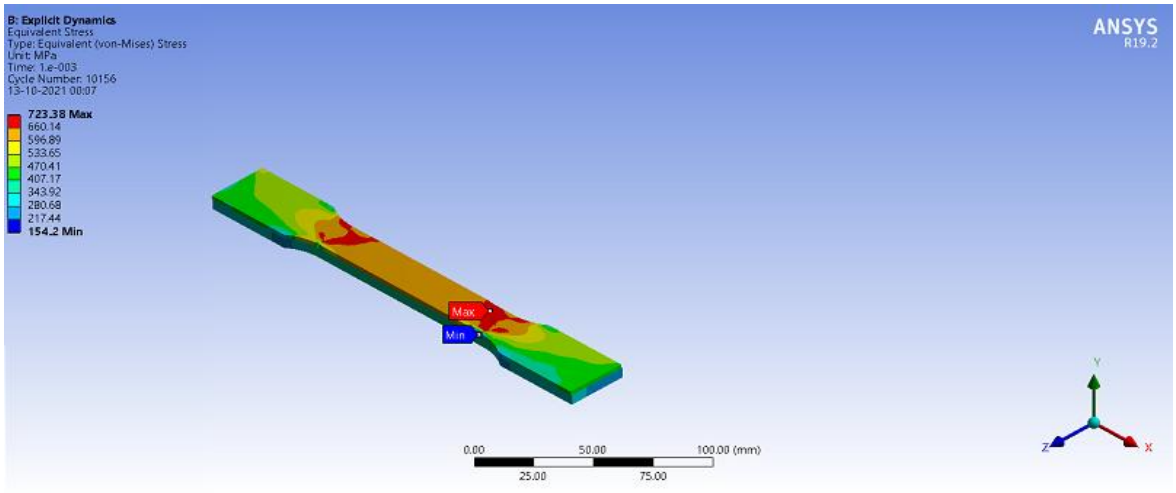

Fig.61. Equivalent(Von-Mises) Stress of Specimen TC-5-2-6

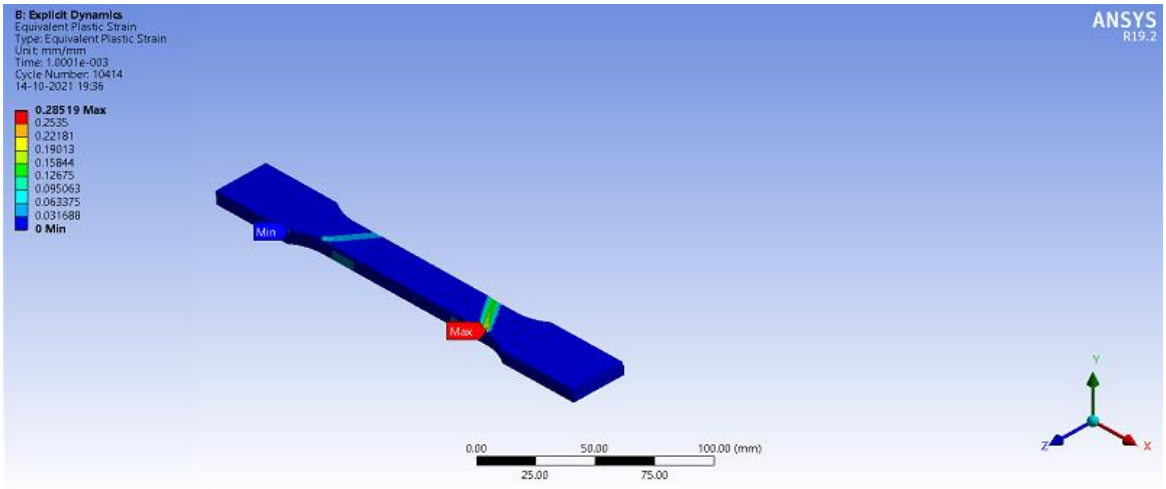

Fig.62. Equivalent Plastic Strain of Specimen TC-5-2-6

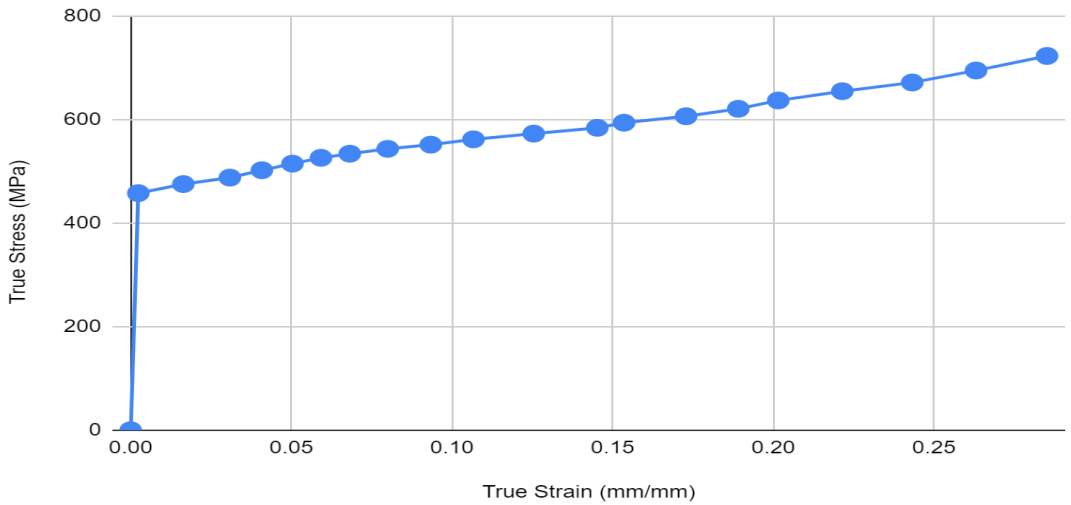

Graph.24. True Stress-True Strain curve of Specimen TC-5-2-6

Specimen TC-5-2-7

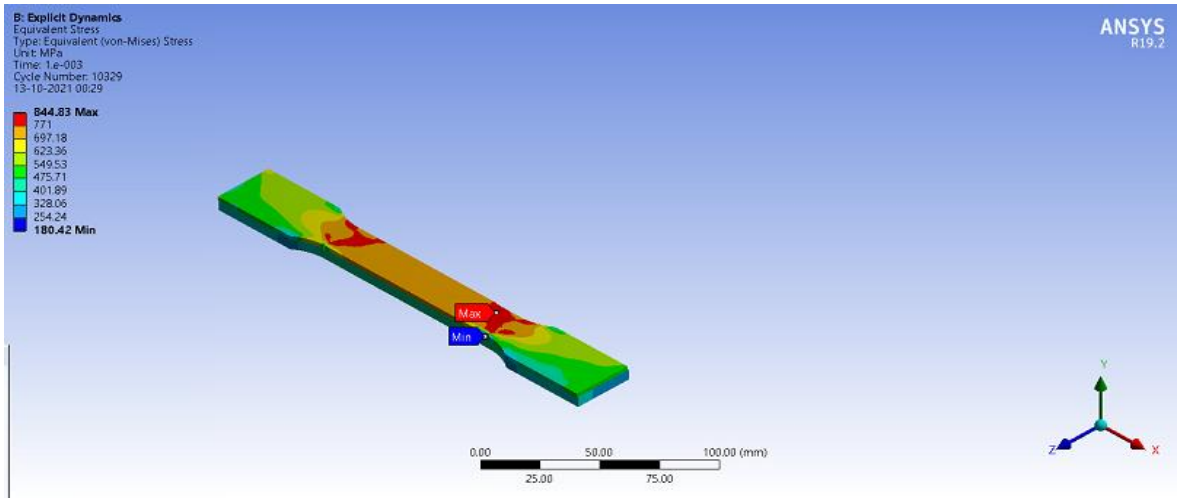

Fig.63. Equivalent(Von-Mises) Stress of Specimen TC-5-2-7

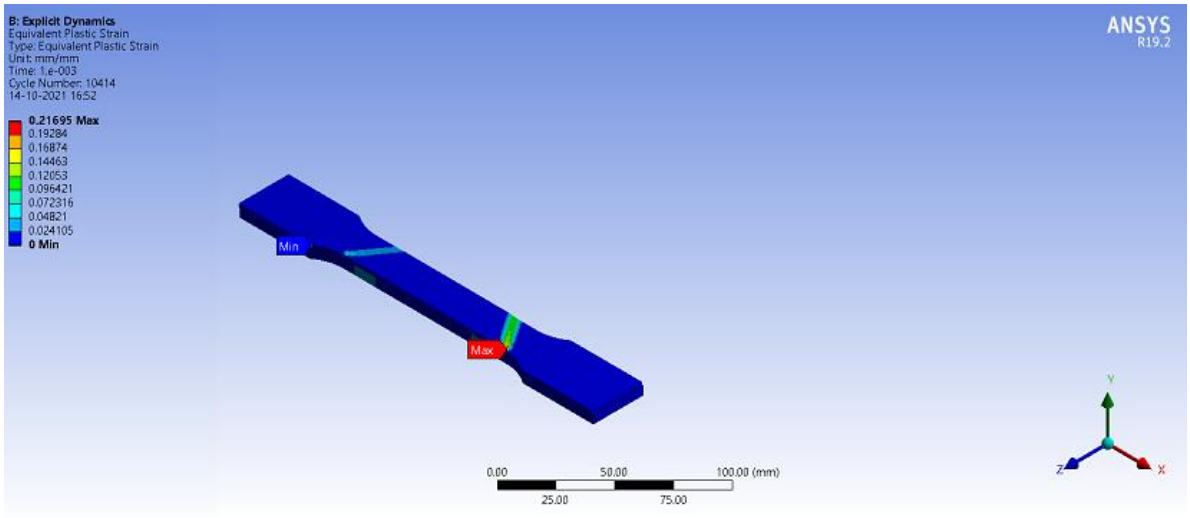

Fig.64. Equivalent Plastic Strain of Specimen TC-5-2-7

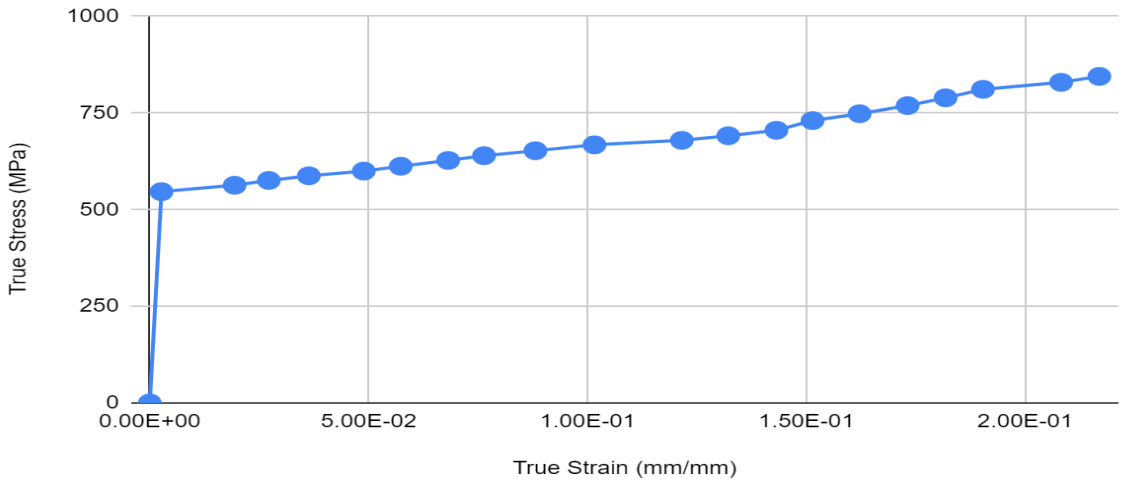

Graph.25. True Stress-True Strain curve of Specimen TC-5-2-7

Specimen TC-5-2-8

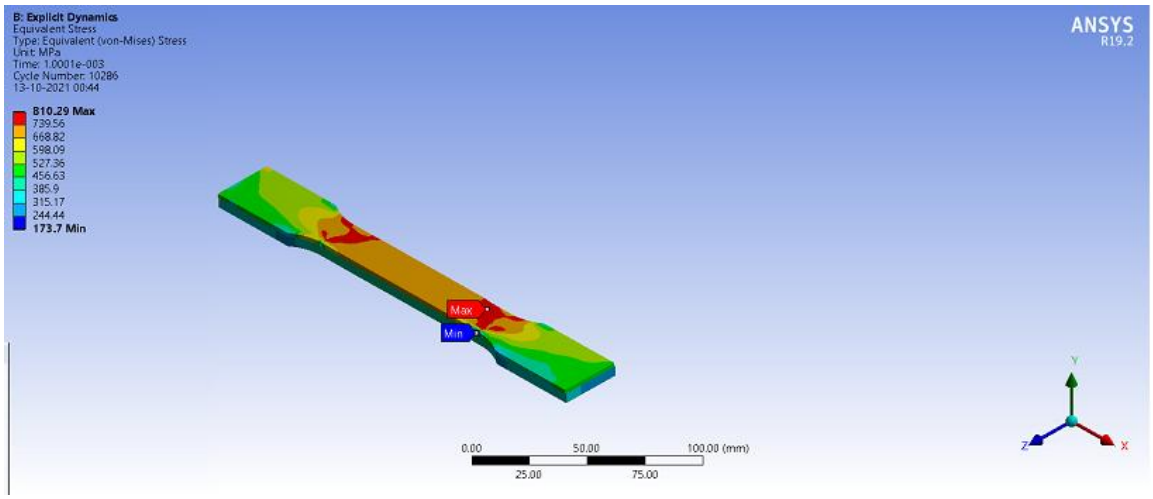

Fig.65. Equivalent(Von-Mises) Stress of Specimen TC-5-2-8

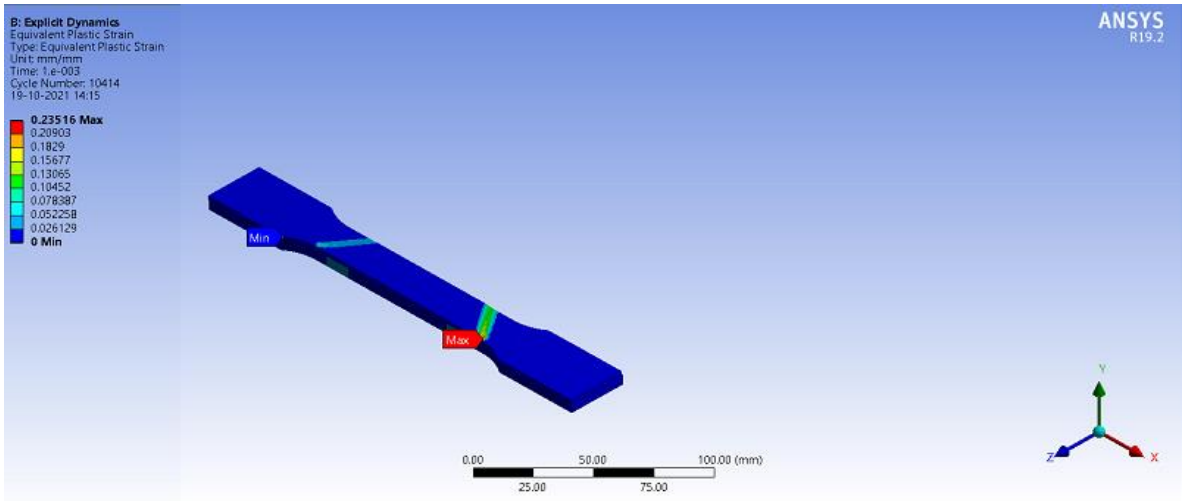

Fig.66. Equivalent Plastic Strain of Specimen TC-5-2-8

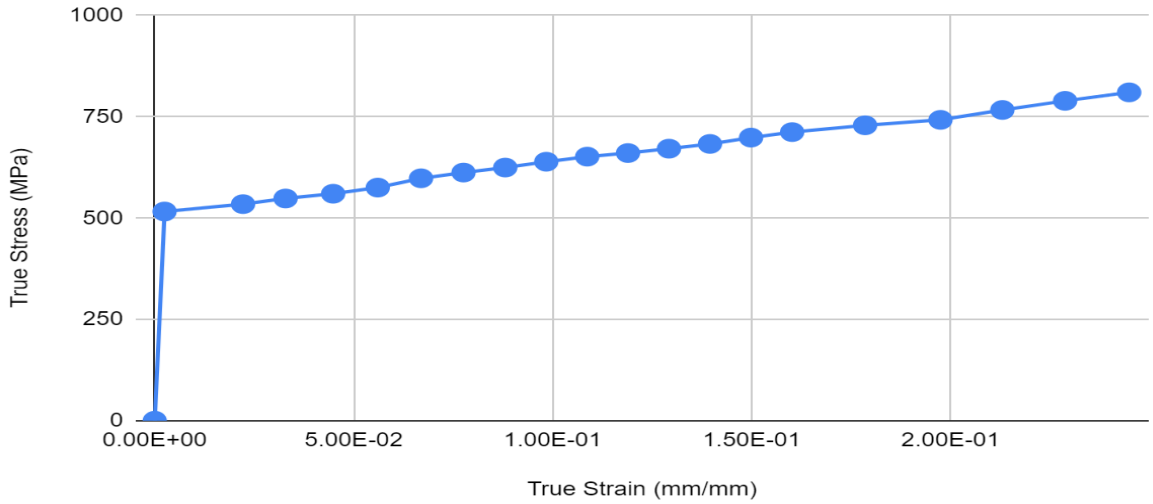

Graph.26. True Stress-True Strain curve of Specimen TC-5-2-8

Specimen TC-5-2-9

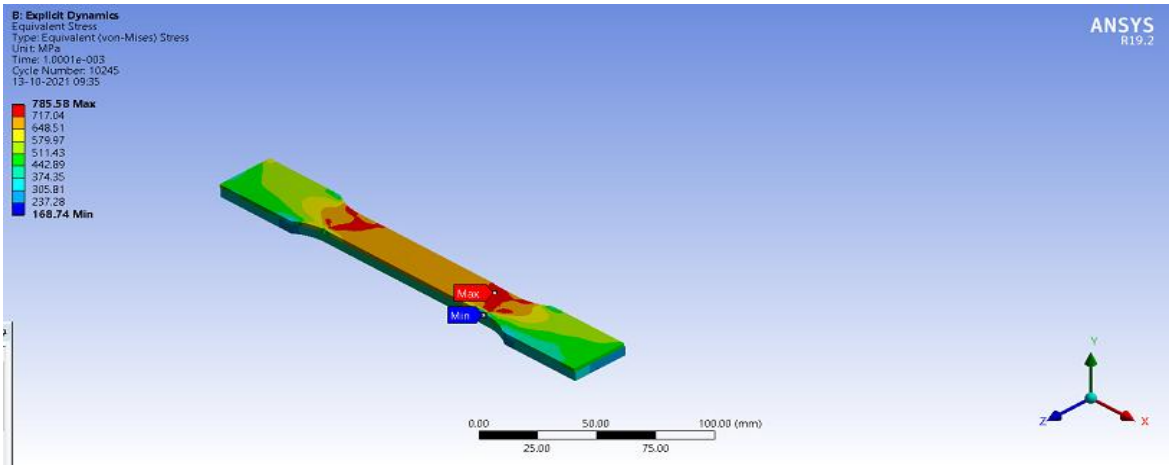

Fig.67. Equivalent(Von-Mises) Stress of Specimen TC-5-2-9

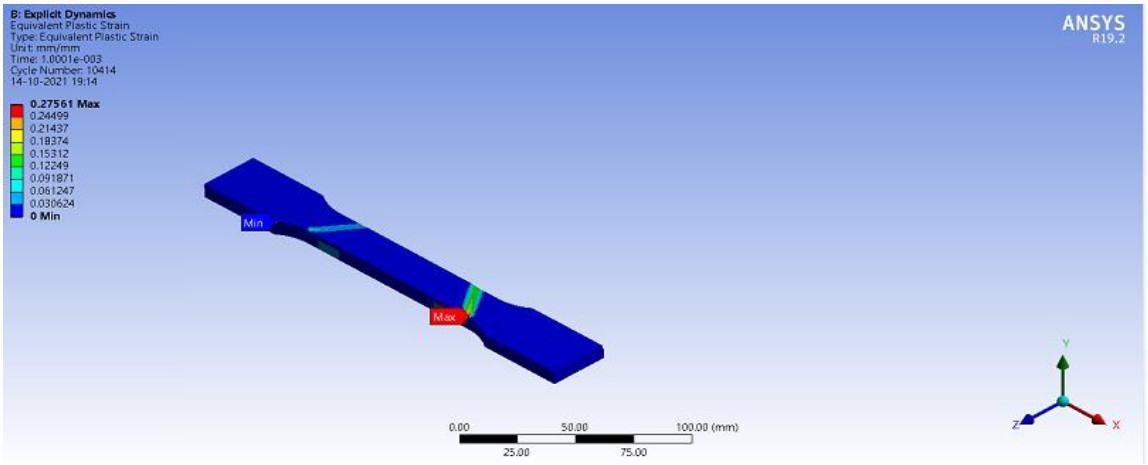

Fig.68. Equivalent Plastic Strain of Specimen TC-5-2-9

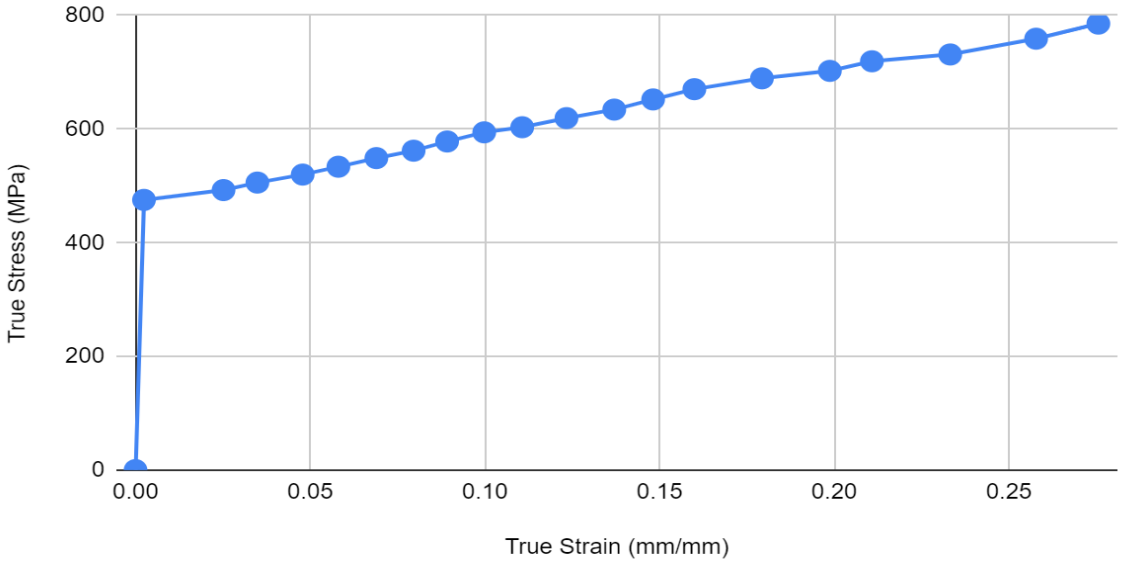

Graph.27. True Stress-True Strain curve of Specimen TC-5-2-9

Specimen TC-2-2-1

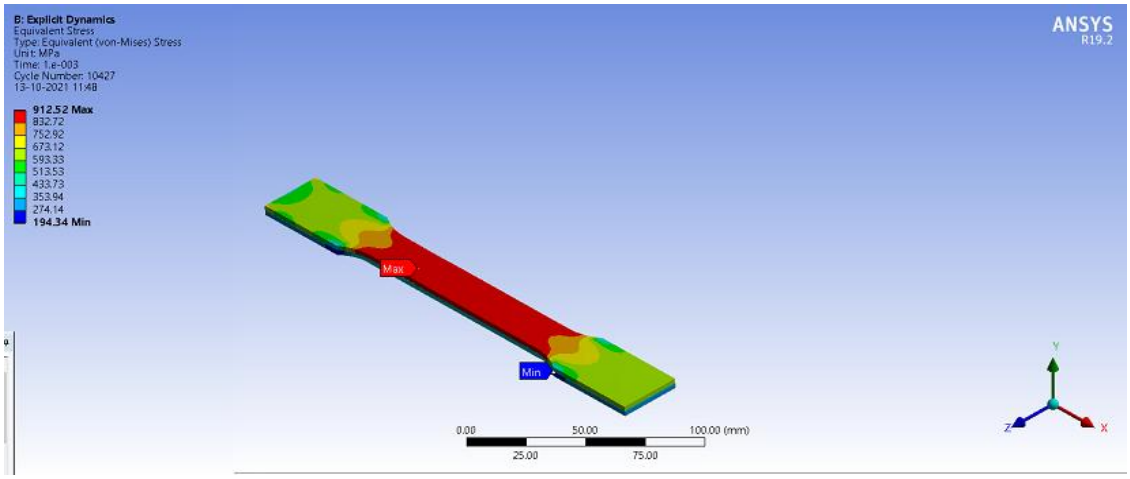

Fig.69. Equivalent(Von-Mises) Stress of Specimen TC-2-2-1

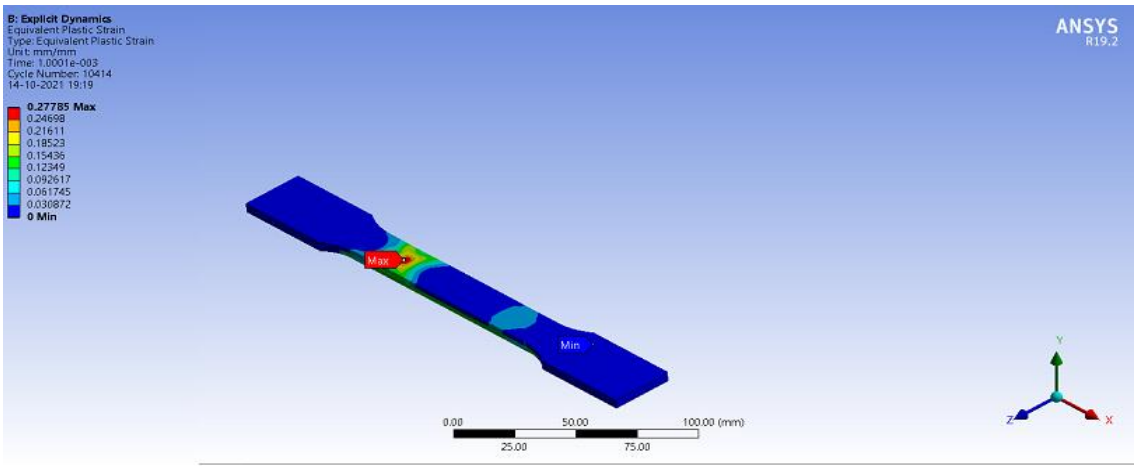

Fig.70. Equivalent Plastic Strain of Specimen TC-2-2-1

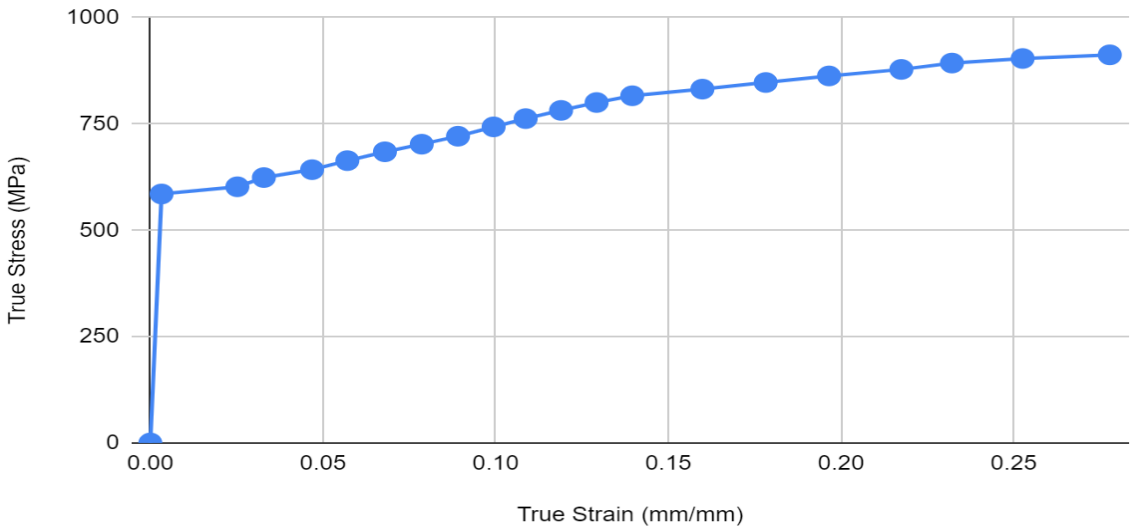

Graph.28. True Stress-True Strain curve of Specimen TC-2-2-1

Specimen TC-2-2-2

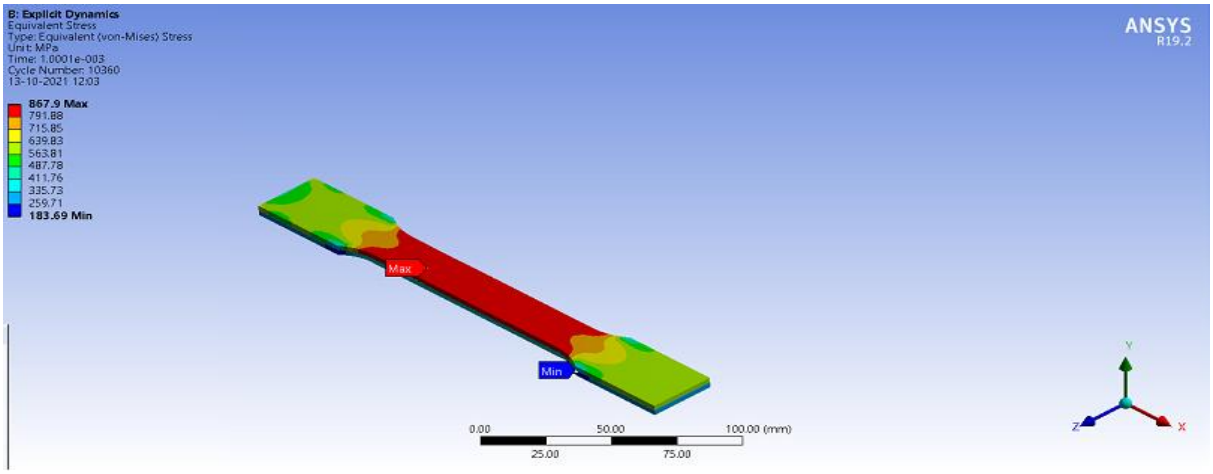

Fig.71. Equivalent(Von-Mises) Stress of Specimen TC-2-2-2

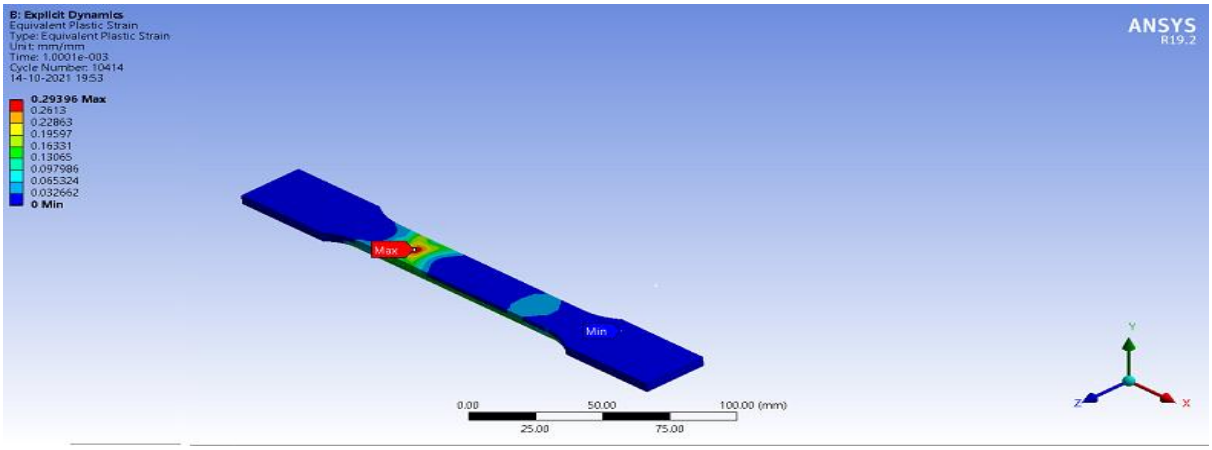

Fig.72. Equivalent Plastic Strain of Specimen TC-2-2-2

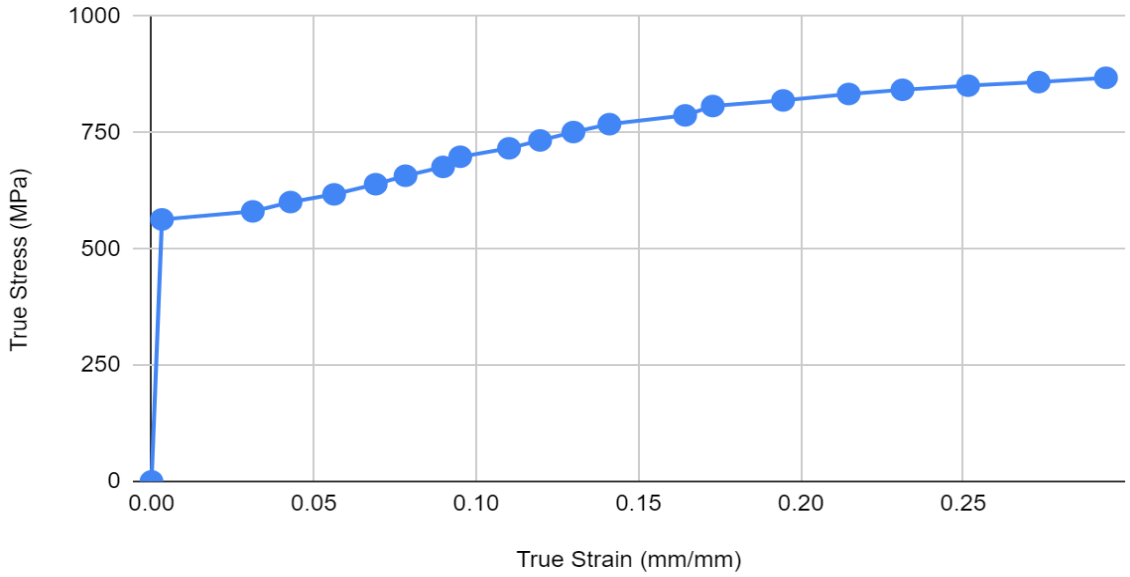

Graph.29. True Stress-True Strain curve of Specimen TC-2-2-2

Specimen TC-2-2-3

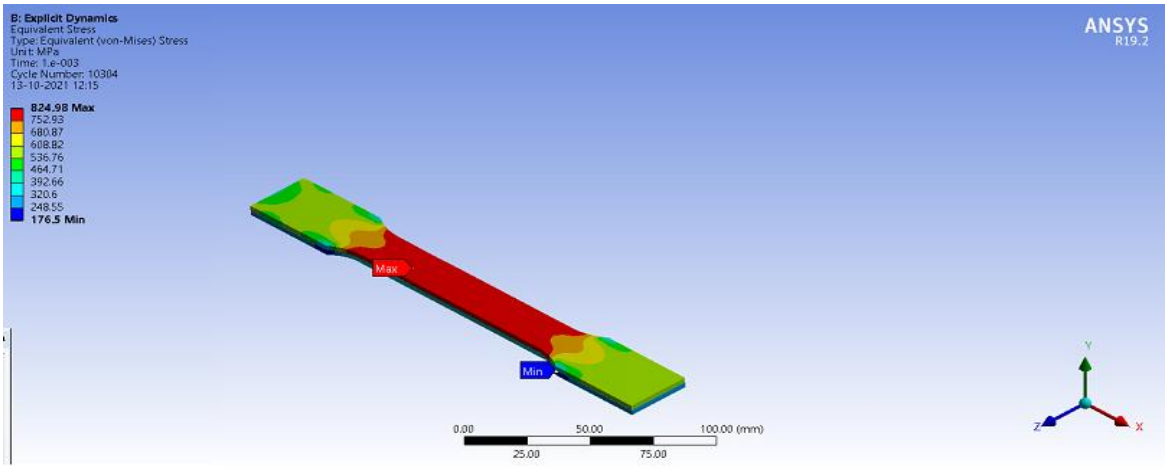

Fig.73. Equivalent(Von-Mises) Stress of Specimen TC-2-2-3

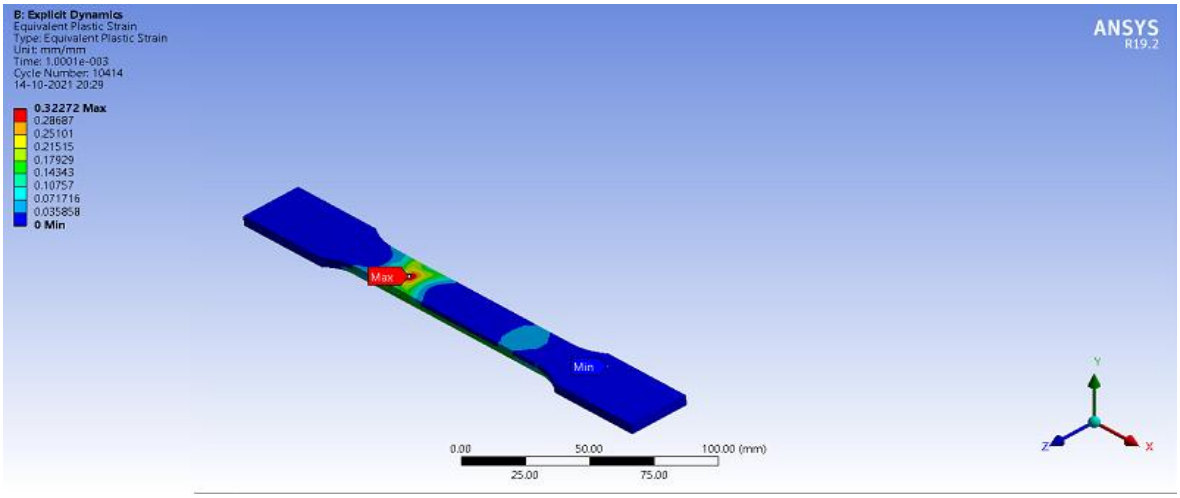

Fig.74. Equivalent Plastic Strain of Specimen TC-2-2-3

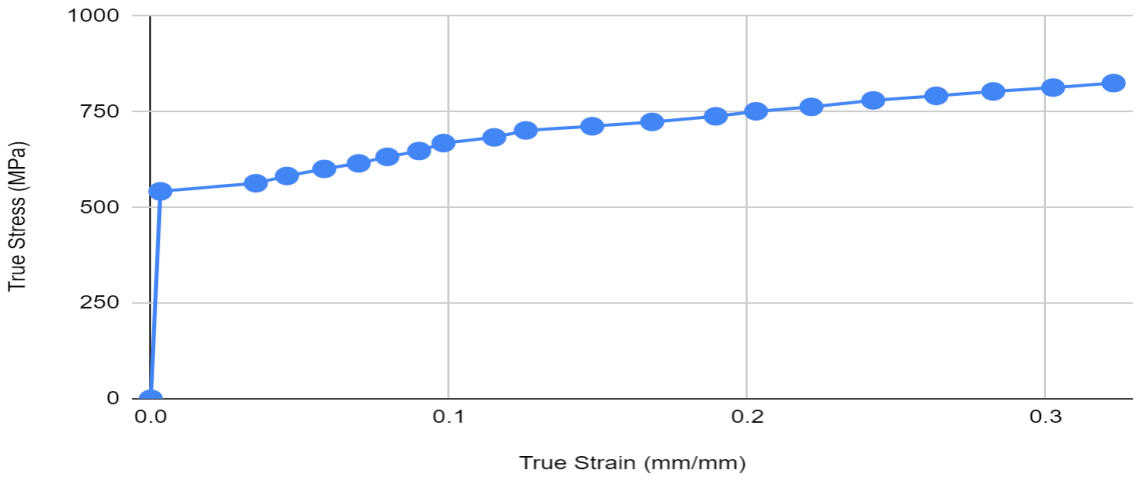

Graph.30. True Stress-True Strain curve of Specimen TC-2-2-3

Specimen TC-2-2-4

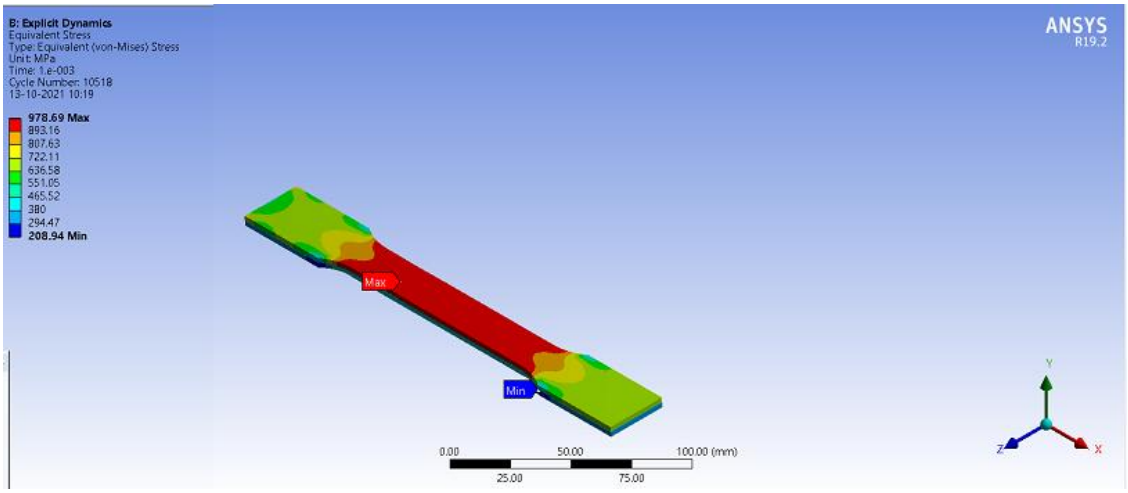

Fig.75. Equivalent(Von-Mises) Stress of Specimen TC-2-2-4

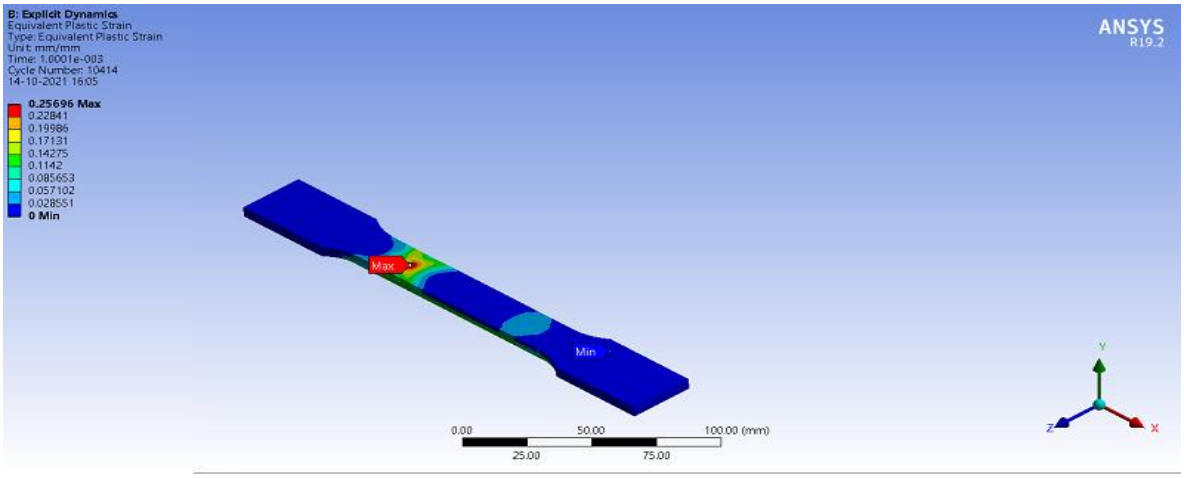

Fig.76. Equivalent Plastic Strain of Specimen TC-2-2-4

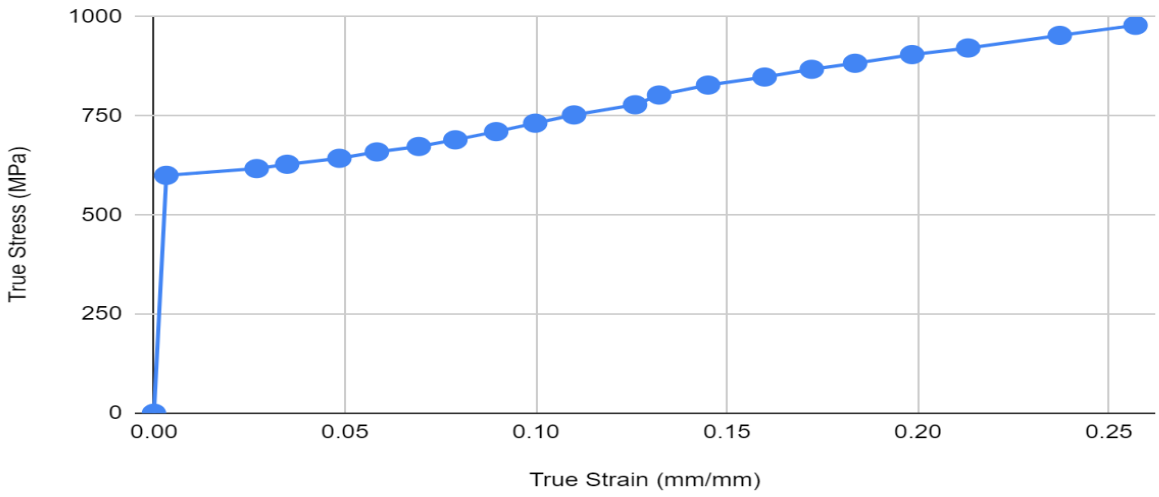

Graph.31. True Stress-True Strain curve of Specimen TC-2-2-4

Specimen TC-2-2-5

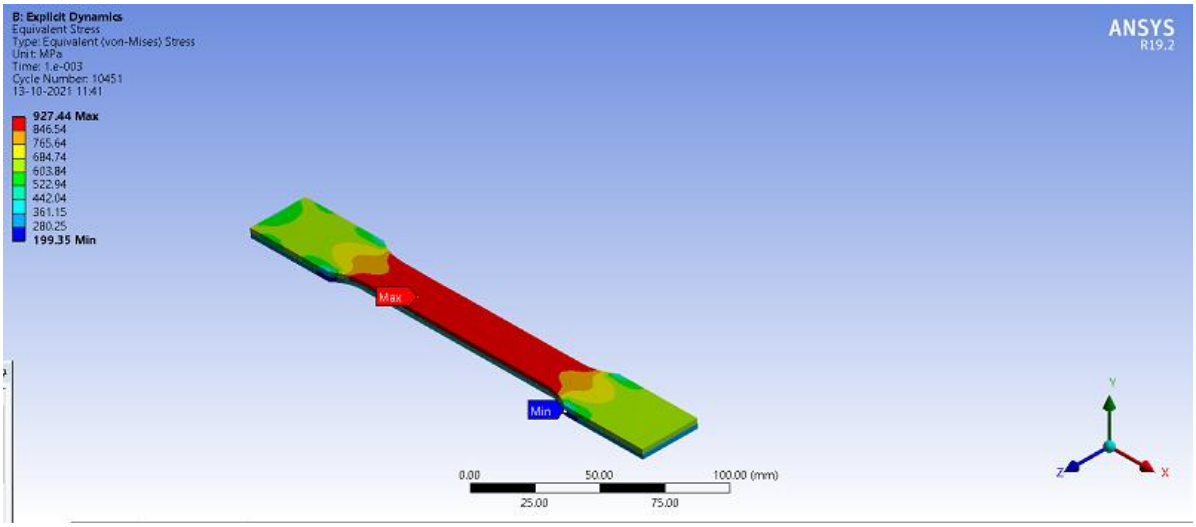

Fig.77. Equivalent(Von-Mises) Stress of Specimen TC-2-2-5

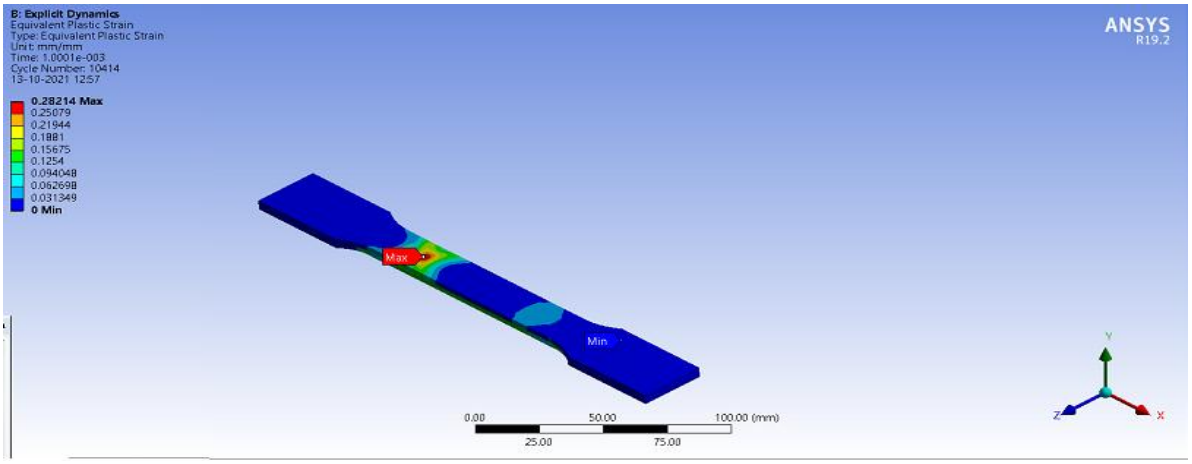

Fig.78. Equivalent Plastic Strain of Specimen TC-2-2-5

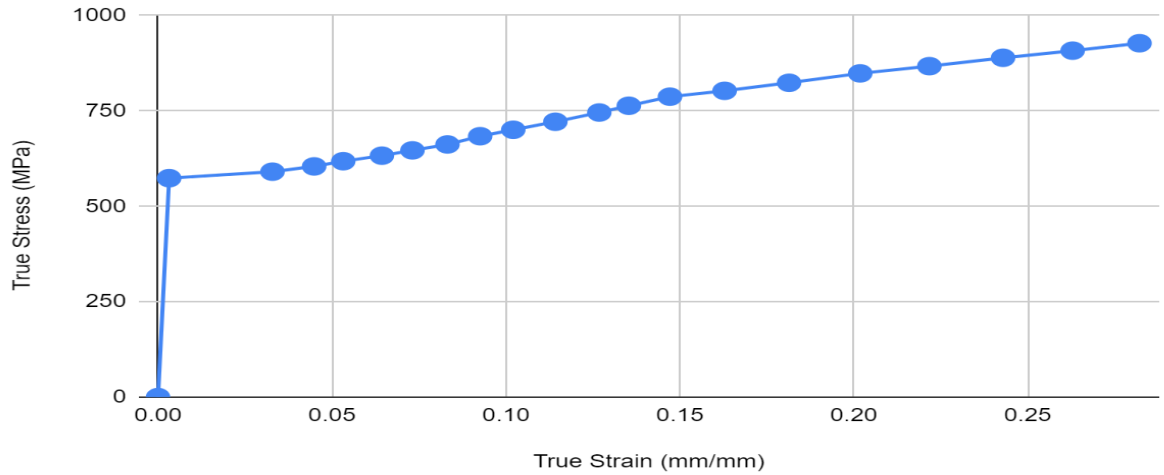

Graph.32. True Stress-True Strain curve of Specimen TC-2-2-5

Specimen TC-2-2-6

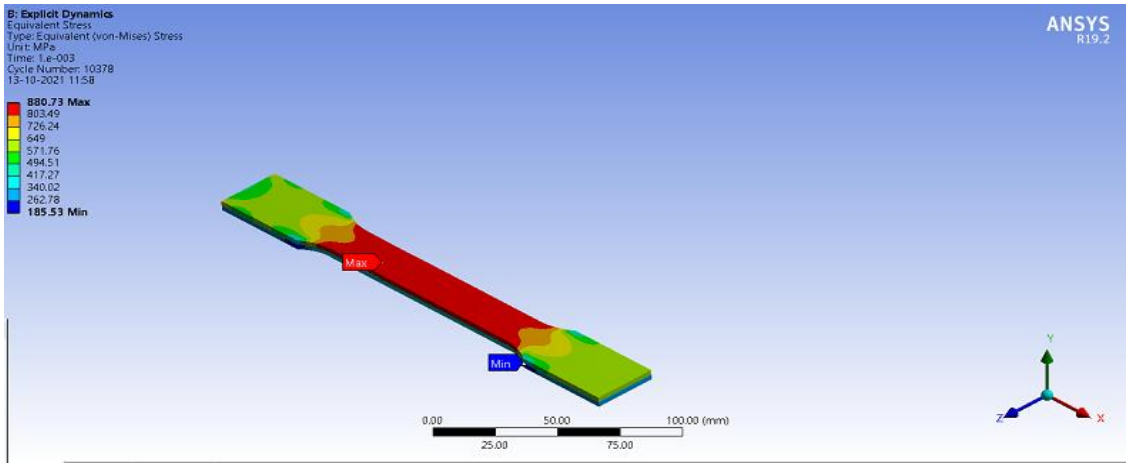

Fig.79. Equivalent(Von-Mises) Stress of Specimen TC-2-2-6

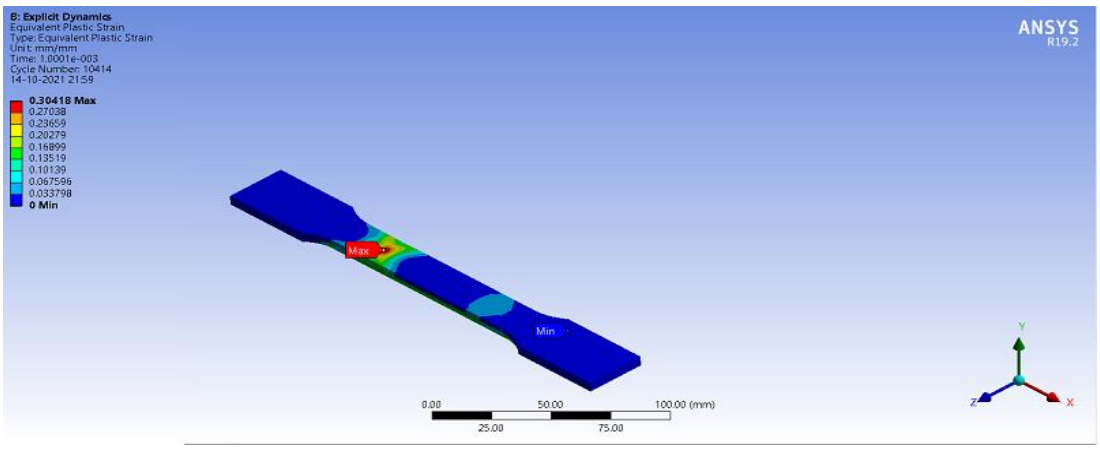

Fig.80. Equivalent Plastic Strain of Specimen TC-2-2-6

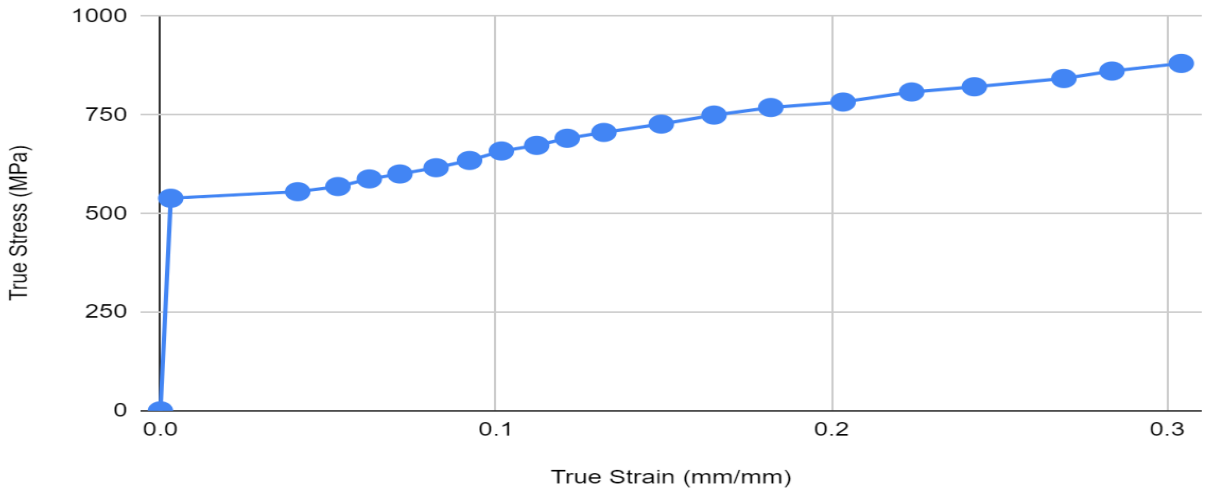

Graph.33. True Stress-True Strain curve of Specimen TC-2-2-6

Specimen TC-2-2-7

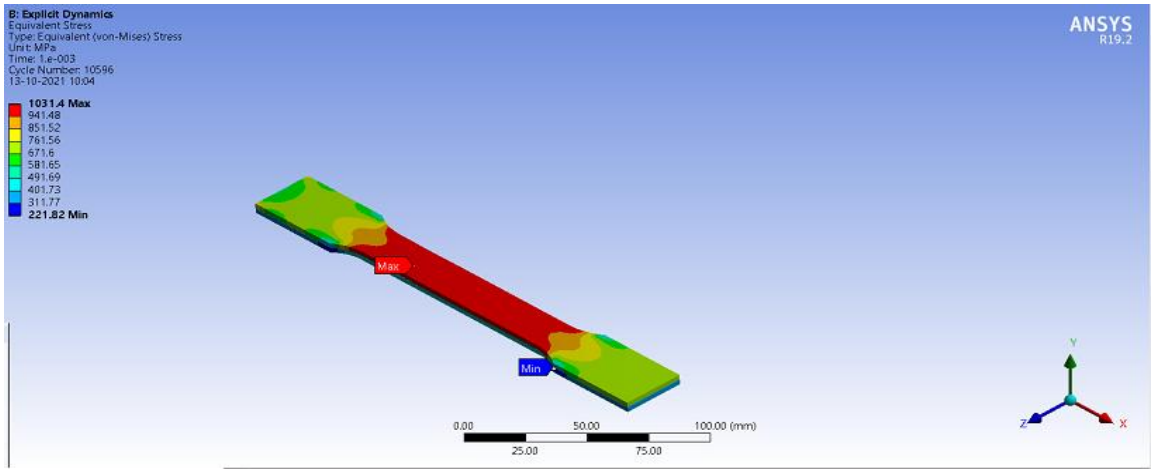

Fig.81. Equivalent(Von-Mises) Stress of Specimen TC-2-2-7

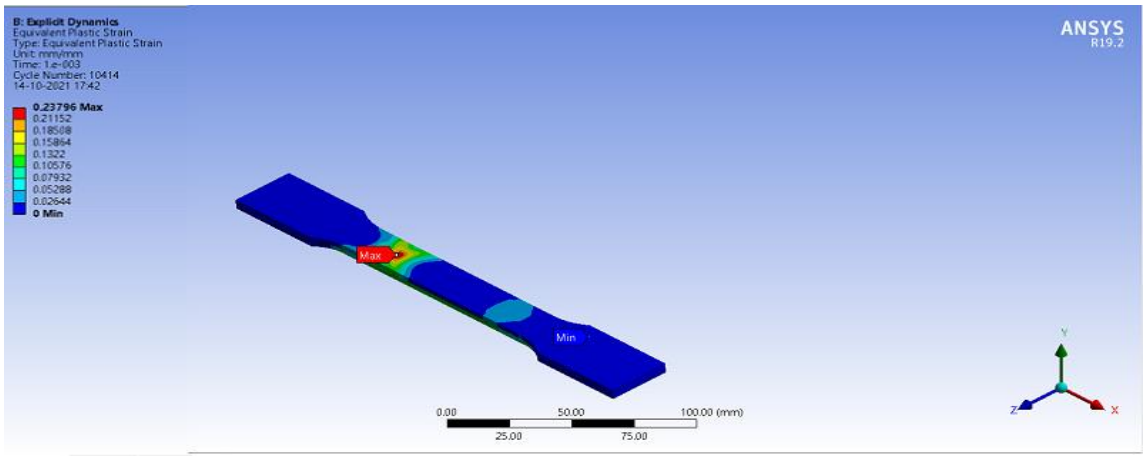

Fig.82. Equivalent Plastic Strain of Specimen TC-2-2-7

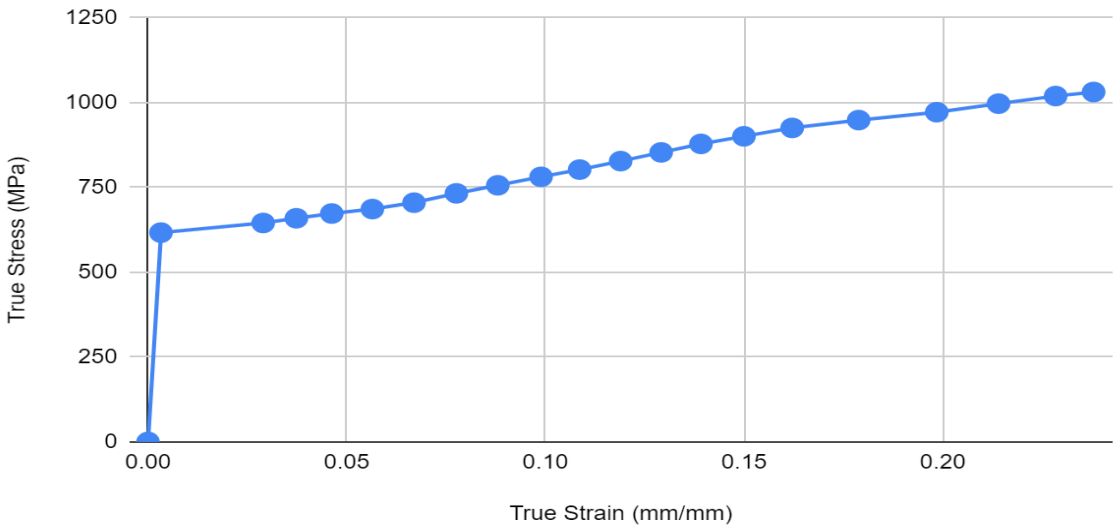

Graph.34. True Stress-True Strain curve of Specimen TC-2-2-7

Specimen TC-2-2-8

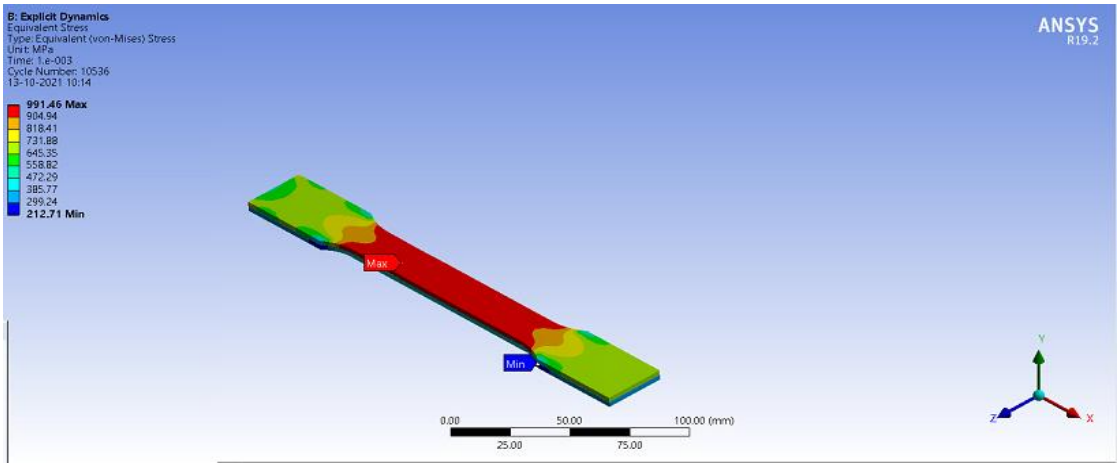

Fig.83. Equivalent(Von-Mises) Stress of Specimen TC-2-2-8

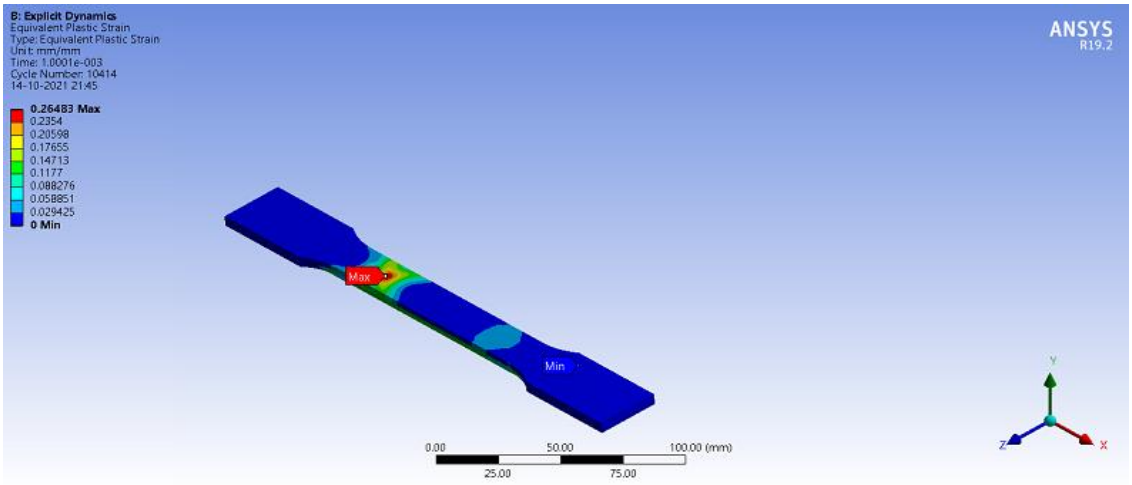

Fig.84. Equivalent Plastic Strain of Specimen TC-2-2-8

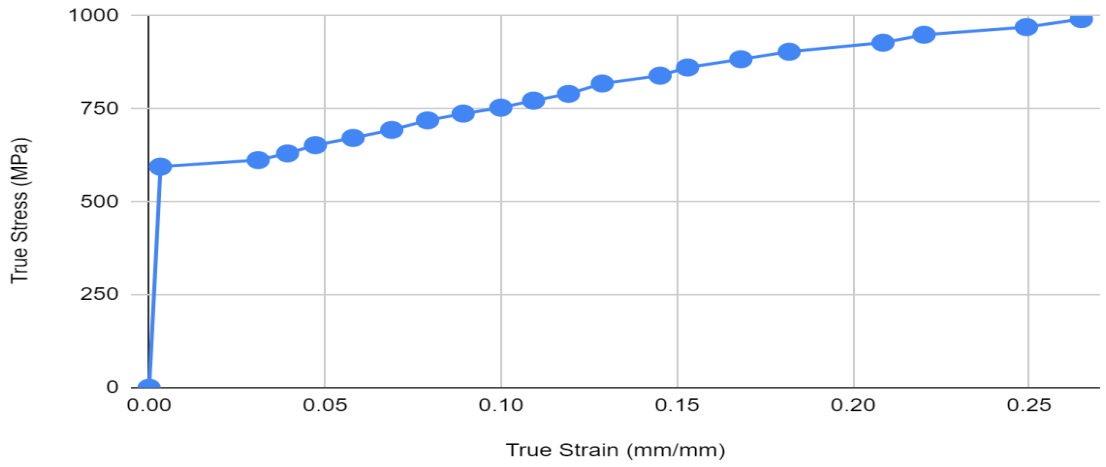

Graph.35. True Stress-True Strain curve of Specimen TC-2-2-8

Specimen TC-2-2-9

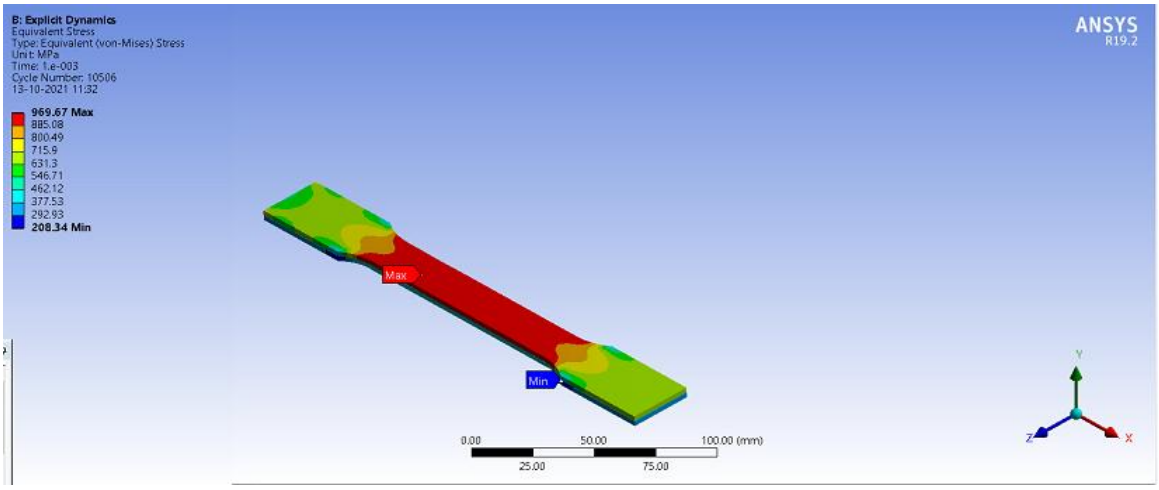

Fig.85. Equivalent(Von-Mises) Stress of Specimen TC-2-2-9

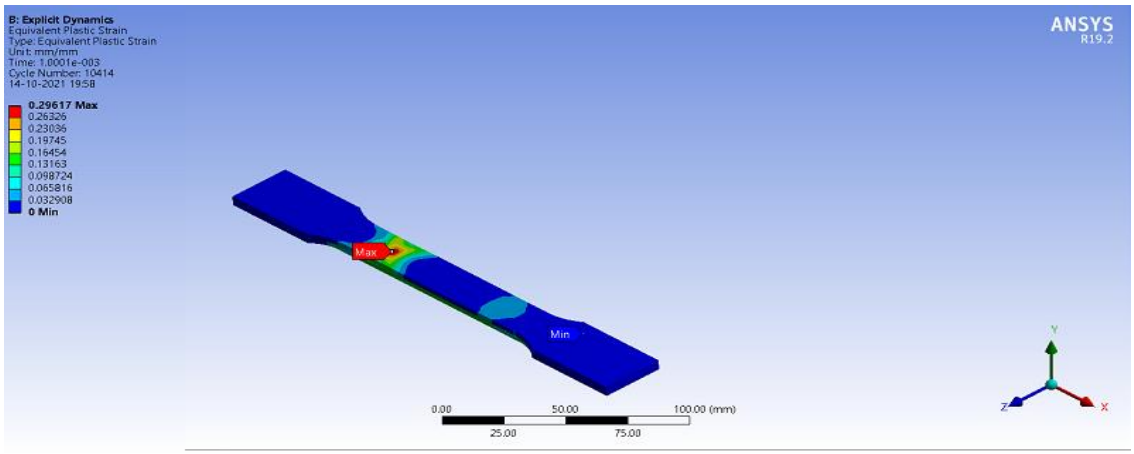

Fig.86. Equivalent Plastic Strain of Specimen TC-2-2-9

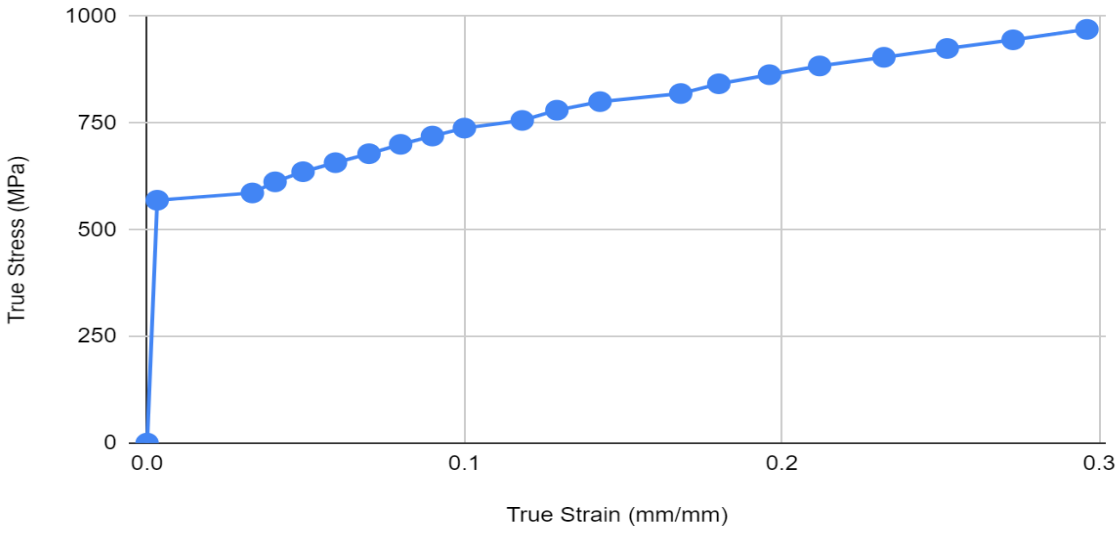

Graph.36. True Stress-True Strain curve of Specimen TC-2-2-9

Specimen TC-0-2-1

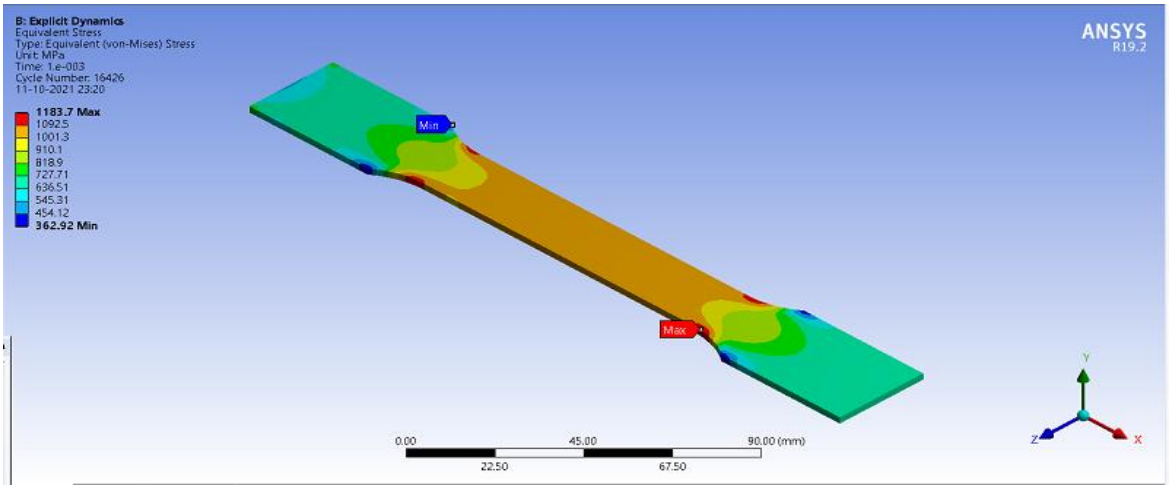

Fig.87. Equivalent(Von-Mises) Stress of Specimen TC-0-2-1

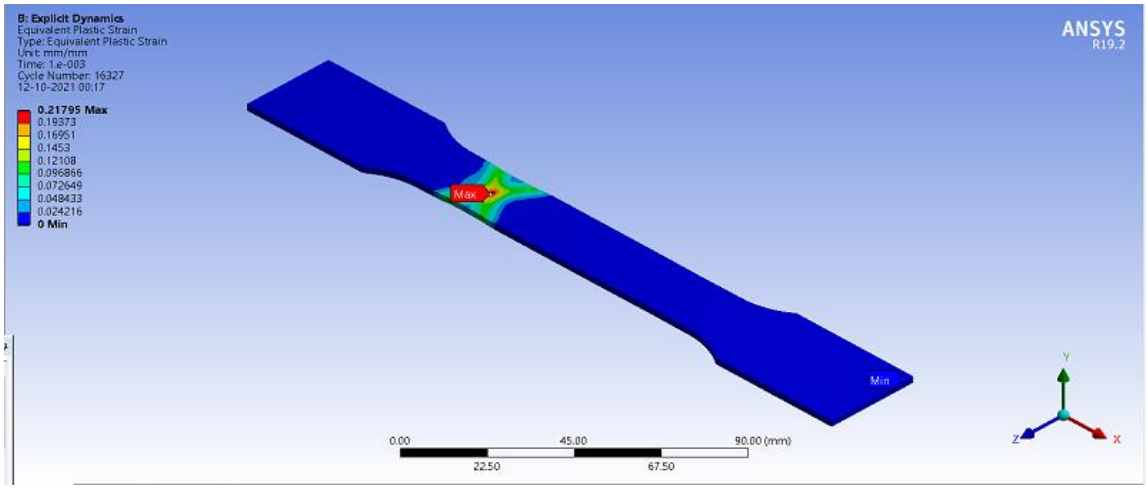

Fig.88. Equivalent Plastic Strain of Specimen TC-0-2-1

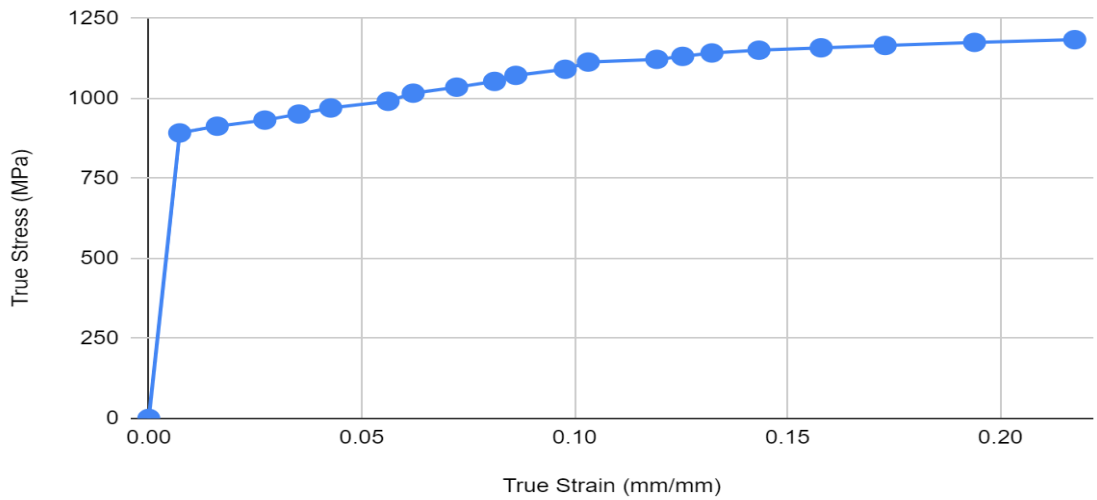

Graph.37. True Stress-True Strain curve of Specimen TC-0-2-1

Specimen TC-0-2-2

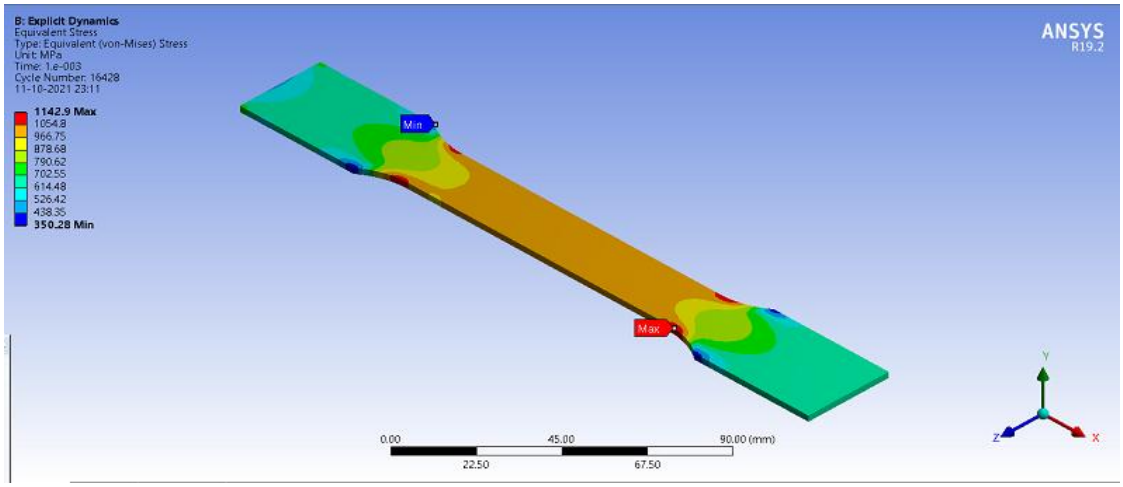

Fig.89. Equivalent(Von-Mises) Stress of Specimen TC-0-2-2

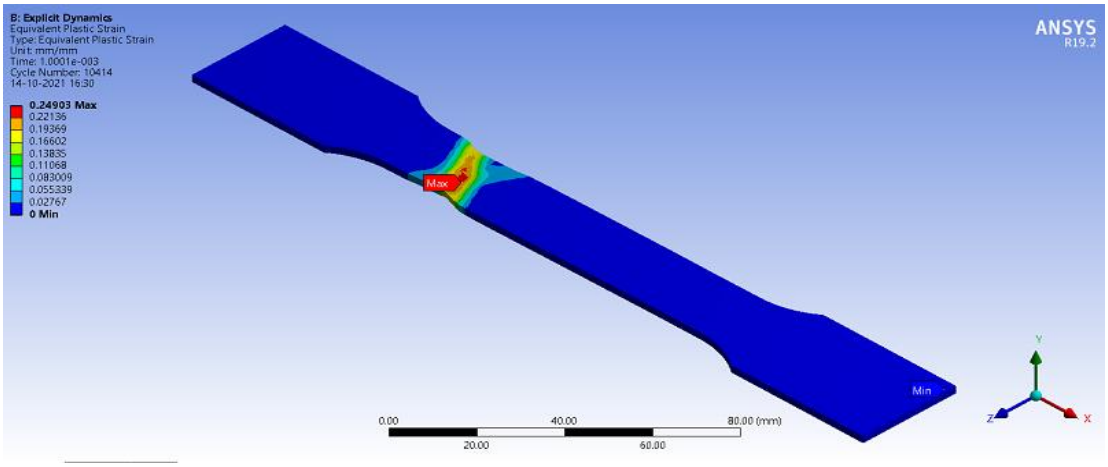

Fig.90. Equivalent Plastic Strain of Specimen TC-0-2-2

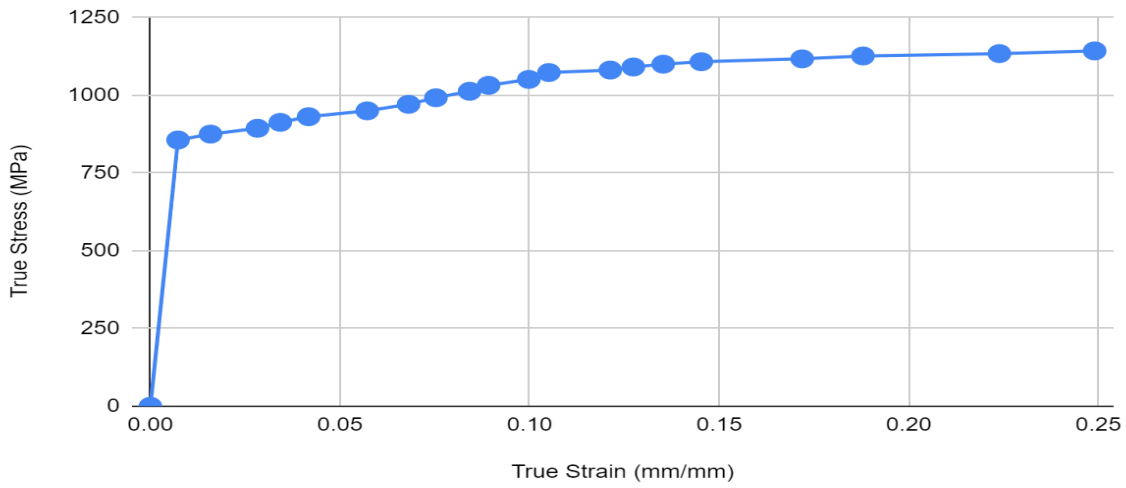

Graph.38. True Stress-True Strain curve of Specimen TC-0-2-2

Specimen TC-0-2-3

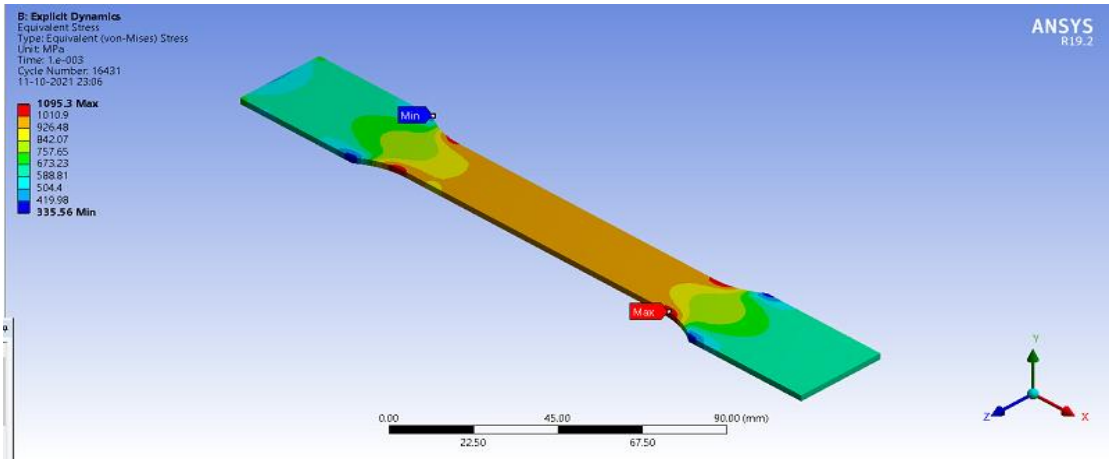

Fig.91. Equivalent(Von-Mises) Stress of Specimen TC-0-2-3

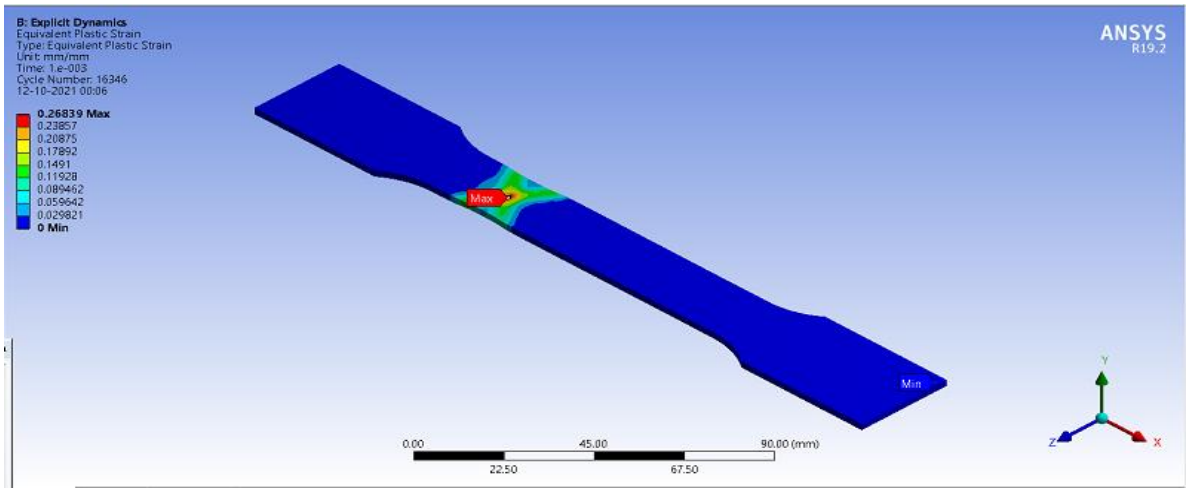

Fig.92. Equivalent Plastic Strain of Specimen TC-0-2-3

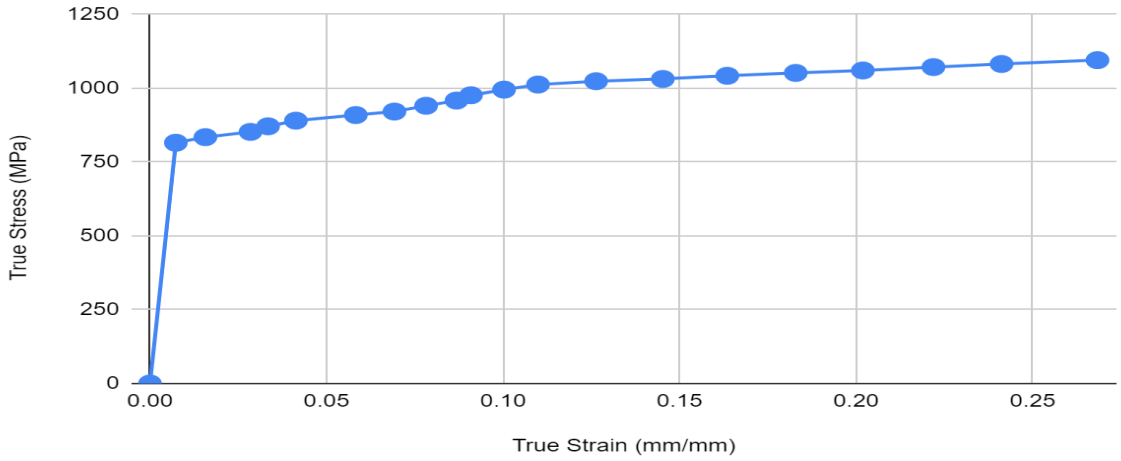

Graph.39. True Stress-True Strain curve of Specimen TC-0-2-3

Specimen TC-0-2-4

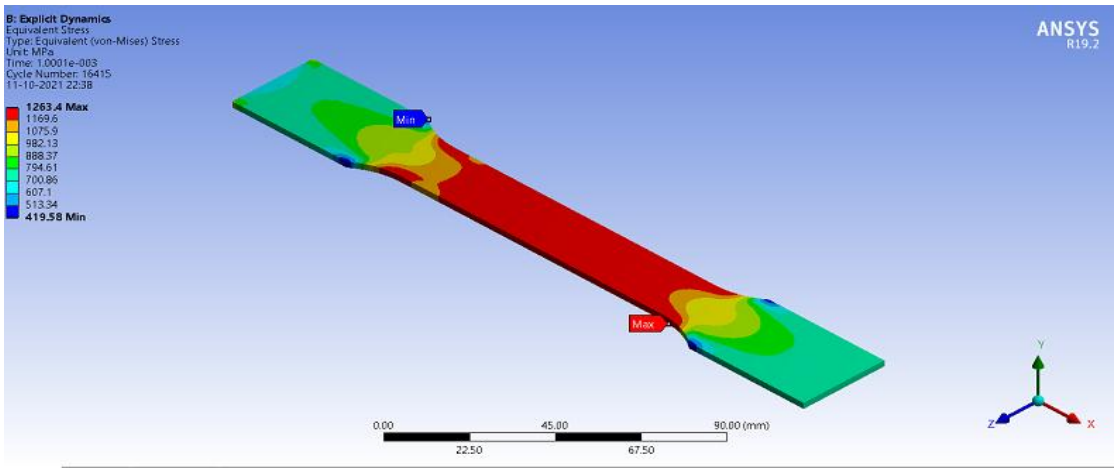

Fig.93. Equivalent(Von-Mises) Stress of Specimen TC-0-2-4

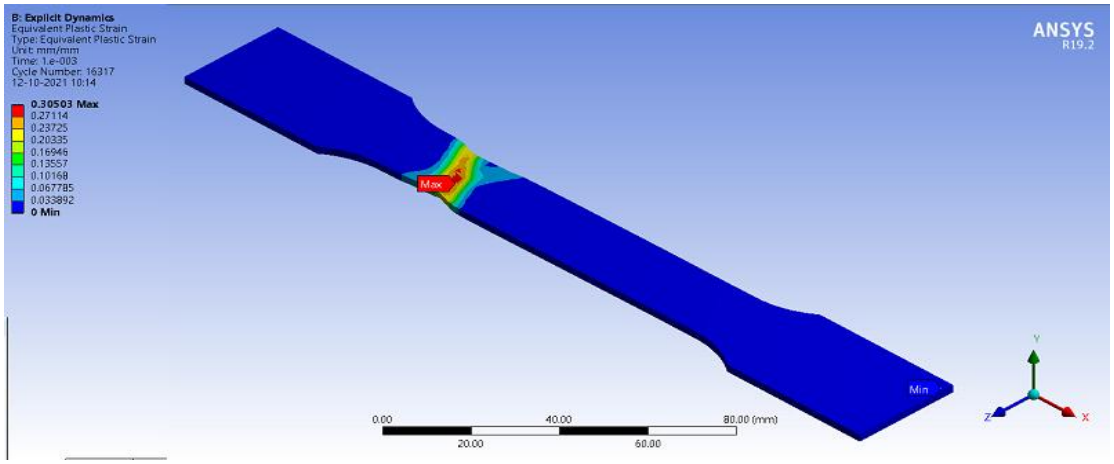

Fig.94. Equivalent Plastic Strain of Specimen TC-0-2-4

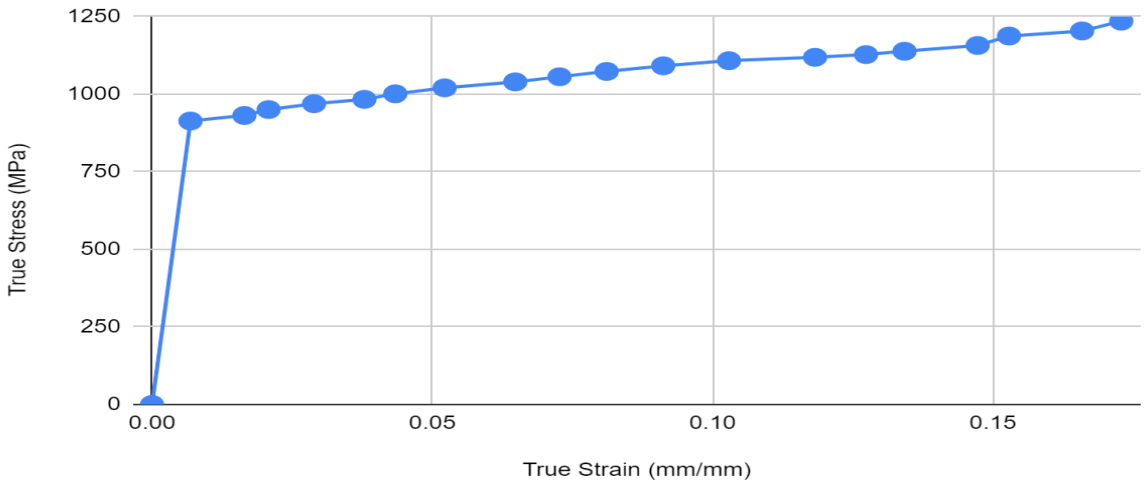

Graph.40. True Stress-True Strain curve of Specimen TC-0-2-4

Specimen TC-0-2-5

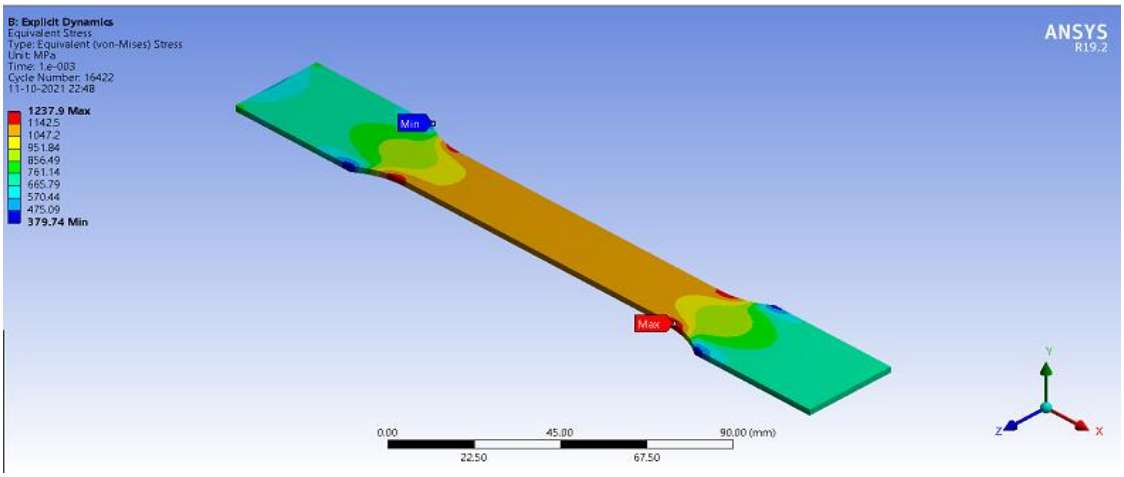

Fig.95. Equivalent(Von-Mises) Stress of Specimen TC-0-2-5

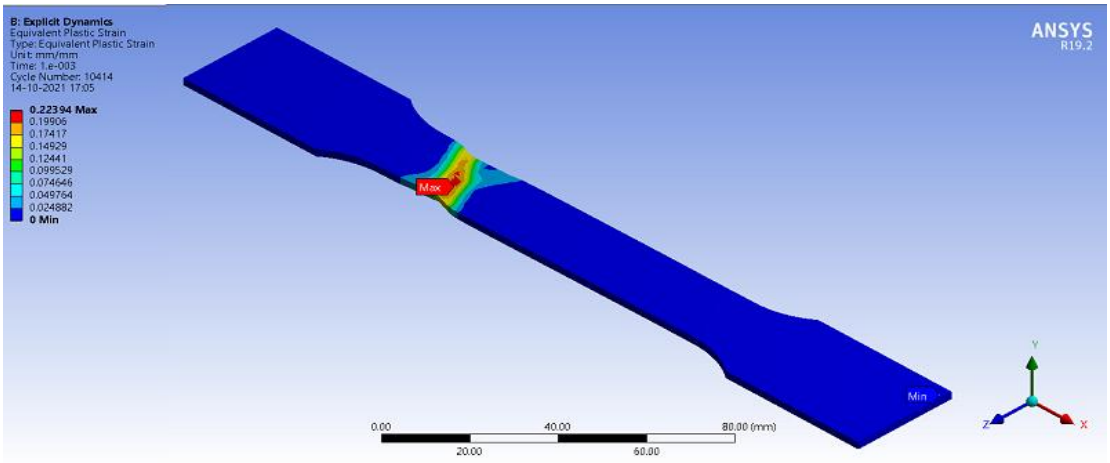

Fig.96. Equivalent Plastic Strain of Specimen TC-0-2-5

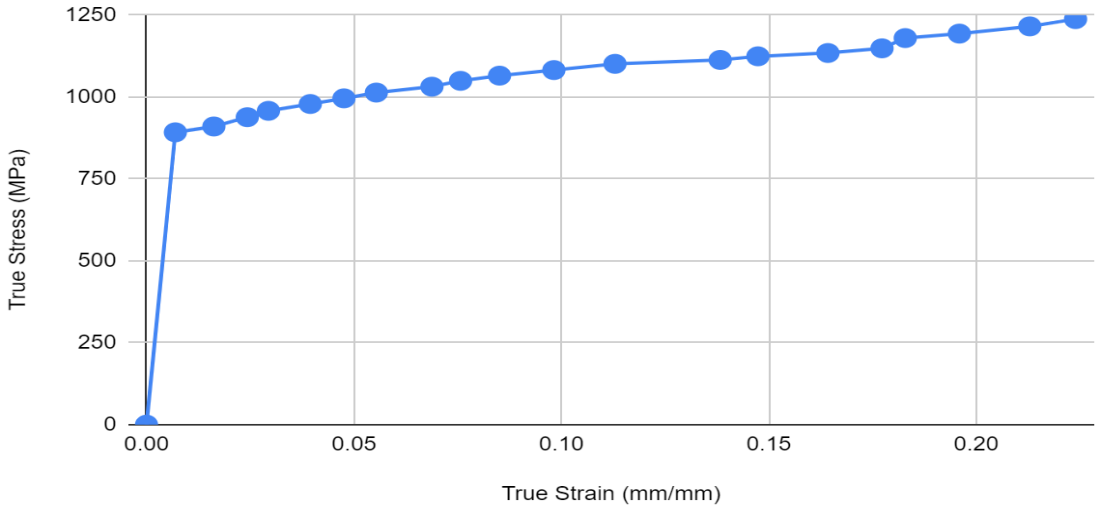

Graph.41. True Stress-True Strain curve of Specimen TC-0-2-5

Specimen TC-0-2-6

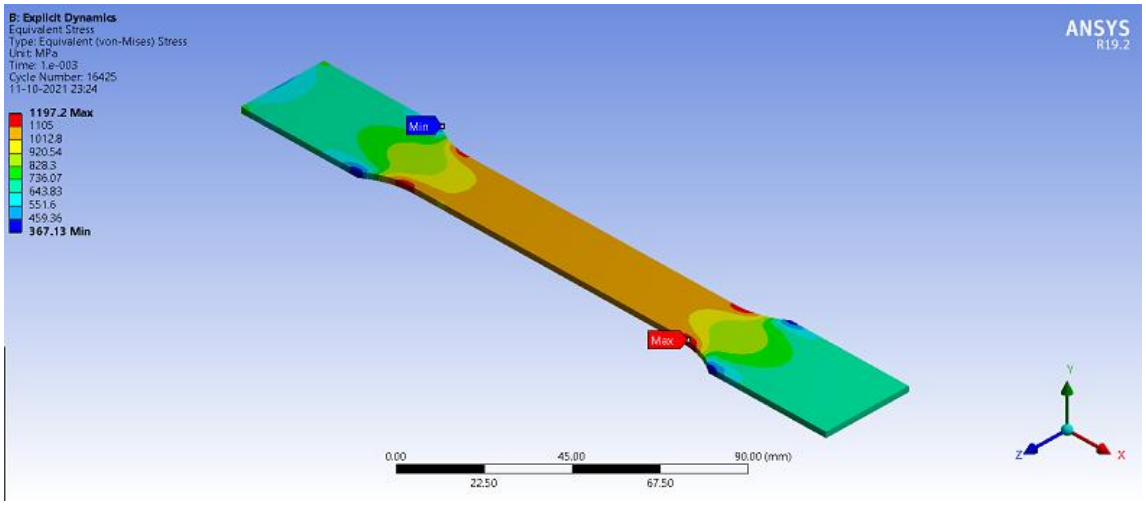

Fig.97. Equivalent(Von-Mises) Stress of Specimen TC-0-2-6

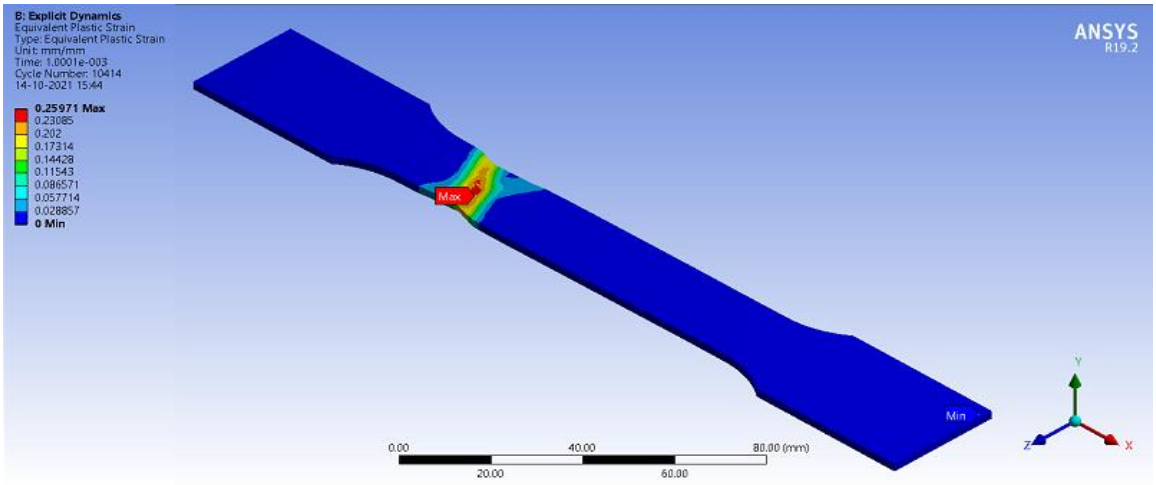

Fig.98. Equivalent Plastic Strain of Specimen TC-0-2-6

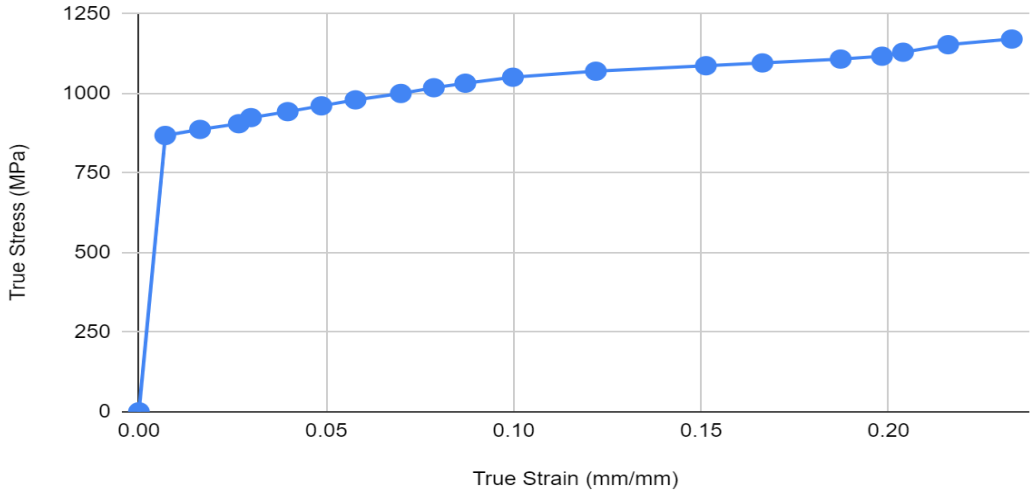

Graph.42. True Stress-True Strain curve of Specimen TC-0-2-6

Specimen TC-0-2-7

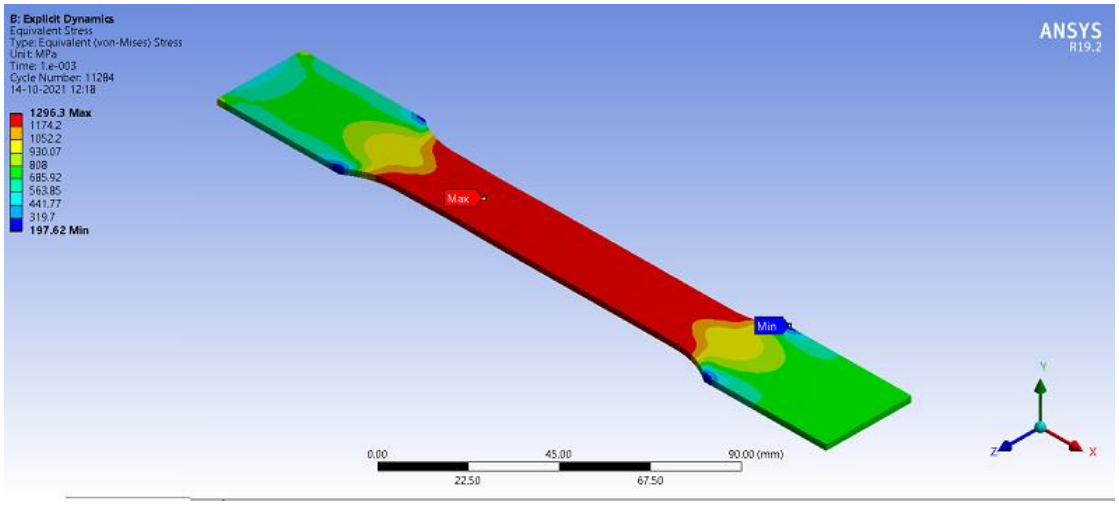

Fig.99. Equivalent(Von-Mises) Stress of Specimen TC-0-2-7

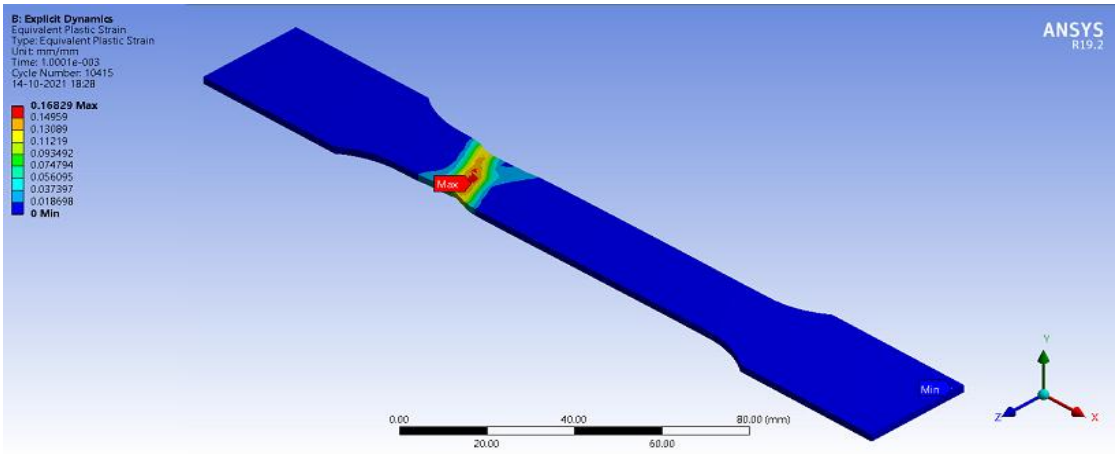

Fig.100. Equivalent Plastic Strain of Specimen TC-0-2-7

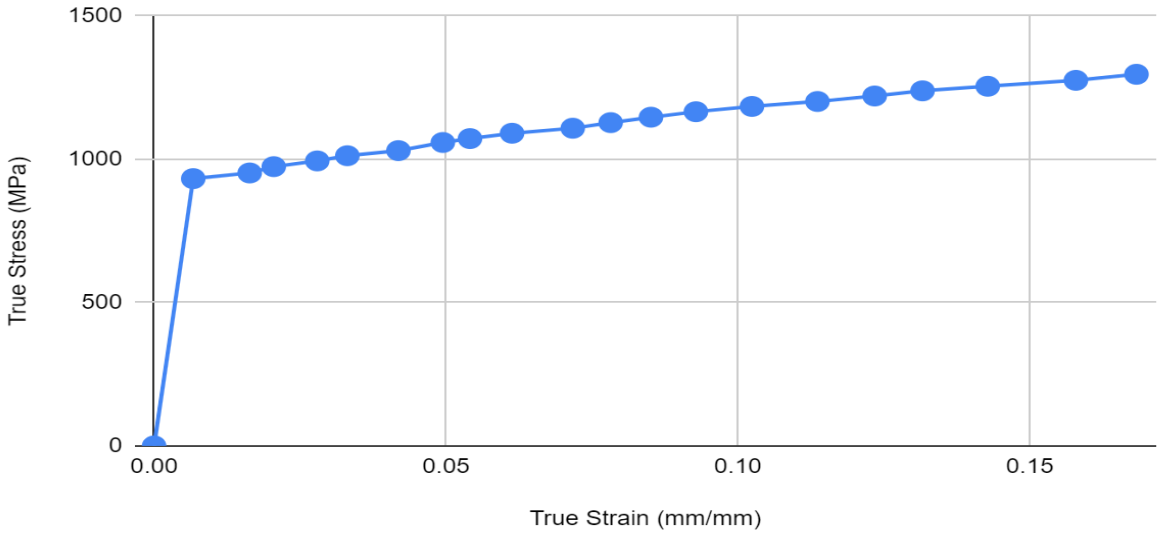

Graph.43. True Stress-True Strain curve of Specimen TC-0-2-7

Specimen TC-0-2-8

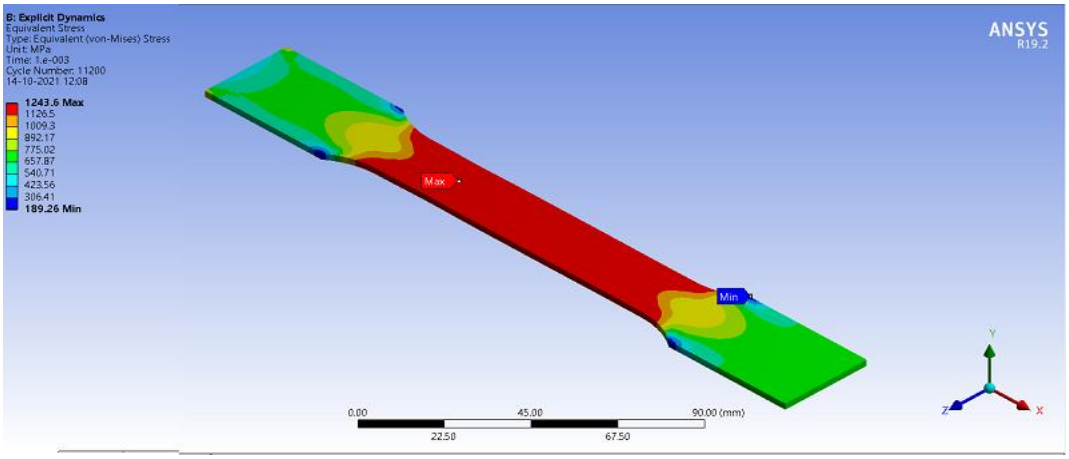

Fig.101. Equivalent(Von-Mises) Stress of Specimen TC-0-2-8

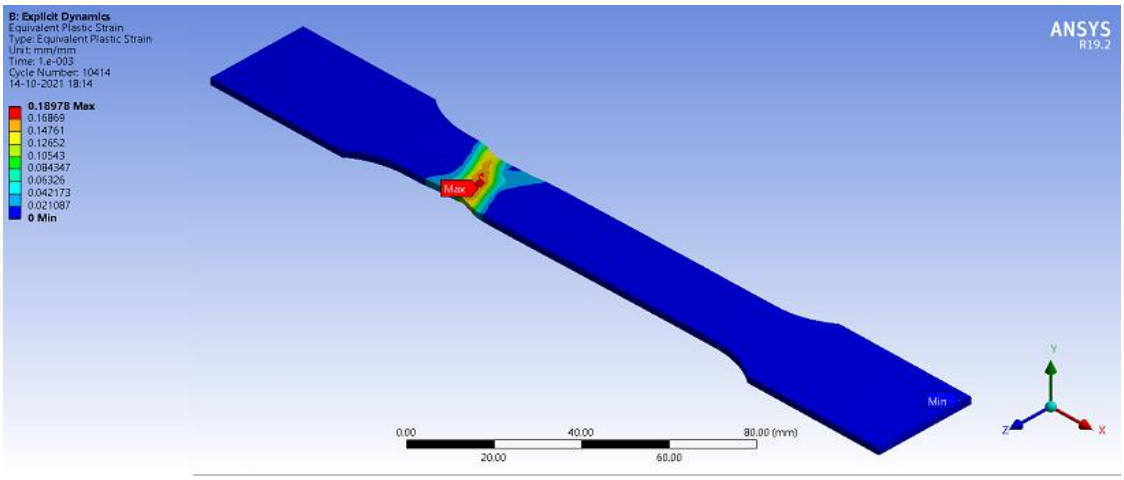

Fig.102. Equivalent Plastic Strain of Specimen TC-0-2-8

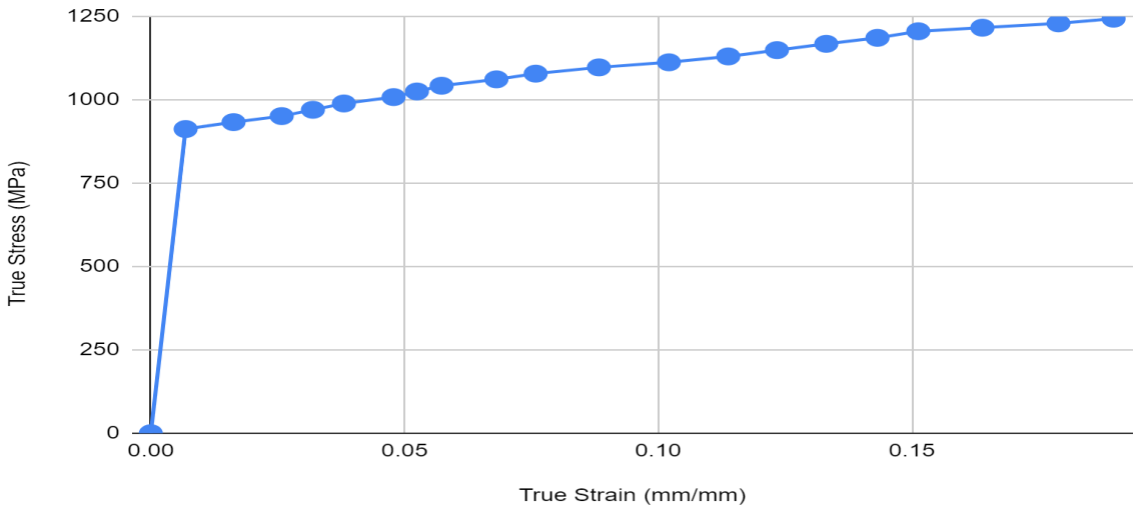

Graph.44. True Stress-True Strain curve of Specimen TC-0-2-8

Specimen TC-0-2-9

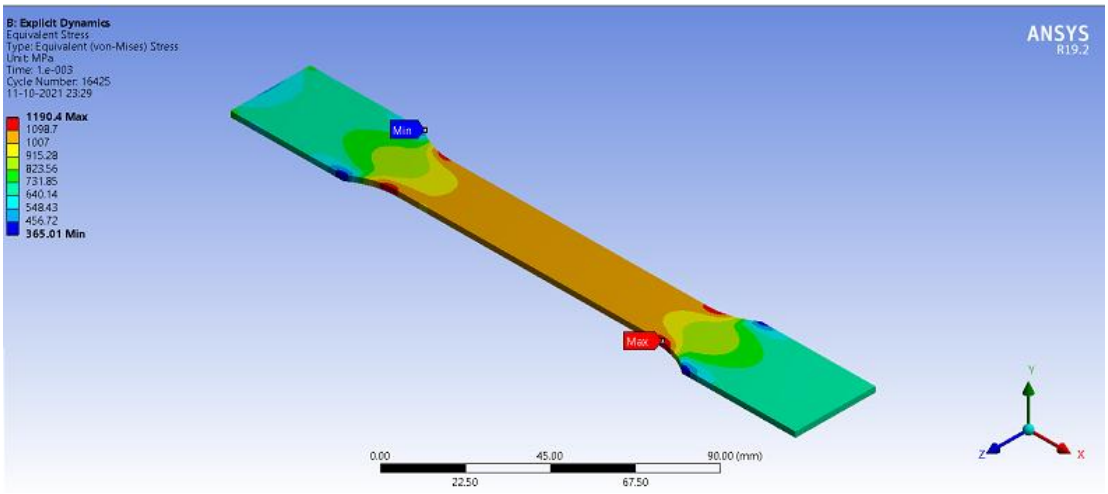

Fig.103. Equivalent(Von-Mises) Stress of Specimen TC-0-2-9

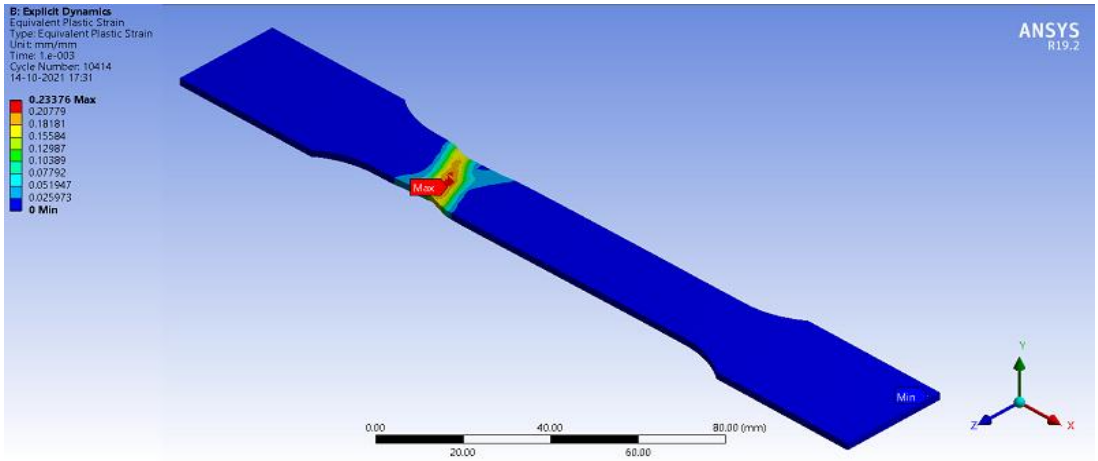

Fig.104. Equivalent Plastic Strain of Specimen TC-0-2-9

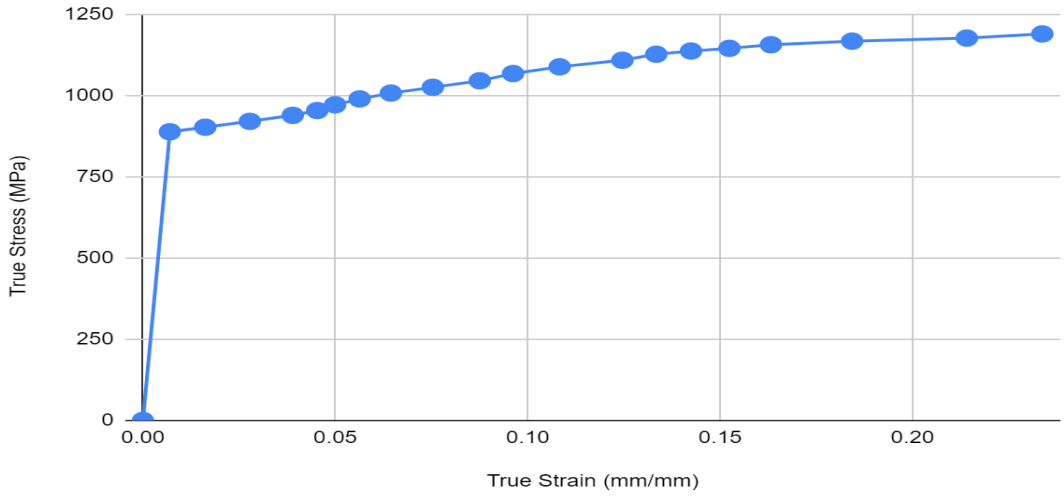

Graph.45. True Stress-True Strain curve of Specimen TC-0-2-9

CHAPTER-6
CALCULATION AND RESULT

CALCULATION

6.1 Determination of material constant

6.1.1 Material Constant A, B, and n

The material constant A was determined from the stress-strain curve at a reference strain rate of 1/sec and the reference temperature of 293K.

For the determination of material constant B and n, taking deformation temperature T= Tref= 293K and the deformation strain rate $\acute{\varepsilon} = \acute{\varepsilon}ref = 1/sec$.

Then equation(1) is modified into as follows

$$\sigma = (A + B\varepsilon^n) \text{.....(2)}$$

In this equation, the influence of strain rate strengthening and thermal softening effects are neglected.

Then by rearranging equation 2 and taking natural logarithm on both sides.

Modified Equation -

$$\ln(\sigma - A) = n \ln\varepsilon + \ln B \text{……(3)}$$

Then draw a linear relationship plot between $\ln(\sigma - A)$ and $\ln\varepsilon$, the intercept of the line on the Y-axis will give the value of B, and the slope of the line will give the value of n.

6.1.2 Material Constant C

To determine material constant C, taking deformation temperature T = Tref = 293K

Then the equation 1 can be written as

$$\sigma = (A + B\varepsilon^n)(1 + C \ln\acute{\varepsilon}^*) \text{.....(4)}$$

The influence of thermal softening effects is neglected here. The value of material constants A, B, and n were put in equation 4 then by rearranging the equation 4

Modified Equation-

$$\sigma /(A + B\varepsilon^n) = (1 + C \ln\acute{\varepsilon}^*) \text{.....(5)}$$

Plot a graph between $\sigma /(A + B\varepsilon^n)$ and $\ln\acute{\varepsilon}^*$ by considering flow stress values at three strain rates (1 /sec,10 /sec, and 100/sec) and the slope of the line gives the value of constant C.

6.1.3 Material Constant, m

To determine the material constant m, taking $\dot{\varepsilon} = \dot{\varepsilon}ref = 1\ s^{-1}$. Then the equation 1 can be written as

$$\sigma = (A + B\varepsilon^n)(1 - T * m) \text{.....(6)}$$

For this, the influence of strain rate strengthening effects is ignored. Equation 6 is rearranged and takes a natural logarithm.

$$\ln(1 - \sigma/ (A + B\varepsilon^{n})) = m \ln T^{*} \text{.....(7)}$$

By putting the values of A, B, and n into equation 7 and plot the graph between ln(1 − σ/ (A + B^ε n)) and lnT* for the flow stress values of two different temperatures (673K and 973K). The slope of the fitted curve gives the value of material constant m.

RESULT

6.2 Material Constants for Clad Ratio-0.17, clad ratio-0.29, and clad ratio-0.5

6.2.1 Material Constants for Clad Ratio-0.17

- **Material Constant A-** The material constant A was determined to be 440.46 MPa from the stress-strain curve at a reference strain rate of 1/sec and reference temperature of 293K.
- **Material Constant B and n**-Material constant B is the intercept of the line as shown in fig 105 which gives a value of log(B)=5.558 then B = 259.3 and n is the slope of the line which gives a value of 0.394.

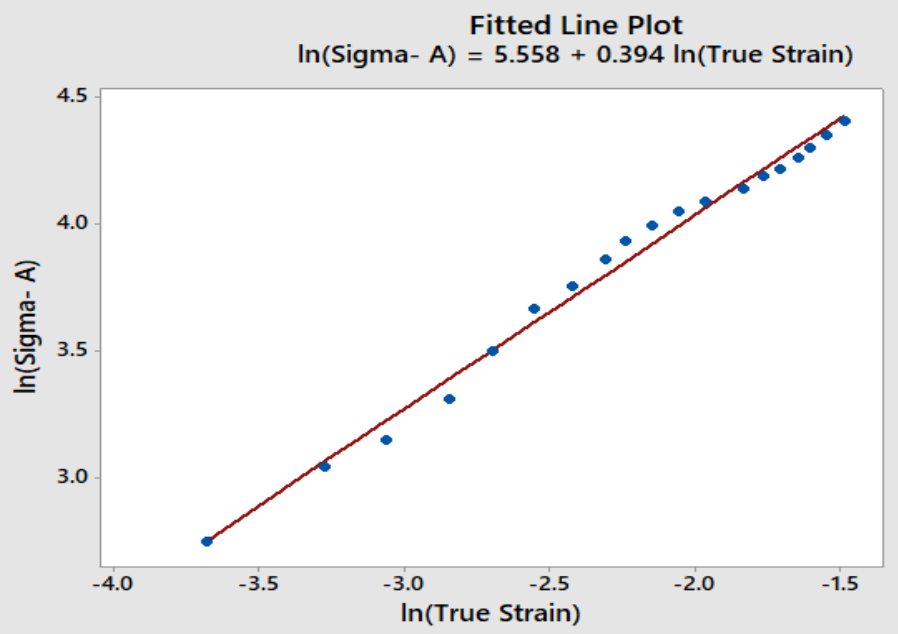

Fig.105. Plot between ln(σ − A) and lnε for clad ratio-0.17 under reference conditions

- **Material Constant C-** C is the slope of the line as shown in fig.106 which gives a value of 0.03599.

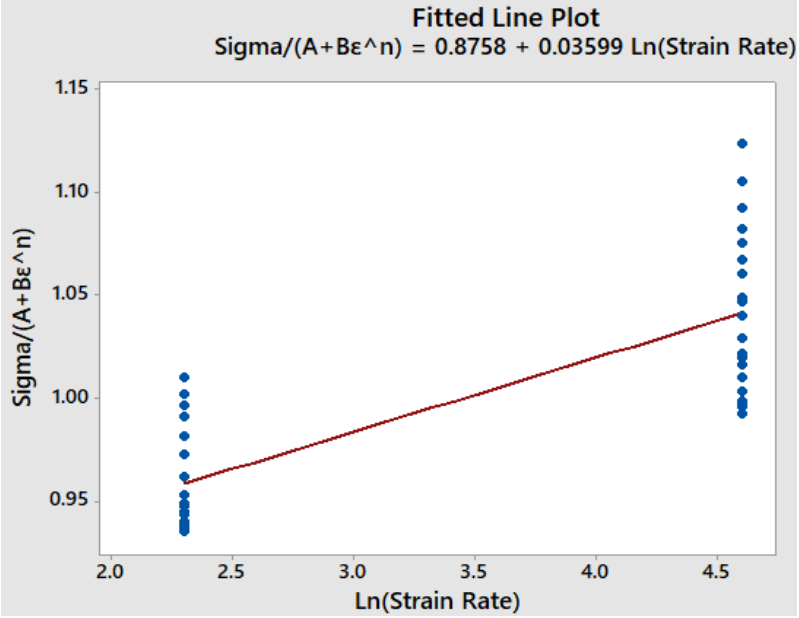

Fig.106. Plot between $\sigma/(A+B\varepsilon^n)$ and $\ln\dot{\varepsilon}^*$ for clad ratio-0.17 under the reference conditions

- **Material Constant, m-** The slope of the fitted curve as shown in fig.107 gives the value of material constant m as 0.2196

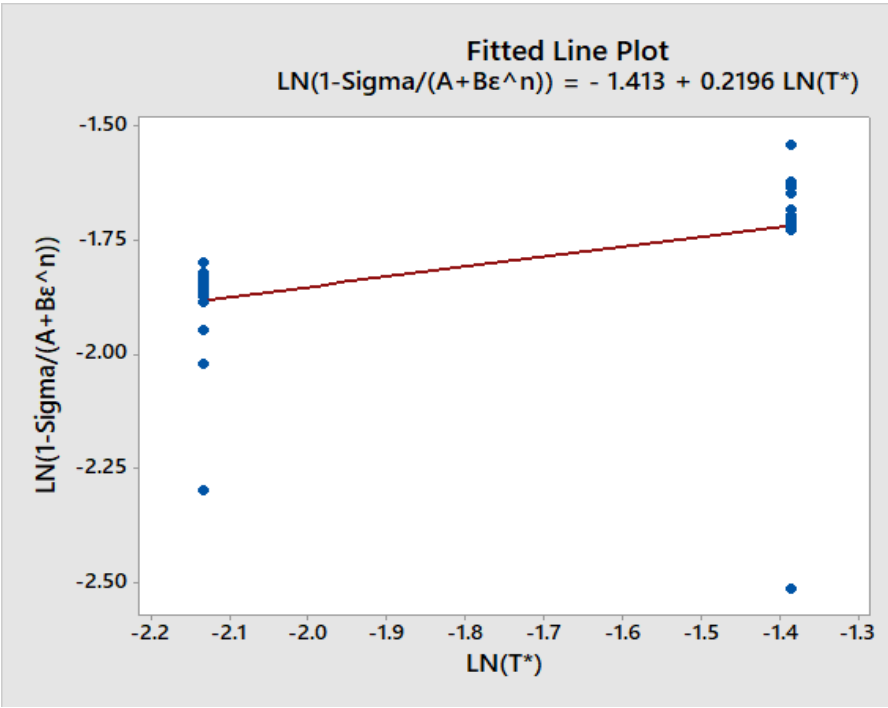

Fig.107. Plot between $\ln(1-\sigma/(A+B\varepsilon^n))$ and lnT* for clad ratio-0.17 under the reference conditions.

6.2.2 Material Constant for Clad Ratio-0.29

- **Material Constant A-** The material constant A was determined to be 496.52 MPa from the stress-strain curve at a reference strain rate of 1/sec and reference temperature of 293K.
- **Material Constant B and n**-Material Constant B is the intercept of the line as shown in fig.108 which gives a value of ln(B)= 5.901 then B=365.402 and n is the slope of the line which gives a value of 0.412.

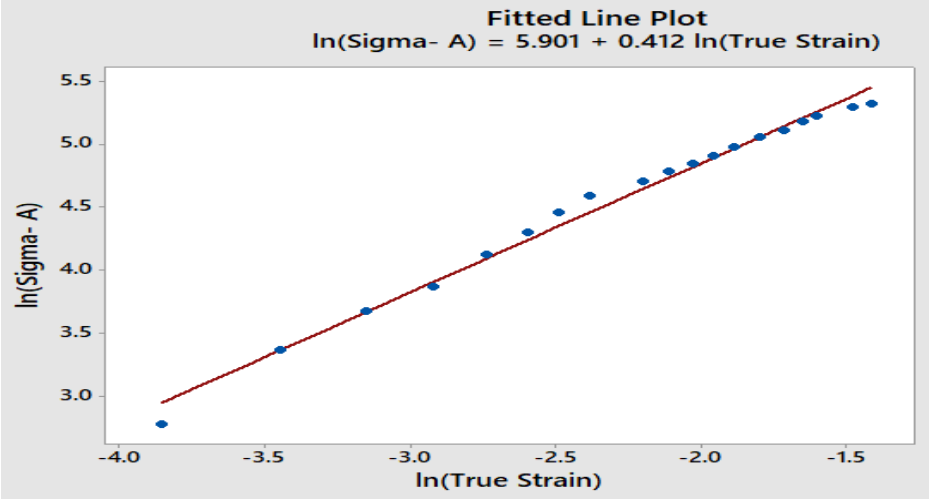

Fig.108. Plot between ln(σ − A) and lnε for clad ratio-0.29 under reference Conditions

- **Material Constant C-** C is the slope of the line as shown in fig.109 which gives a value of 0.03061.

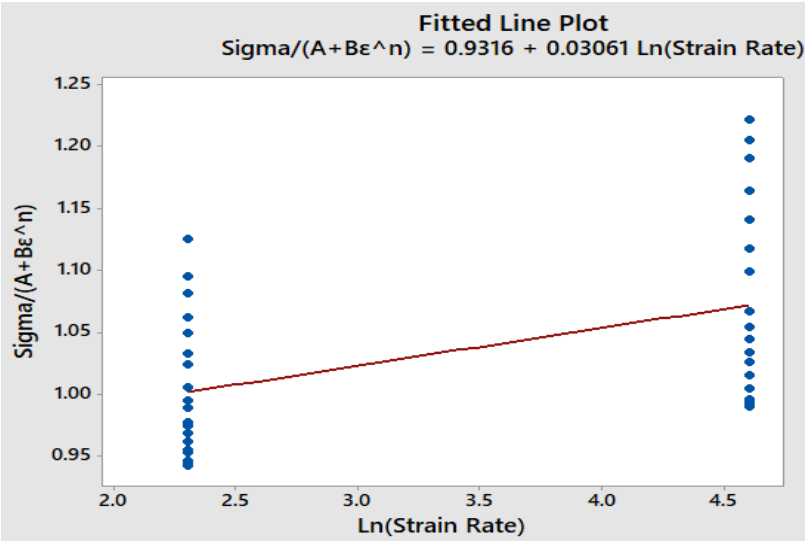

Fig.109. Plot between σ /(A+Bε^{n}) and lnε$^{\cdot}$* for clad ratio-0.29 under the reference conditions.

- **Material Constant, m-** The slope of the fitted curve as shown in fig.110 gives the value of material constant m as 0.3864.

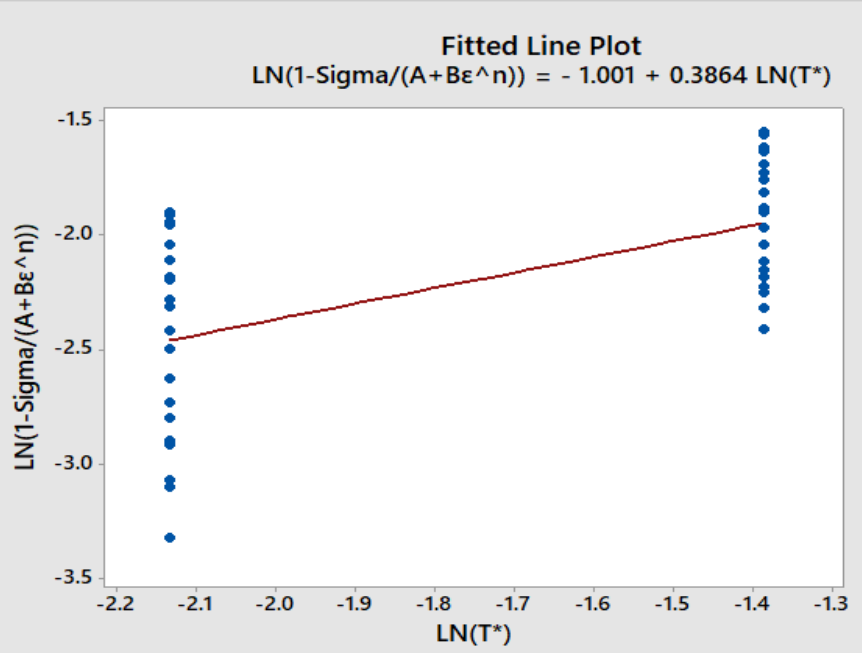

Fig.110. Plot between ln (1 − σ /(A+Bε n)) and lnT* for clad ratio-0.29 under the reference conditions.

6.2.3 Material Constant for Clad Ratio-0.5

- **Material Constant A-** The material constant A was determined to be 585.39 MPa from the stress-strain curve at a reference strain rate of 1/sec and reference temperature of 293K.
- **Material Constant B and n-** Material Constant B is the intercept of the line as shown in fig.111 which gives a value of ln(B)= 6.182 then B=483.95 and n is the slope of the line which gives a value of 0.445.

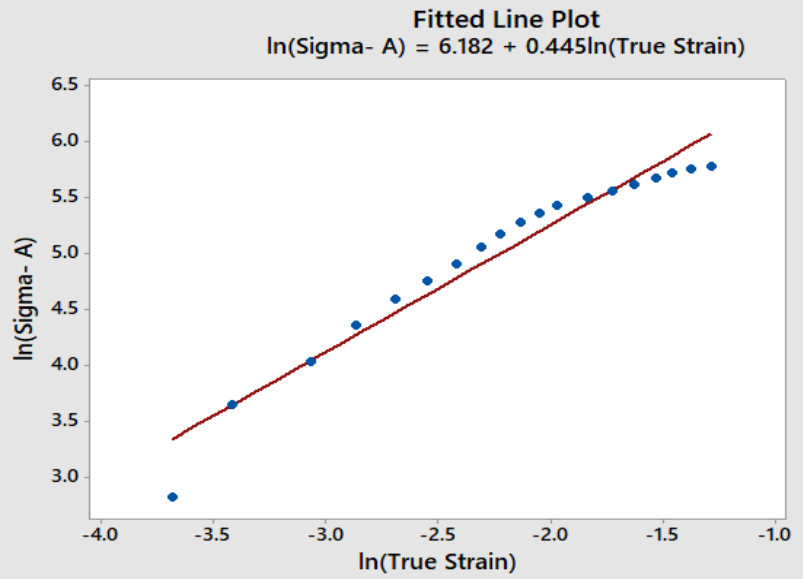

Fig.111. Plot between ln(σ − A) and lnε for clad ratio-0.5 under reference conditions.

Material Constant C- C is the slope of the line as shown in fig.112 which gives a value of 0.02759.

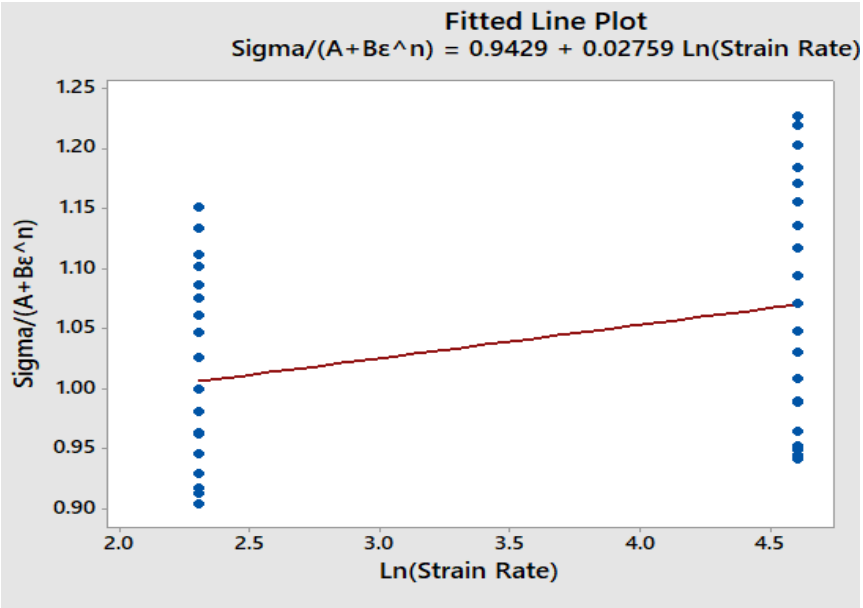

Fig.112. Plot between ln(σ − A) and lnε for clad ratio-0.5 under reference conditions.

- **Material Constant, m-** The slope of the fitted curve as shown in fig 113 gives the value of material constant m as 0.4768.

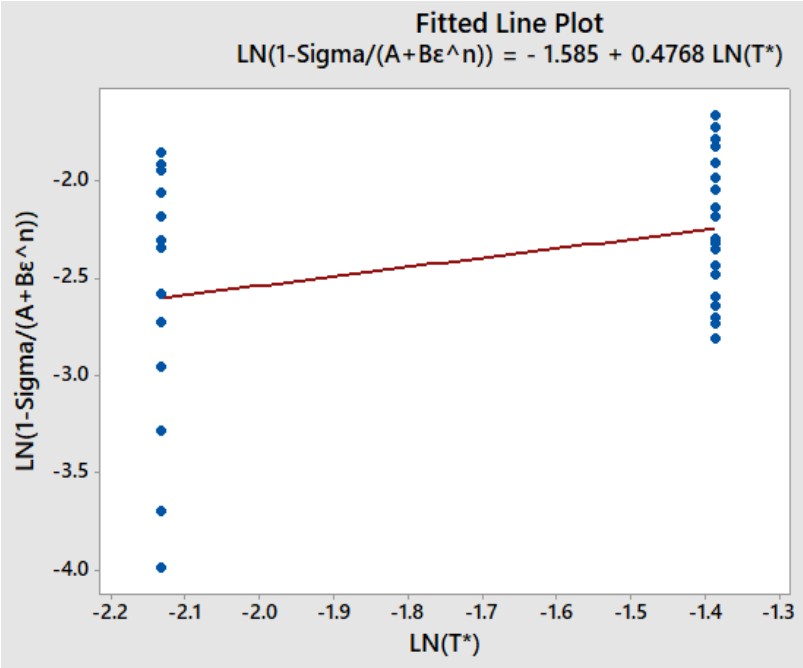

Fig.113. Plot between ln $(1 - \sigma / (A+B\varepsilon^n))$ and lnT* for clad ratio-0.29 under the reference conditions.

Table.11. Calculated J-C parameters for clad ratio-0.17,0.29 and 0.5.

Clad Ratio	A	B	n	C	m
0.17	457.71	259.3	0.394	0.03599	0.2196
0.29	496.52	365.402	0.412	0.03061	0.3864
0.5	585.39	483.95	0.445	0.02759	0.4768

6.3 Effect of Temperature and Strain Rate on the stress-strain curve of TC-bimetallic steel

- **Temperature-** The stress-strain curve and the flow stress are dependent on the temperature of the surrounding area on which the test is conducted. As shown in figures 114, 115, and 116 the value of the temperature increases, the strength decreases, and ductility increases due to the softening effect at higher temperatures. These stress-strain curves are generated by keeping the strain rate constant with varying temperatures.

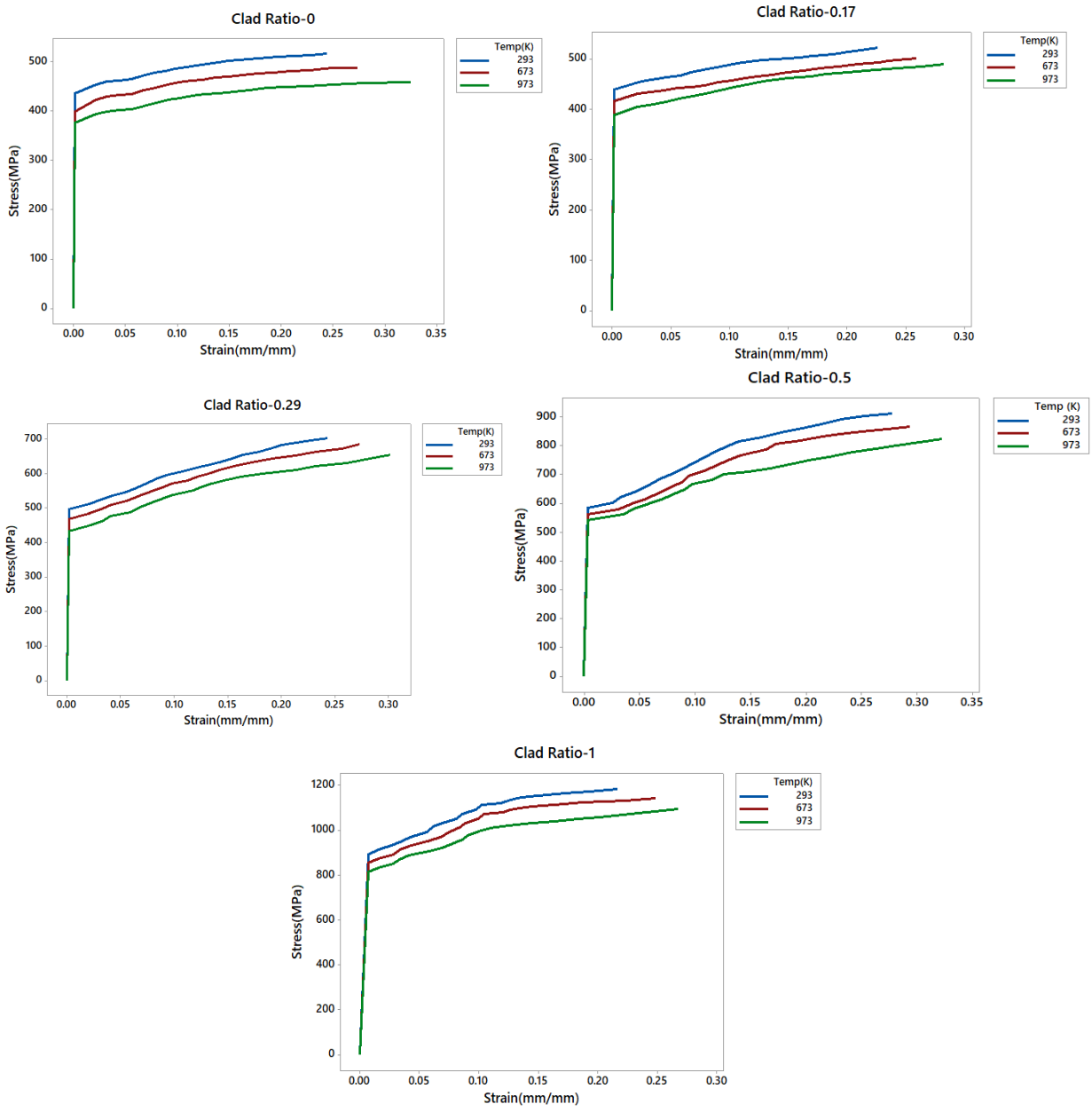

Fig.114. True Stress-true strain at various temperatures under strain rate of 1/sec.

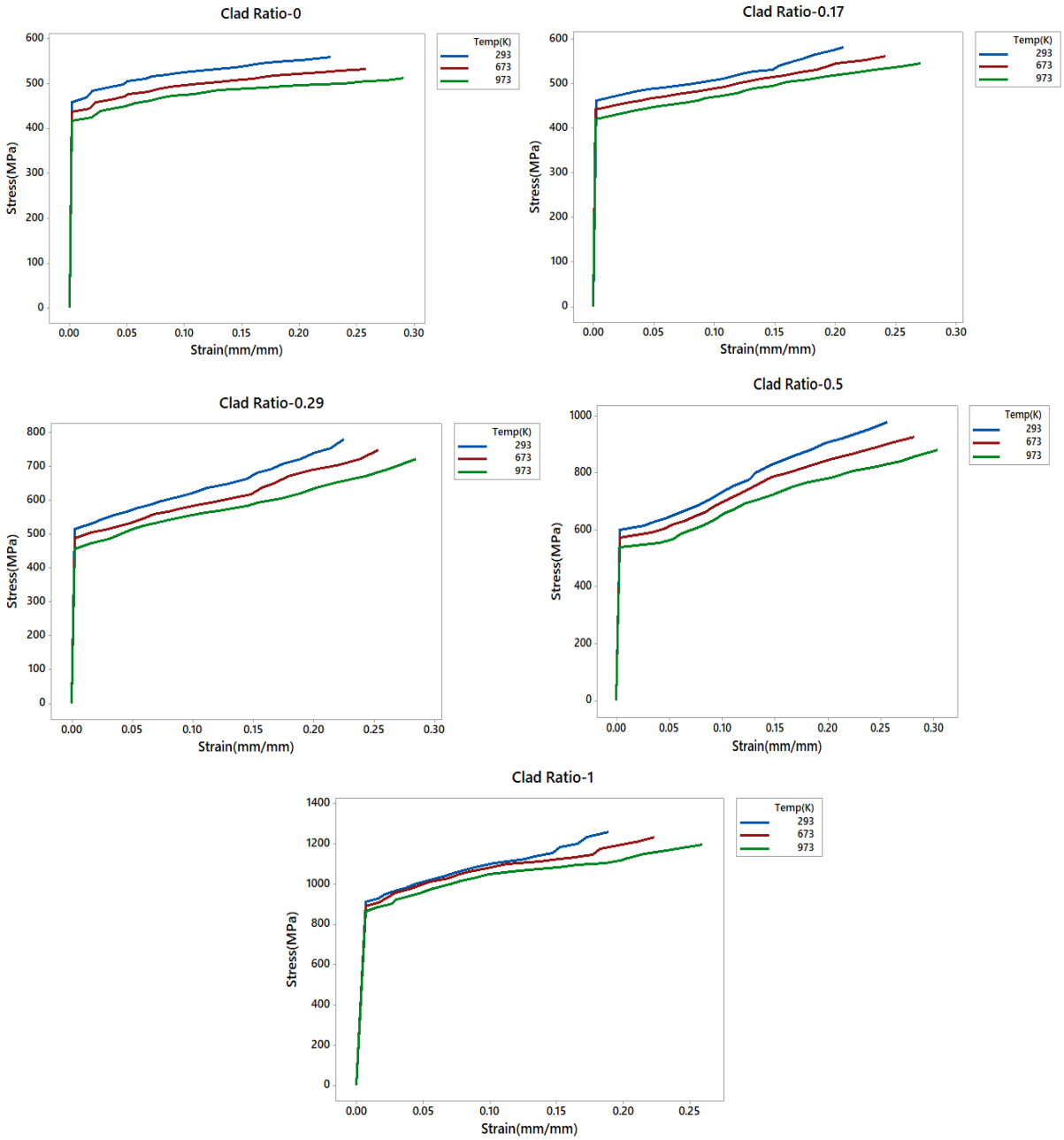

Fig.115. True Stress-true strain at various temperatures under strain rate of 10/sec

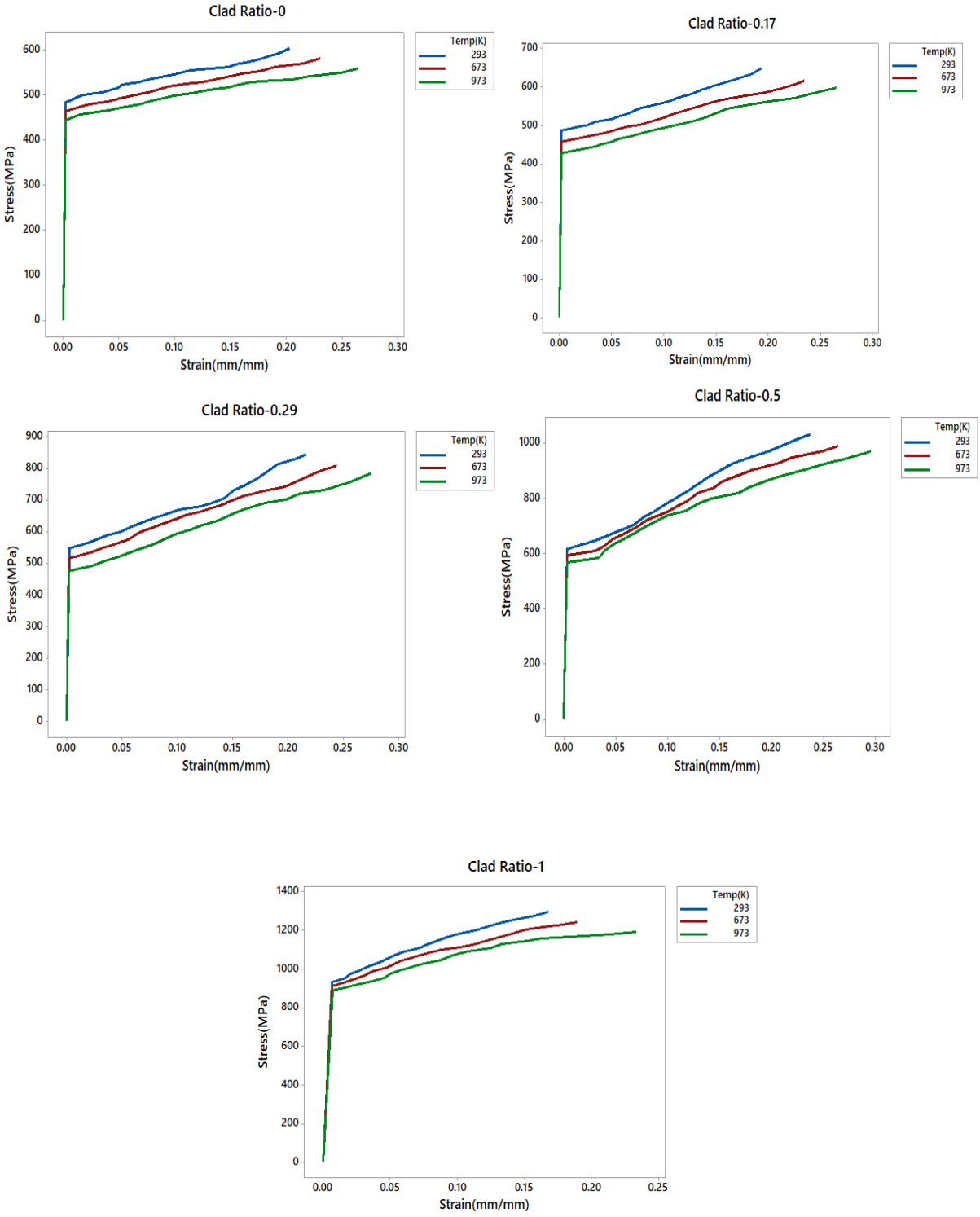

Fig.116. True Stress-true strain at various temperatures under strain rate of 100/sec

- **Strain rate-** As shown in figures.117,118 and 119 as the value of strain rate increases, flow stress increases because flow stress is directly proportional to strain rate. A high strain rate causes the yield point to appear for low-carbon steel which does not show any yield point under normal strain rates. These stress-strain curves are generated by keeping the temperature constant with varying strain rates.

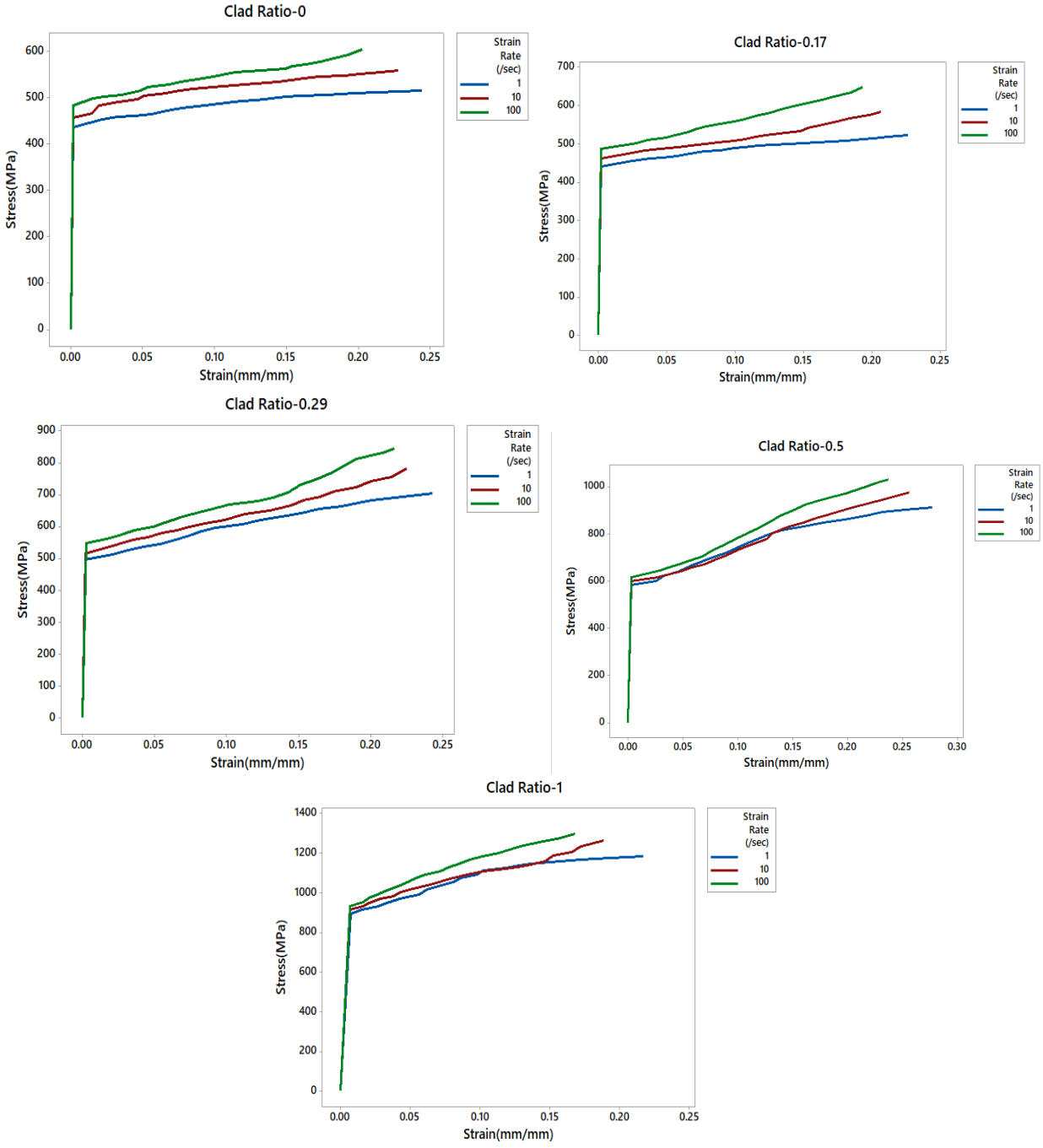

Fig.117. True Stress-true strain at various strain rates under the temperature of 293K

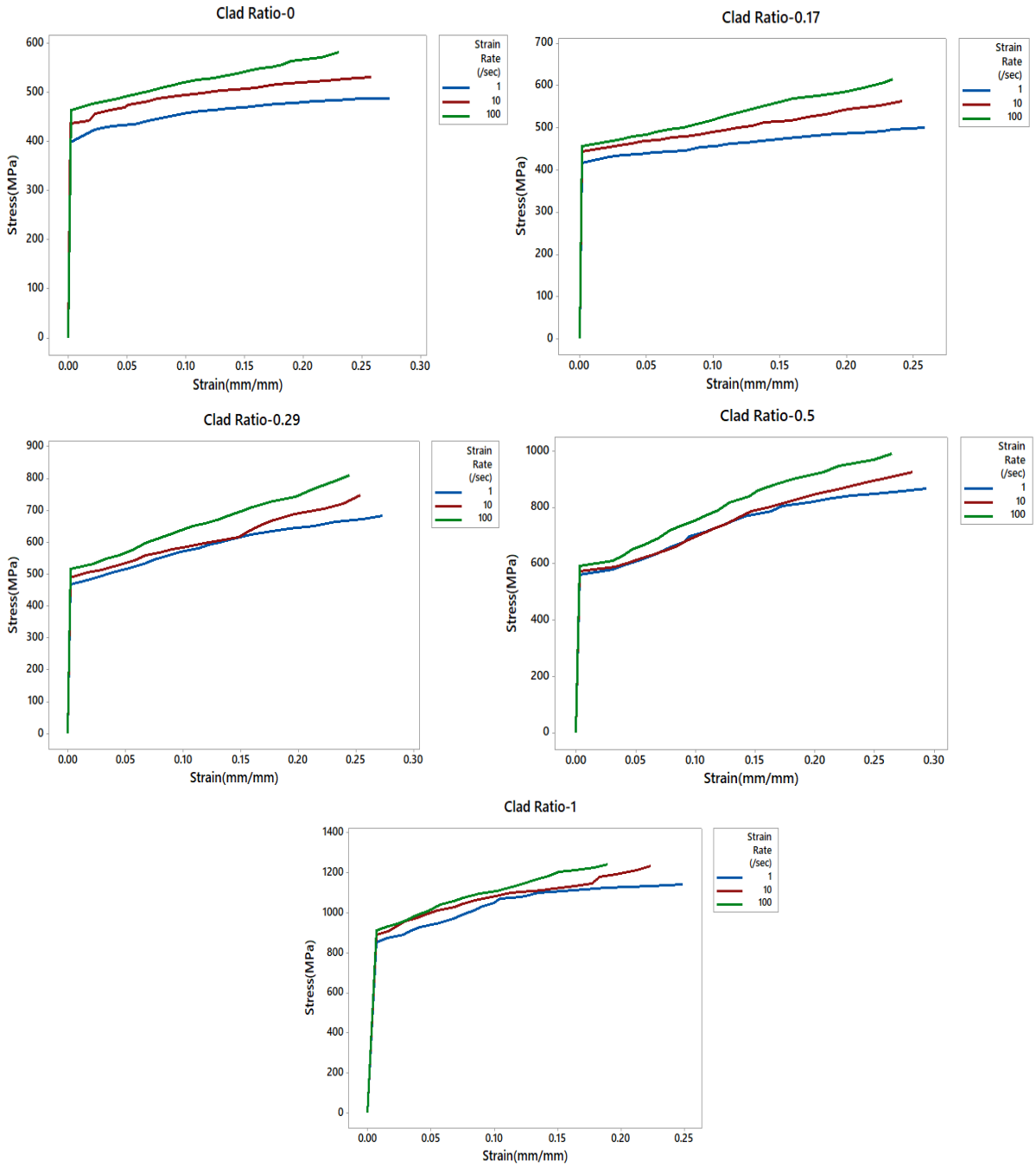

Fig.118. True Stress-true strain at various strain rates under the temperature of 673K

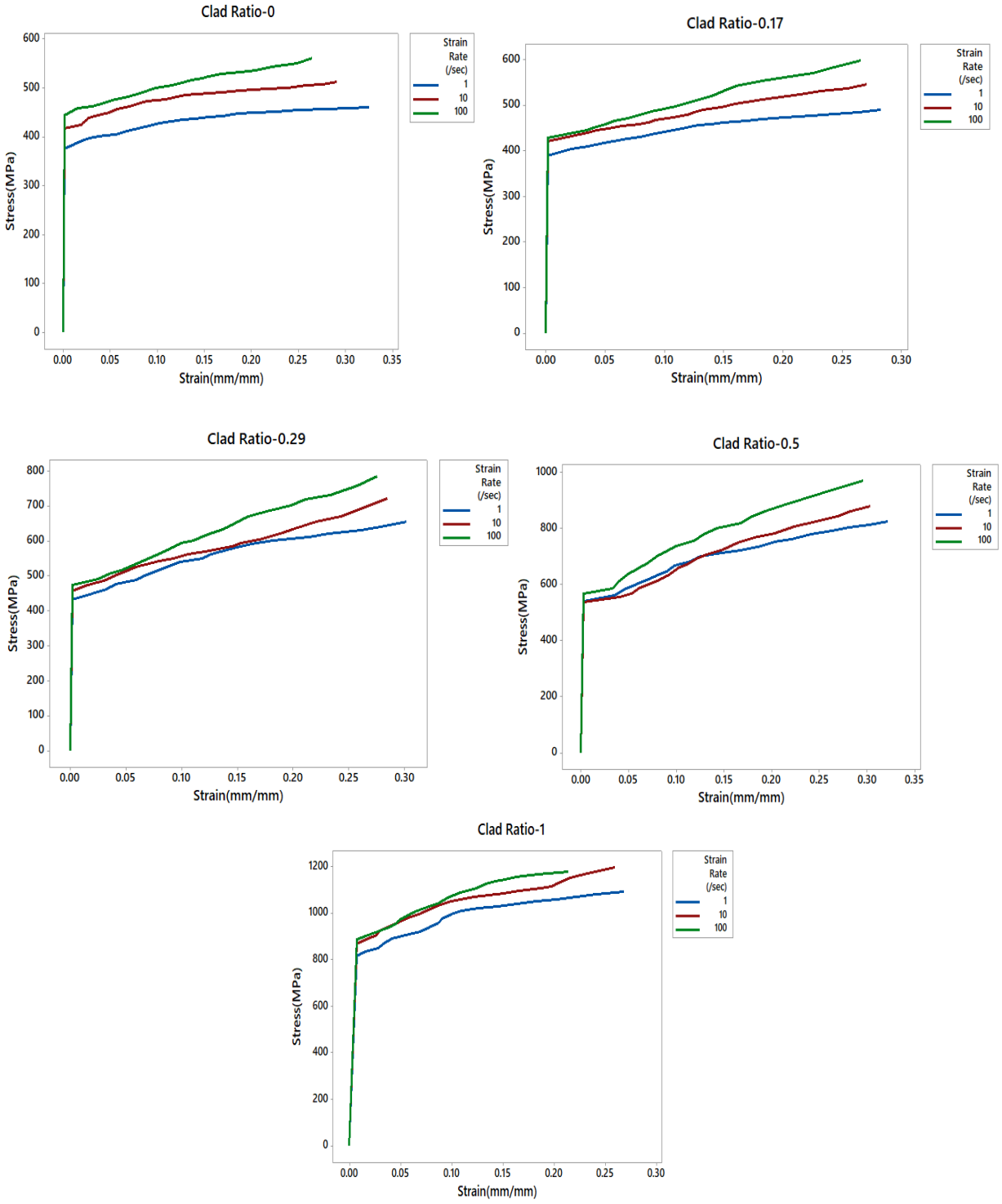

Fig.119. True Stress-true strain at various strain rates under the temperature of 973K

Table.12. Analyzed values of Stress-Strain curve correlated parameters

SPECIMENS	CLAD RATIO (α)	TEMPERATURE (K)	STRAIN RATE (/Sec)	Modulus Of Elasticity (E)	Yield Stress (σy) (MPa)	Ultimate Stress (σu) (MPa)
TC-10-0-1	0	293	1	223.9	436.46	517.19
TC-10-0-2	0	673	1	216.46	400.76	489.29
TC-10-0-3	0	973	1	210.31	376.68	459.79
TC-10-0-4	0	293	10	225.85	457.71	559.07
TC-10-0-5	0	673	10	220.48	437.87	532.88
TC-10-0-6	0	973	10	215.49	417.87	512.7
TC-10-0-7	0	293	100	230.78	485.09	604.86
TC-10-0-8	0	673	100	226.79	464.88	582.8
TC-10-0-9	0	973	100	221.46	444.9	560.19
TC-10-2-1	0.17	293	1	210.36	451.15	542.4
TC-10-2-2	0.17	673	1	204.58	416.49	501.34
TC-10-2-3	0.17	973	1	198.87	389.28	489.94
TC-10-2-4	0.17	293	10	214.48	472.34	582.12

TC-10-2-5	0.17	673	10	209.58	453.41	563.3
TC-10-2-6	0.17	973	10	206.48	434.78	545.88
TC-10-2-7	0.17	293	100	219.69	498.46	647.6
TC-10-2-8	0.17	673	100	215.38	476.25	616.25
TC-10-2-9	0.17	973	100	210.38	458.46	598.45
TC-5-2-1	0.29	293	1	196.28	496.52	703.04
TC-5-2-2	0.29	673	1	190.38	468.66	684.99
TC-5-2-3	0.29	973	1	185.46	432.86	655.13
TC-5-2-4	0.29	293	10	199.38	516.39	781.58
TC-5-2-5	0.29	673	10	195.49	489.98	750.22
TC-5-2-6	0.29	973	10	192.38	458.29	723.38
TC-5-2-7	0.29	293	100	204.53	546.58	844.83
TC-5-2-8	0.29	673	100	200.87	516.34	810.29
TC-5-2-9	0.29	973	100	196.49	475.39	785.58
TC-2-2-1	0.50	293	1	179.95	585.39	912.52
TC-2-2-2	0.50	673	1	174.67	563.36	867.9

TC-2-2-3	0.50	973	1	169.58	542.18	824.98
TC-2-2-4	0.50	293	10	184.87	600.14	978.69
TC-2-2-5	0.50	673	10	179.54	573.76	927.44
TC-2-2-6	0.50	973	10	174.98	538.92	880.73
TC-2-2-7	0.50	293	100	189.26	616.93	1031.4
TC-2-2-8	0.50	673	100	184.82	594.62	991.46
TC-2-2-9	0.50	973	100	178.69	569.22	969.67
TC-0-2-1	1.00	293	1	122.91	892.34	1183.7
TC-0-2-2	1.00	673	1	117.48	856.46	1142.9
TC-0-2-3	1.00	973	1	111.24	815.46	1095.3
TC-0-2-4	1.00	293	10	133.35	913.46	1263.4
TC-0-2-5	1.00	673	10	128.38	892.26	1237.9
TC-0-2-6	1.00	973	10	123.5	868.24	1197.2
TC-0-2-7	1.00	293	100	138.96	932.43	1296.3
TC-0-2-8	1.00	673	100	133.021	912.53	1243.6
TC-0-2-9	1.00	973	100	126.83	889.12	1190.4

6.4 Effect of Clad ratio on Yield stress, Modulus of Elasticity, and Ultimate stress.

- **Yield Stress** - As the value of the clad ratio increases the yield plateau of Stress-Strain curves of the Titanium- Clad bimetallic steels disappears gradually, and the value of equivalent yield strength increases.

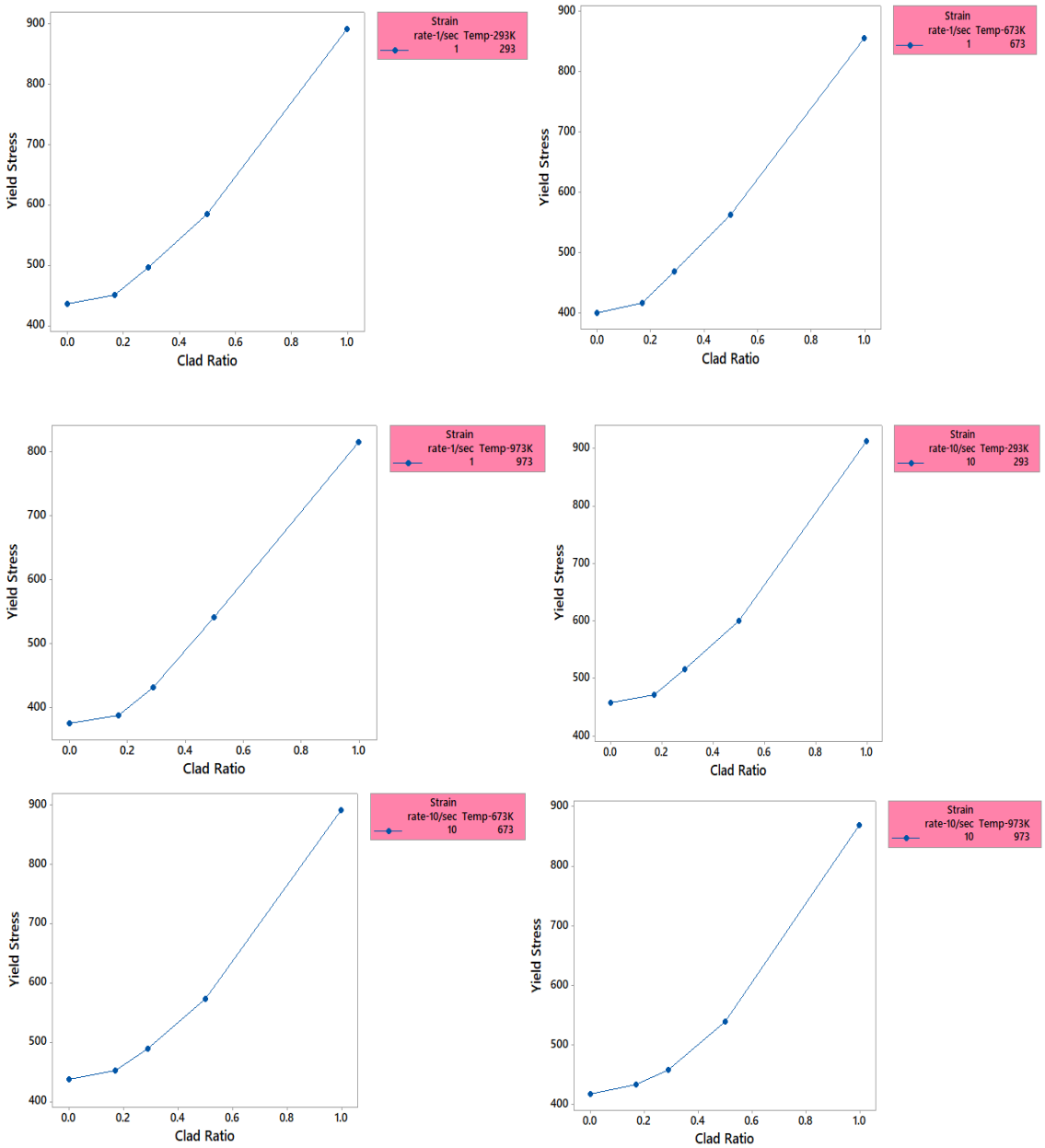

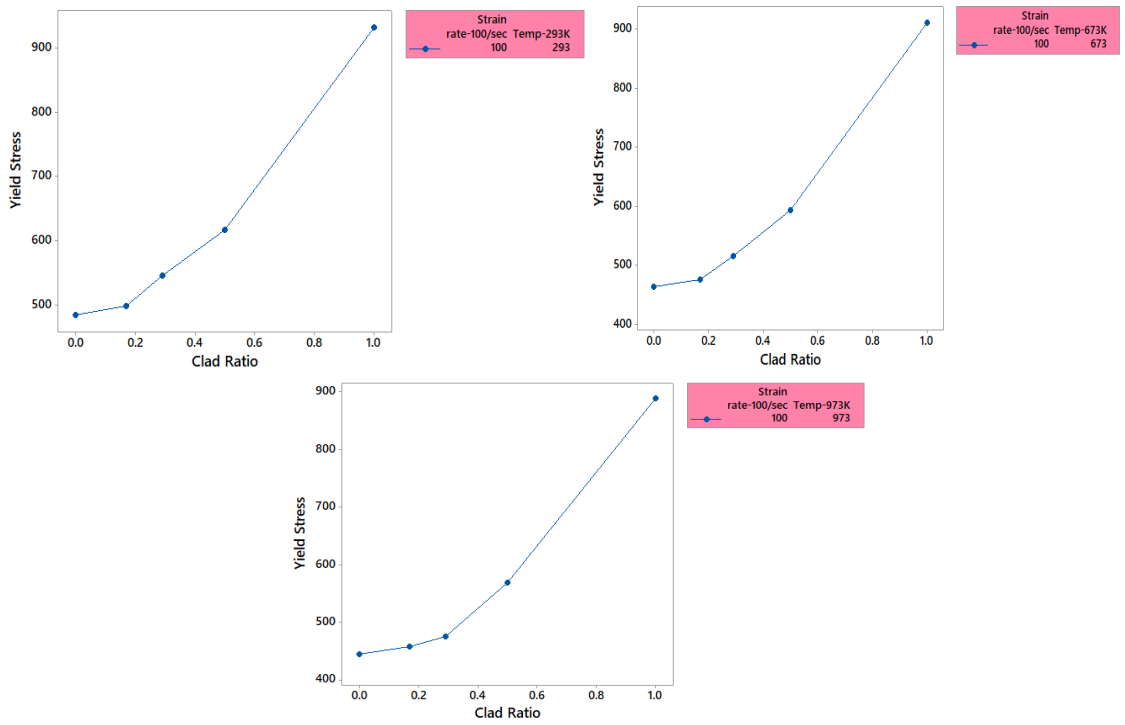

Fig.120. Effect of clad ratio on Yield stress (σy)

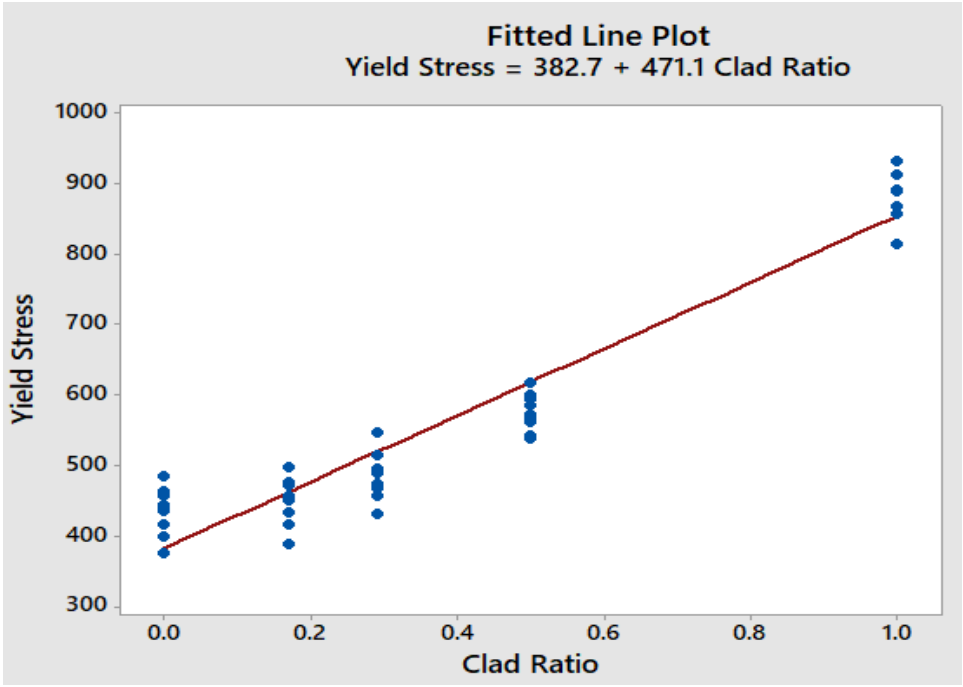

Fig.121. Fitted line plot between Yield stress (σy) and clad ratio.

- **Modulus Of Elasticity** - As the value of clad ratio increases, the elastic modulus is reduced. So inverse relation is seen between clad ratio and modulus of elasticity.

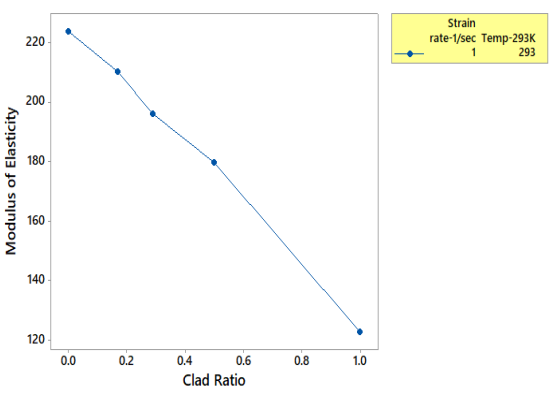
Strain
rate-1/sec Temp-293K
1 293
Modulus of Elasticity
Clad Ratio

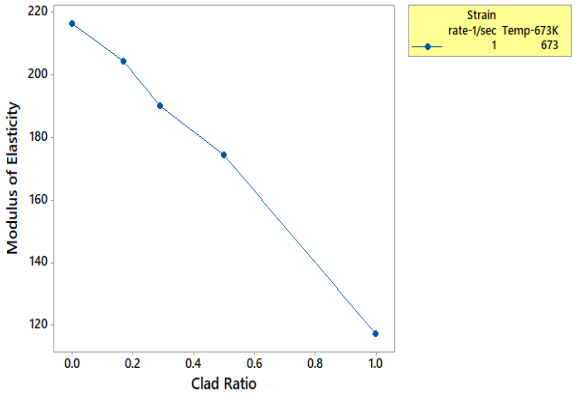
Strain
rate-1/sec Temp-673K
1 673
Modulus of Elasticity
Clad Ratio

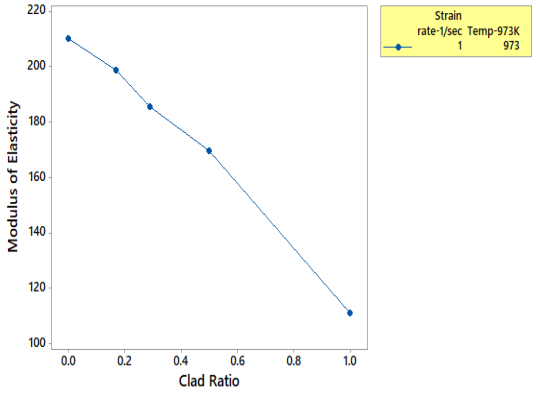
Strain
rate-1/sec Temp-973K
1 973
Modulus of Elasticity
Clad Ratio

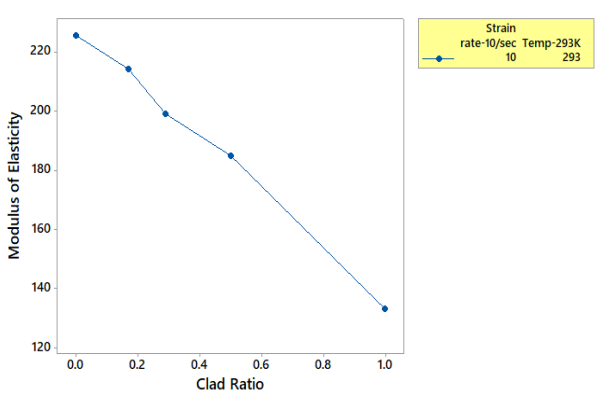
Strain
rate-10/sec Temp-293K
10 293
Modulus of Elasticity
Clad Ratio

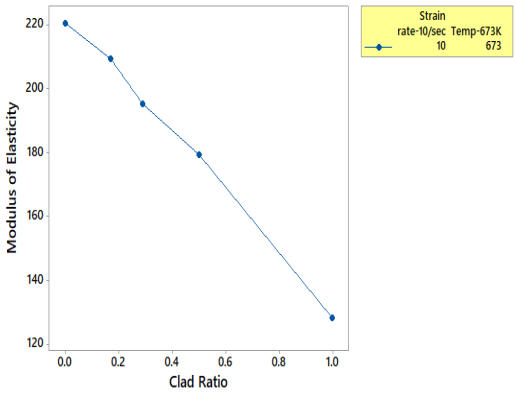
Strain
rate-10/sec Temp-673K
10 673
Modulus of Elasticity
Clad Ratio

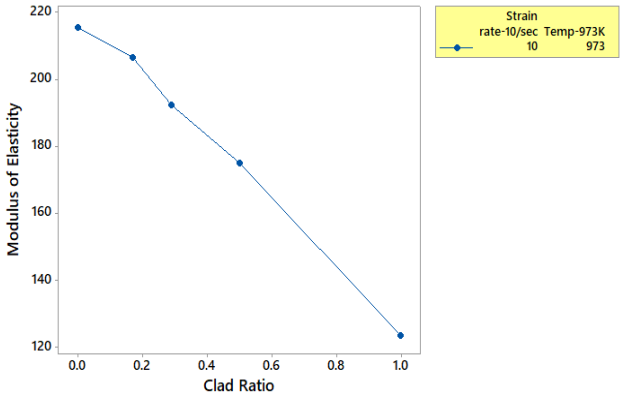
Strain
rate-10/sec Temp-973K
10 973
Modulus of Elasticity
Clad Ratio

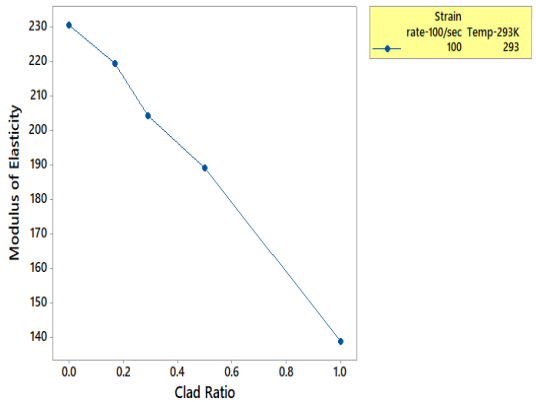
Strain
rate-100/sec Temp-293K
100 293
Modulus of Elasticity
Clad Ratio

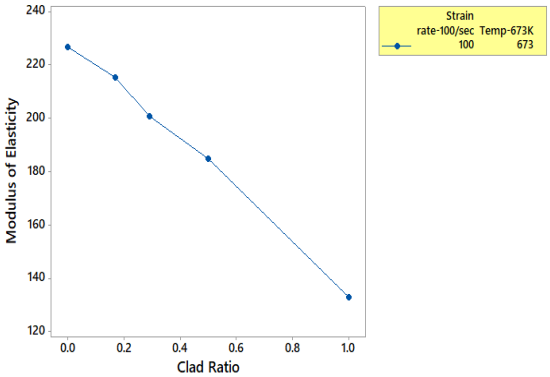
Strain
rate-100/sec Temp-673K
100 673
Modulus of Elasticity
Clad Ratio

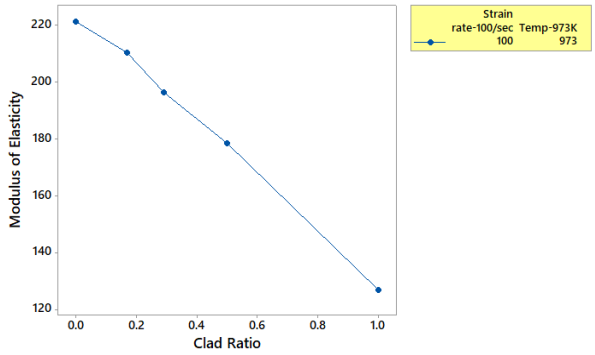

Fig.122. Effect of clad ratio on Modulus Of Elasticity(E)

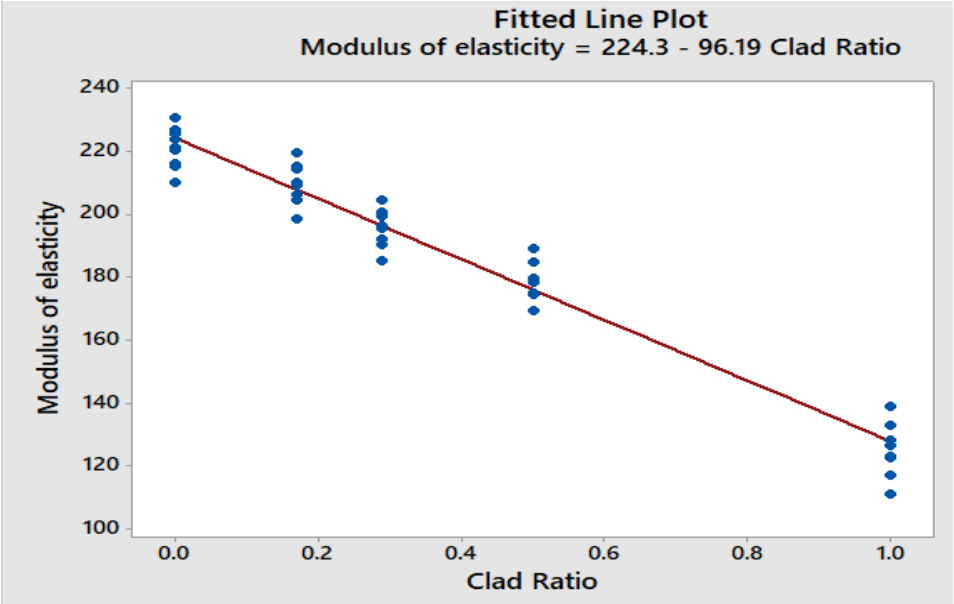

Fig.123. Fitted line plot between Modulus of Elasticity and clad ratio.

- **Ultimate Strength:** As the clad ratio of TC clad bimetallic steel increases the value of ultimate strength also increases. So direct relation is seen between clad ratio and modulus of elasticity.

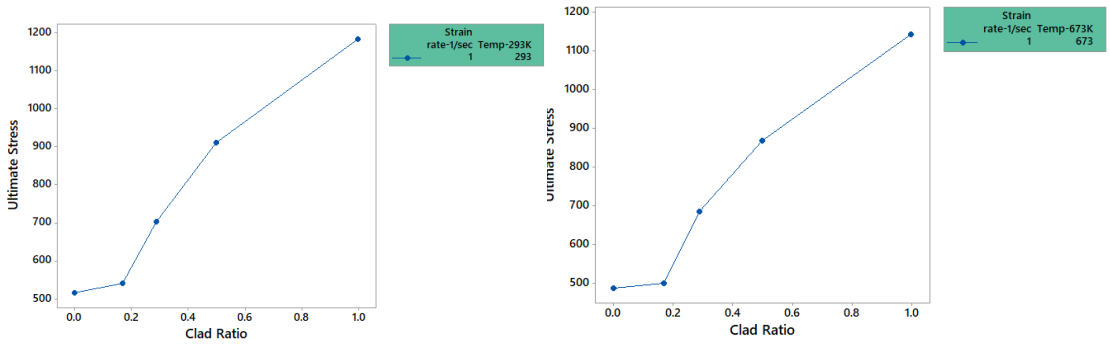

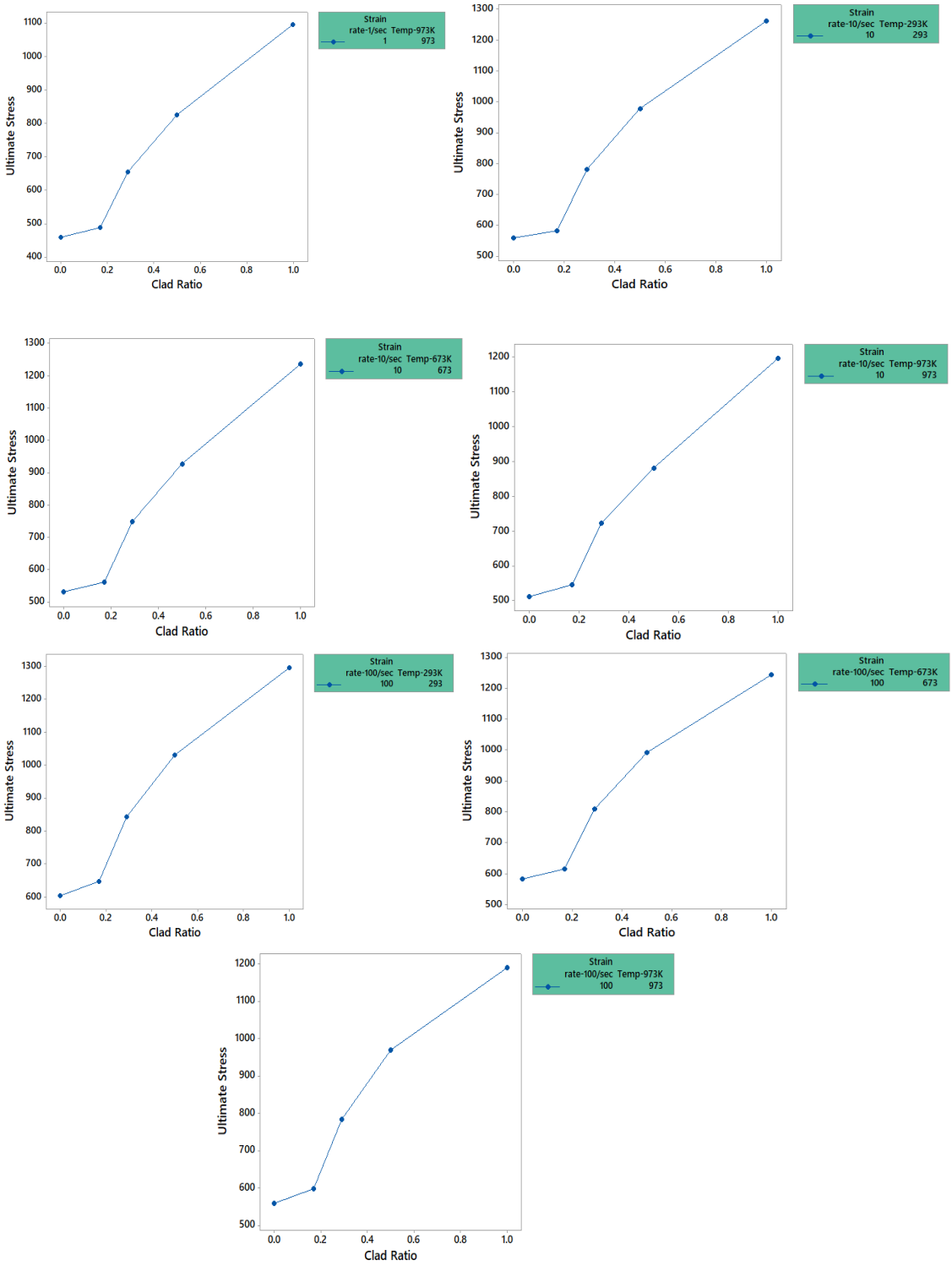

Fig.124. Effect of clad ratio on Ultimate Stress (σu)

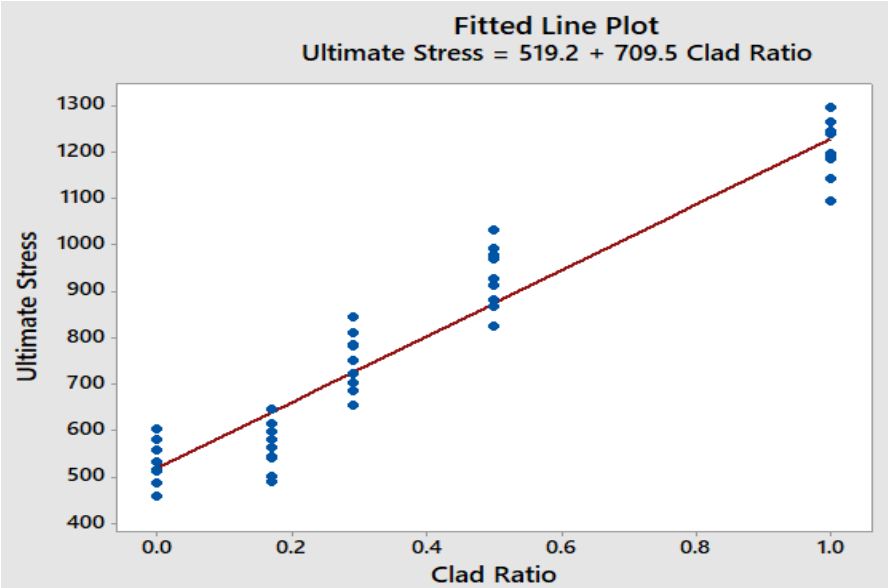

Fig.125. Fitted line plot between Ultimate stress and clad ratio.

CHAPTER-7

CONCLUSION

The analytical True stress- True strain curves of the Titanium-clad bimetallic steel plates having various clad ratios were obtained, where the clad ratio is defined as the ratio of the cladding layer thickness(tc) to the thickness of total plate(t). Johnson-cook parameters for different clad ratios 0.17,0.29 and 0.5 are obtained using the Johnson-cook parameters of Titanium grade5 and AISI 1006 steel. Analytical results depict that as the clad ratio, there are significant changes in the stress-strain curves & their significant parameters like Ultimate Stress, Yield Stress, Modulus of Elasticity for the titanium-clad bimetallic steels. TC bimetallic steels' true stress- true strain curves were found to be the intermediate curves between those of their parent and clad materials, that is AISI 1006 steel and titanium grade 5. The true stress-true strain curves of the Titanium clad bimetallic steels with clad ratios approaching 0 & 1 were similar to those of AISI 1006 steel & titanium grade 5, respectively. From the table, it was depicted that as the value of clad ratio increases, the value of Johnson-cook parameter 'A' increases which mean yield plateau of Stress-Strain curves of the Titanium- Clad bimetallic steels disappears gradually, and the value of equivalent yield strength increases, the value of Johnson-cook parameter 'B'(Strain hardening constant)and 'n' (Strain hardening coefficient) increases which mean, the initial work hardening is less rapid but continues to high strains, the value of 'C' (strengthening coefficient of strain rate) decreases which mean flow stress value decreases in curves which continue to high strains, the value of 'm'(thermal softening coefficient) increases which means that as the temperature increases softening effect increases which reduce the flow stress value and increases the ductility of the material.

REFERENCES

1. Liu, X., Bai, R., Uy, B., & Ban, H. (2019). Material properties and stress-strain curves for titanium-clad bimetallic steels. Journal of Constructional Steel Research, 162, 105756. https://doi.org/10.1016/j.jcsr.2019.105756
2. Rozumek, D., & Bański, R. (2012). Crack growth rate under cyclic bending in the explosively welded steel/titanium bimetals. Materials and Design, 38, 139–146. https://doi.org/10.1016/j.matdes.2012.02.014
3. Prasanthi, T. N., Kirana, R., & Saroja, S. (2016). Explosive cladding and post-weld heat treatment of mild steel and titanium. Materials and Design, 93, 180–193. https://doi.org/10.1016/j.matdes.2015.12.120
4. Chu, Q., Zhang, M., Li, J., & Yan, C. (2017). Experimental and numerical investigation of microstructure and mechanical behavior of titanium/steel interfaces prepared by explosive welding. Materials Science and Engineering A, 689(December 2016), 323–331. https://doi.org/10.1016/j.msea.2017.02.075
5. Chu, Q., Tong, X., Xu, S., Zhang, M., Li, J., Yan, F. X., & Yan, C. (2020). Interfacial Investigation of Explosion-Welded Titanium/Steel Bimetallic Plates. Journal of Materials Engineering and Performance, 29(1), 78–86. https://doi.org/10.1007/s11665-019-04535-9
6. Li, J., Vivek, A., & Daehn, G. (2021). Improved properties and thermal stability of a titanium-stainless steel solid-state weld with a niobium interlayer. Journal of Materials Science and Technology, 79, 191–204. https://doi.org/10.1016/j.jmst.2020.11.050
7. Saroj, S., Sahu, A., & Masanta, M. (2020). Geometrical assessment and mechanical characterization of single-line Inconel 825 layer fabricated on AISI 304 steel by TIG cladding method. Surfaces and Interfaces, 20(June), 100631. https://doi.org/10.1016/j.surfin.2020.100631
8. Chu, Q., Tong, X., Xu, S., Zhang, M., Yan, F., Cheng, P., & Yan, C. (2020). The formation of intermetallics in Ti/steel dissimilar joints welded by Cu-Nb composite filler. Journal of Alloys and Compounds, 828, 154389. https://doi.org/10.1016/j.jallcom.2020.154389
9. Saboktakin, M., Razavi, G. R., & Monajati, H. (2011). The Investigate Metallurgical Properties of Roll BondingTitanium Clad Steel. International Journal of Applied Physics and Mathematics, March 2015, 177–180. https://doi.org/10.7763/ijapm.2011.v1.34
10. Mahmood, Y., Guo, B., Chen, P., Zhou, Q., & Bhatti, A. A. (2020). Numerical study of an interlayer effect on explosively welded joints. International Journal of Multiphysics, 14(1), 69–80. https://doi.org/10.21152/1750-9548.14.1.69
11. Bae, D. S., Chae, Y. R., Lee, S. P., Lee, J. K., Park, S. S., Lee, Y. S., & Lee, S. M. (2011). Effect of post heat treatment on bonding interfaces in Ti/Mild steel/Ti clad

materials. Procedia Engineering, 10, 996–1001. https://doi.org/10.1016/j.proeng.2011.04.164
12. Chai, X. yang, Pan, T., Chai, F., Luo, X. bing, Su, H., Yang, Z. gang, & Yang, C. fu. (2018). Interlayer engineering for titanium clad steel by hot roll bonding. Journal of Iron and Steel Research International, 25(7), 739–745. https://doi.org/10.1007/s42243-018-0106-3
13. Jiang, H., Yan, X., Liu, J., Duan, X., & Zeng, S. (2014). Influence of asymmetric rolling parameters on the microstructure and mechanical properties of titanium explosive clad plate. Xiyou Jinshu Cailiao Yu Gongcheng/Rare Metal Materials and Engineering, 43(11), 2631–2636. https://doi.org/10.1016/s1875-5372(15)60016-9
14. Karolczuk, A., Kowalski, M., Bański, R., & Zok, F. (2013). Fatigue phenomena in explosively welded steel-titanium clad components subjected to push-pull loading. International Journal of Fatigue, 48, 101–108. https://doi.org/10.1016/j.ijfatigue.2012.10.007
15. Kaya, Y., & Eser, G. (2019). Production of ship steel—titanium bimetallic composites through explosive cladding. Welding in the World, 63(6), 1547–1560. https://doi.org/10.1007/s40194-019-00771-8
16. Kurosawa, F. (1988). Analytical study on the Fe/Ti interface in titanium- clad steels. Surface and Interface Analysis, 12(3), 203–210. https://doi.org/10.1002/sia.740120306
17. Li, B., Chen, Z., He, W., Zhou, T., Wang, Y., Peng, L., Li, J., & Liu, Q. (2019). Effect of titanium grain orientation on the growth of compounds at diffusion bonded titanium/steel interfaces. Materials Characterization, 148(November 2018), 243–251. https://doi.org/10.1016/j.matchar.2018.12.029
18. Liangyu, L., Yong, S., Jian, C., Yu, F., Xiaoyuan, X., & Jin, Y. (2020). Study on microstructure and properties of TA1-304 stainless steel explosive welding cladding plate. Materials Research Express, 7(2), 1–10. https://doi.org/10.1088/2053-1591/ab7357
19. Luo, Z., Wang, G., Xie, G., Wang, L., & Zhao, K. (2013). Interfacial microstructure and properties of a vacuum hot roll-bonded titanium-stainless steel clad plate with a niobium interlayer. Acta Metallurgica Sinica (English Letters), 26(6), 754–760. https://doi.org/10.1007/s40195-013-0283-9
20. Prasanthi, T. N., Sudha, C., Ravikirana, Saroja, S., Naveen Kumar, N., & JanakiRam, G. D. (2015). Friction welding of mild steel and titanium: Optimization of process parameters and evolution of interface microstructure. Materials and Design, 88, 58–68. https://doi.org/10.1016/j.matdes.2015.08.141
21. Saboktakin, M., Razavi, G., & Monajati, H. (2011). The Effect of Copper Interlayer on Metallurgical Properties of Roll Bonding Titanium Clad Steel. 15, 10–14.
22. Bhanu Kiran, V.T., Krishna, M., Praveen, M. and Pattar, N., Numerical Simulation of Multilayer Hardfacing on Low Carbon Steel, International Journal of Engineering and Technology, Vol.3, No.1, pp.53-63, 2011.
23. X-, S. A. T. M., & Marshall, G. C. (1965). MEMORANDUM. October.

24. Szymlek, K. (2008).Review of Titanium and Steel Welding Methods. Advances in Materials Sciences, 8(1). https://doi.org/10.2478/v10077-008-0023-4
25. Kumar Saha, M., & Das, S. (2018). Gas Metal Arc Weld Cladding and its Anti-Corrosive Performance- A Brief Review. Athens Journal of Technology & Engineering, 5(2), 155–174. https://doi.org/10.30958/ajte.5-2-4
26. Szymlek K.: Technologia platerowania blach stalowych tytanem. VI Seminarium Naukowe Studentów i Młodych Inżynierów Mechaników. Gdańsk, 5-6 grudnia 2002. pp. 39-47.
27. J. Z. Wang, X. B. Yan, W. Q. Wang, Rare Metal Mater. Eng. 39 (2010) 309-312
28. Samson K., Szymlek K., Walczak W.: Próba optymalizacji parametrów zgrzewania wybuchowego tytanu ze stalą i aluminum. Materiały konferencji naukowo-technicznej. VII Konferencja Spawalnicza Szczecin 2002 "Postęp w technologiach spawania w osłonach gazowych". Międzyzdroje, 21-23.05.2002. pp. 205-212
29. Yang, D. han, Luo, Z. an, Xie, G. ming, Jiang, T., Zhao, S., & Misra, R. D. K. (2019). Interfacial microstructure and properties of a vacuum roll-cladding titanium-steel clad plate with a nickel interlayer. Materials Science and Engineering A, 753(February), 49–58. https://doi.org/10.1016/j.msea.2019.03.008
30. Japan Soc. Corros. Eng.: Boshoku Gijyutsu Binrann , Nikkan kougyo Shinbun Corp.,, pp. 197-198 , (1985) .
31. H.B. Bomberger, P.J. Cambourelis, and G.E. Hutchinson,"Corrosion Properties of Titanium in Marine Environments," J. Electrochem.Soc., Vol. 101, p. 442, (1954).
32. W.L. Wheatfall, "Metal Corrosion in Deep-Ocean Environments," U.S. Navy Marine Engineering Laboratory, Research and Development Phase Report 429/66, Annapolis, Maryland, January (1967).
33. M.A. Pelensky, J.J. Jawarski, A. Gallaccio, "Air, Soil and Sea Galvanic Corrosion Investigation at Panama Canal Zone," p. 94, ASTM STP 576, (1967)
34. D.H. Bae, S.J. Jung, Y.R. Cho, W.S. Jung, H.S. Jung, C.Y. Kang and D.S. Bae, Effect of Pre-Heat Treatment on Bonding Properties in Ti/Al/STS Clad Materials, J. Kor. Ins. Met. & Mater., 2009; 47:573-9
35. D.H. Bae, Y.J. Choi, W.S. Chung, D.S. Bae and Y.R. Cho, Effect of Tension-Test Temperature on Fracture Behavior and Mechanical Properties in STS/Al/Cu Clad Materials, J. Kor. Ins. Met. & Mater, 2009; 47:811-8.
36. Song, J., Kostka, A., Veehmayer, M., & Raabe, D. (2011). Hierarchical microstructure of explosive joints: Example of titanium to steel cladding. Materials Science and Engineering A, 528(6), 2641–2647. https://doi.org/10.1016/j.msea.2010.11.092
37. Ramirez, J. E. (2014). Mechanical behavior of titanium-clad steel welded joints. Welding Journal, 93(10), 369s-378s
38. Qian, X., & Duan, X. (2019). Constitutive model and cutting simulation of titanium alloy Ti6Al4V after heat treatment. Materials, 12(24), 1–13. https://doi.org/10.3390/ma1224145
39. Bataev, I. A., Tanaka, S., Zhou, Q., Lazurenko, D. V., Junior, A. M. J., Bataev, A. A., Hokamoto, K., Mori, A., & Chen, P. (2019). Towards better understanding of explosive welding by combination of numerical simulation and experimental study. Materials and Design, 169(March 2019), 107649. https://doi.org/10.1016/j.matdes.2019.107649